Plants as a Battery Exploring Crop Flexibility to Buffer Enviromental Fluctuations Cristina Zepeda

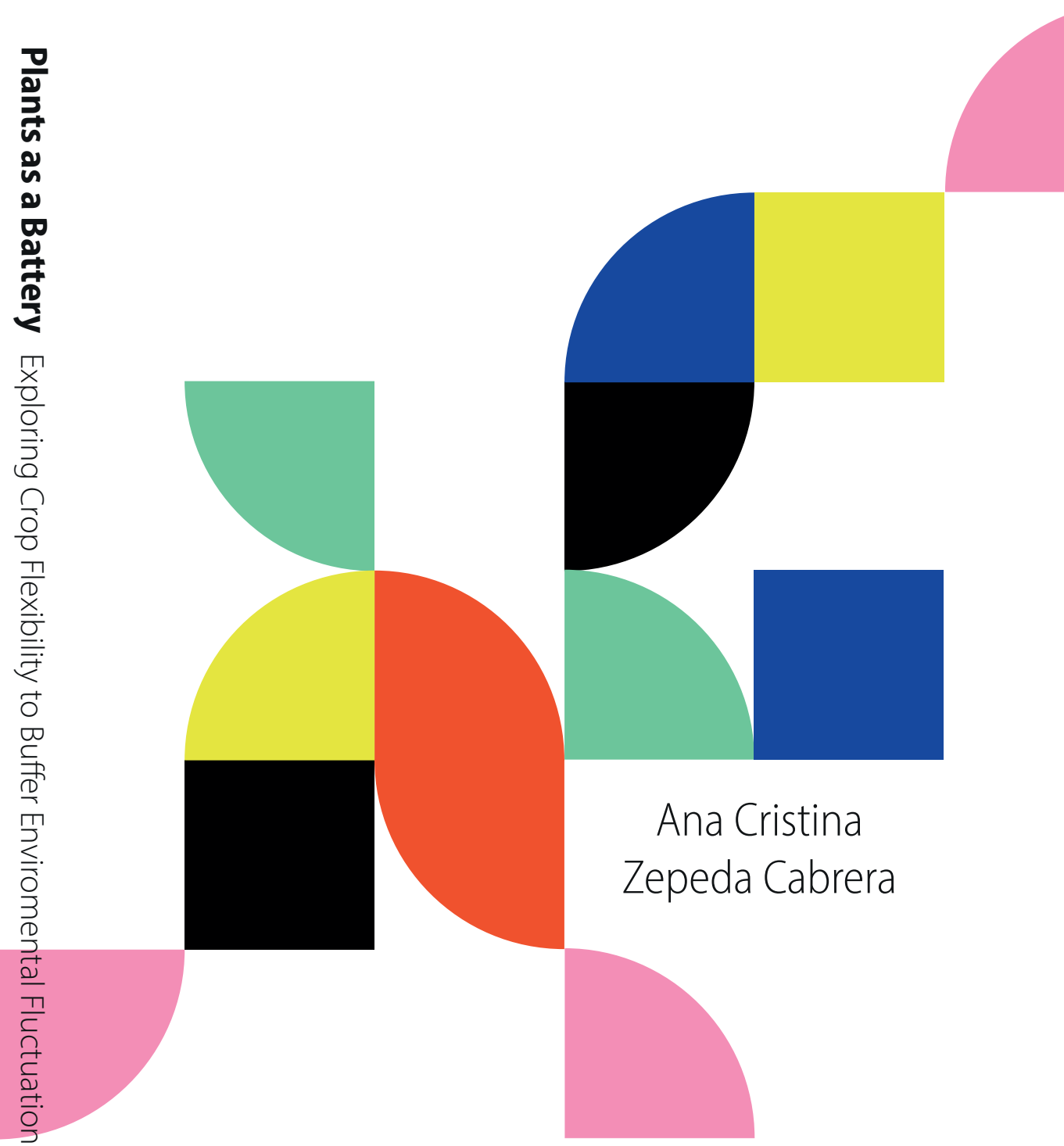

Ana Cristina
Zepeda Cabrera

PLANTS AS A BATTERY

Exploring Crop Flexibility to Buffer Enviromental Fluctuations

Propositions

1. The limits for temperature integration in vegetative plants are determined by the plants' ability to accumulate and remobilize carbon.
   (this thesis)

2. Crop models that exclude simulation of reproductive processes fail at predicting fruit yield.
   (this thesis)

3. An energy crisis is the most effective incentive for individuals and organizations to adopt energy-saving behaviors.

4. Forrester diagrams are an essential communication tool for collaboration between engineers and biologists.

5. Self-compassion is an essential skill in academia.

6. Flex desk policy makes efficient use of office space in the short-term but reduces productivity and well-being of employees in the long-term.

7. Mandatory cooking lessons in Dutch high schools are necessary to improve food culture in the Netherlands.

8. The prevalence of burnout in the Netherlands is mostly attributed to the societal stigma surrounding mental health treatment, especially the reluctance of individuals to seek help from a psychologist.

Propositions belonging to the thesis, entitled
Plants as a battery: Exploring Crop Flexibility to Buffer Environmental Fluctuations

Ana Cristina Zepeda Cabrera
Wageningen, 01 June 2023

Plants as a Battery

Exploring Crop Flexibility to Buffer Environmental Fluctuations

Ana Cristina Zepeda Cabrera

Thesis committee

Promotor
Prof. Dr Leo F.M. Marcelis
Professor of Horticulture and Product Physiology
Wageningen University & Research

Co-promotor
Dr Ep Heuvelink
Associate professor of Horticulture and Product Physiology
Wageningen University & Research

Other members
Prof. Dr Niels P.R. Anten, Wageningen University & Research
Dr Oliver Körner, Leibniz-Institute of Vegetable and Ornamental Crops, Germany
Dr Cecilia Stanghellini, Wageningen University & Research
Dr Ad de Koning, Ridder, Harderwijk

This research was conducted under the auspices of the C.T. de Wit Graduate School for Production Ecology and Resource Conservation (PE&RC).

Plants as a Battery

Exploring Crop Flexibility to Buffer Environmental Fluctuations

Ana Cristina Zepeda Cabrera

Thesis

submitted in fulfilment of the requirements for the degree of doctor
at Wageningen University
by the authority of the Rector Magnificus,
Prof. Dr A.P.J. Mol,
in the presence of the
Thesis Committee appointed by the Academic Board
to be defended in public
on Thursday 01 June 2023
at 01:30 p.m. in the Omnia Auditorium.

Ana Cristina Zepeda Cabrera
Plants as a Battery Exploring Crop Flexibility to Buffer Environmental Fluctuations,
178 pages.

PhD thesis, Wageningen University, Wageningen, the Netherlands (2022)
With references, with summary in English

ISBN: 978-94-6447-686-6
https://doi.org/10.18174/629897

you do not just wake up and become the butterfly

-growth is a process

(rupi kaur)

To my other half, my sister Juli

Table of Contents

Chapter 1

General introduction

Ana Cristina Zepeda

1.1 Greenhouse horticulture and energy consumption

Greenhouse horticulture in the Netherlands is known to be the most intensive and advanced form of production (Hemming et al., 2019). Precise control of the indoor climate allows for consistent crop production with high yields, regardless of external weather conditions (Bot, 2001). However, rigid climate set points require high energy inputs, particularly during the cold and dark winter months in temperate (northern) climates (Van Beveren et al., 2015). The intensification of horticultural production in the Netherlands also leads to environmental issues, with the sector accounting for 6.5% of the country's total CO_2 emissions in 2018 (RIVM, 2021). Particularly, the use of natural gas in boilers and in combined heat and power generators (CHP) accounts for 10% of the natural gas consumption in the Netherlands. In recent years, the illumination of greenhouses has further contributed to electricity consumption (Van der Velden & Smit, 2019). As a result of the increasing gas and electricity consumption, the Dutch government and horticulture sector developed a long-term agreement to reduce energy consumption and CO_2 emissions. This agreement states that from 2050, all new greenhouses must be energy-neutral (Landbouw & Zaken, 2020). The current sharp increase in energy prices further incentivizes the reduction of energy consumption (PBL, 2022). Energy reduction can be reached by technical measures such as the use of cover materials or thermal screens (Bot, 2001), by breeding for new cultivars that are better adapted to low temperatures (Van Der Ploeg & Heuvelink, 2005), or by a flexible greenhouse climate management based on plant physiological processes (Körner & Challa, 2003).

1.2 Flexible climate control: an old concept or a potential solution?

In order to reduce energy consumption in the greenhouse, more sustainable control strategies have been developed, such as flexible temperature and humidity control (De Koning, 1990; Dieleman & Meinen, 2007; Körner & Challa, 2004) or dynamic lighting (Bhuiyan & Iersel, 2021; Körner et al., 2006). These strategies are possible because crops are robust to changes in temperature, light, humidity, and CO_2. Traditionally, production in controlled environments has focused on maintaining the 'perfect' constant climate while reducing any environmental fluctuations (Poorter et al., 2016). This has resulted in very rigid climate set points. Given that plants in nature are exposed to a wide range of fluctuating conditions on various time scales (from second to minutes, diurnally, day-to-day, and seasonally) (Athanasiou et al., 2010; Bhuiyan & Iersel, 2021; Poorter et al., 2016; Vialet-Chabrand et al., 2017), we might

question ourselves whether it is ideal to maintain such strict constant climate set points in controlled environments. Rapid fluctuations in light (seconds to hours) (e.g. Bhuiyan & Iersel, 2021; Zhang & Kaiser, 2020), or day-to-day fluctuations in light and temperature (e.g. Dieleman & Meinen, 2007; Klopotek & Kläring, 2014) may not necessarily have detrimental effects on plant growth. The ability of crops to tolerate fluctuations in light and temperature provides increased flexibility to deviate from strict climate set points in controlled environments. This can profoundly impact energy use efficiency, as flexible climate set points can reduce energy consumption in greenhouse up to 20% (Körner & Challa, 2004; van Beveren et al., 2015).

The concept of temperature integration, which refers to the maintenance of a mean temperature with specified upper and lower limits over specified time intervals (Körner & Challa, 2003), has been studied for over 30 years (e.g., Buwalda et al., 2000; De Koning, 1990; Dieleman & Meinen, 2007; Fink, 1993; Hurd & Graves, 1984; Liebig, 1988). Crops can tolerate a certain level of temperature fluctuations without negatively impacting crop production or quality (Buwalda et al., 2000).

The interaction between temperature and light plays a significant role in determining the source-sink balance of plants and their ability to 'integrate' environmental conditions. Photosynthesis acts as the source for assimilates, and this process is highly dependent on light, temperature, and CO_2 (Farquhar et al., 1980). Processes such as respiration, cell expansion, and cell division, on the other hand, act as the sinks for assimilates, and these processes are highly dependent on temperature (Parent et al., 2010). The source-sink balance accounts for asynchronies between the supply of assimilates from photosynthesis and the demand of assimilates for respiration and growth. Within this context, the build-up of C storage over time is interpreted as a passive process that occurs only when C supply exceeds C demand (Cannell & Dewar, 1994; Chapin et al., 1990; Dietze et al., 2014; Kozlowski, 1992; Sala et al., 2012). This interpretation, however, has been challenged several times in the past (e.g., (Cannell & Dewar, 1994; Dietze et al., 2014; Sala et al., 2012). Instead, a more accurate view is that C storage is a constantly 'active' process, where C storage is a sink that competes for carbohydrates, the magnitude of which depends on environmental conditions (Chapin et al., 1990; Dietze et al., 2014). The active C pool, or the C storage that is available for use, allows plants to flexibly respond to environmental fluctuations.

While vegetative plants can tolerate a wide range of temperature and light fluctuations without very detrimental effects on growth, flowering plants are extremely sensitive to temperature (Hedhly, 2011). High or low temperatures, even for just one day, can disrupt pollen development and lead to poor seed set, ultimately resulting in smaller

or abnormal fruits. Therefore, when developing dynamic climate strategies, it is crucial to consider the reproductive response of plants to temperature fluctuations. Despite the clear energy-saving advantages of flexible climate control strategies, these are still not widely used in greenhouse production (Hemming et al., 2019a). One of the identified reasons for this is a lack of reliable crop production models for the wide range of crops and species grown in horticultural practice (Van Beveren et al., 2015).

1.3 Crop flexibility: The role of a dynamic C pool

The two key mechanisms responsible for the active regulation of C storage are: (i) the partitioning of assimilates between soluble sugars and starch, and (ii) the degradation and remobilization of storage compounds. Non-structural carbohydrates (NSC), including glucose, fructose, sucrose, starch, and other sugars, are produced via photosynthesis (Martínez-Vilalta et al., 2016). These compounds are then partitioned among processes such as respiration, structural growth, reproduction, storage, and defence (Chapin et al., 1990; Huang et al., 2018). Structural carbon (SC) is fixed in plant structures, such as cell walls, and cannot be remobilized in the future (Furze et al., 2018; Hilty et al., 2021).

1.3.1 Partitioning of newly assimilated C between soluble sugars and starch

Soluble sugars and starch serve different functions in plants (MacNeill et al., 2017). The allocation of newly assimilated C between these two compounds is a key process in the active regulation of C storage (Smith & Stitt, 2007). During the day, some fraction of C is allocated to soluble sugars, for the immediate needs of respiration and growth (MacNeill et al., 2017; Ruan, 2014). Other roles of soluble sugars include cell osmoregulation, signalling, and transport (Hartmann & Trumbore, 2016; Ruan, 2014). The remaining fraction is stored as starch to meet the C demand during the following night (Graf et al., 2010a; Graf & Smith, 2011; Stitt & Zeeman, 2012). This mechanism is clearly demonstrated in starchless *Arabidopsis* mutants, which demonstrate lower growth rates than wild-type plants when grown at low light intensities or short days but demonstrate normal growth in continuous light or long days (Gibon et al., 2009; Graf et al., 2010a).

The relative fraction of assimilates partitioned towards starch is strongly dependent on photoperiod, but weakly dependent on light intensity (Chatterton & Silvius, 1980; Mengin et al., 2017; Pilkington et al., 2015). This means that a larger fraction of C is allocated towards starch during short days to anticipate the long night (Graf et al.,

2010b). This process is regulated by the circadian clock, which is set to a 24-hour cycle (Graf et al., 2010b; Millar et al., 2014; Webb et al., 2019).

In deciduous trees, the regulation of C reserves is important for seasonal growth and reproduction (Lacointe et al., 1993; Weber et al., 2019). During summer and autumn, trees actively allocate C towards starch at the expense of immediate growth (Richardson et al., 2013). During winter, when temperatures are low, dormant trees increase the starch synthase pathway (Sperling et al., 2019; Zwieniecki et al., 2015) providing the necessary resources to bloom and resprout in spring when the temperature rises (Zwieniecki et al., 2015).

1.3.2 Remobilization of storage

The second key process in the active regulation of C storage is the degradation of starch into sucrose at night, or in the long term, the remobilization of previously stored starch. On a diel basis, the degradation of starch at night is precisely timed by the circadian clock (Graf et al., 2010b) to ensure that almost all the starch is consumed by dawn. This prevents the plant from periods of starvation that could inhibit growth (Smith & Zeeman, 2020). An important observation here is that this 'near-to-complete' degradation of starch, has been studied almost only in *Arabidopsis* plants grown under source-limiting conditions (light intensities between 90 to 170 µmol m^{-2} s^{-1}) (Gibon et al., 2004, 2009; Pilkington et al., 2015; Scialdone et al., 2013; Sulpice et al., 2014). One of the only studies done under sink-limited conditions showed that starch degradation at night is incomplete and can be accelerated by raising the temperature (Pilkington et al., 2015). These findings are particularly relevant for plants grown in the field, which are often exposed to higher light intensities during spring and summer or in the middle of the day. Incomplete starch remobilization at night can result in a build-up of C reserves that allow plants to cope with sudden changes in C availability or sudden increases in temperatures. An increase in carbohydrate concentration can directly downregulate photosynthesis by inducing phosphate deficiency or a high concentration of triose-phosphate which inhibits RuBP-carboxylase activity (Azcon-Bieto, 1983; Paul & Foyer, 2001a).

1.4 Reproductive processes and climate fluctuations

So far, I have focused on describing the mechanisms that enable plants to regulate their C storage dynamics and adapt to changing environments. However, it is important to note that other processes, such as reproduction and flowering, are highly sensitive to temperature and can be negatively impacted by short-term temperature

stress, leading to a potential decrease in yield. This is particularly relevant in open field and greenhouse production, as future climate projections predict a higher frequency of short episodes of temperature extremes (Pereira et al., 2022). Abortion of flowers and fruits is often modelled as a function of the balance between supply and demand from assimilates (source-sink ratio) (Bertin & Gary, 1993; Marcelis, 1994; Wubs, 2010) where temperature plays an indirect role. For example, high temperatures are associated with high sink strength, and when combined with a relatively low source strength (e.g. by a low light environment or low leaf area index) this typically results in high fruit abortion rates. However, fruit and seed set directly depend on the success of an aggregation of multiple processes, including pollen development, pollination, pollen tube growth, and fertilization of the female gametes (Santiago & Sharkey, 2019). These processes are highly temperature sensitive (Hedhly et al., 2005), and the impact of temperature is a complex function of intensity, duration, and timing of exposure (Sato et al., 2002; Zinn et al., 2010). Currently, these processes are rarely included in crop simulation models, thereby limiting the accuracy and reliability of these models to predict yield under fluctuating temperature conditions. The fruit set process has since long been identified as one of the weak features in crop growth models (Marcelis et al., 1998a).

1.5 Models as a tool to explain crop flexibility

Models are mathematical representations of system dynamics that explain and predict how a system will respond to environmental and other input variables (Hammer et al., 2004). Crop growth models are essential in decision support systems, greenhouse climate control, and prediction and planning of production (Marcelis et al., 1998b). Crop growth models are often driven by the environmental effect on gross photosynthesis and respiration over the course of a day (Poorter et al., 2013). Growth is then modelled as the net result of daily C input from photosynthesis minus C loss through respiration (Gent & Seginer, 2012). However, this approach overlooks the temporary storage of C whenever supply exceeds demand.

A more accurate analysis of C gains and losses of over the diurnal cycle should consider the asynchrony between timing of acquisition of C and utilization of C for growth and respiration (Goudriaan & Van Laar, 1992). For example, Van Henten, (1994), separated the NSC pool from structural growth in his lettuce growth model. However, this model only accounts for growth during the light periods and does not consider how C contributes to growth during the night. Only in case of an excess accumulation of NSC during the day, assimilates are stored transiently for the next light period. Additionally, Van Henten's (1994) model has only been partially validated with respect to total dry weight, but not for the NSC. This raises questions

about the validity of the model's predictions regarding non-structural carbohydrate content. Gent & Seginer, (2012) also explicitly included a NSC pool in their growth model, and while this model has been validated for total dry weight and NSC in tomato, sunflower, and wheat grown under constant environmental conditions; it is not able to predict diurnal growth patterns. This is because their model does not account for the conservation of carbohydrates until dawn. Instead, the model partitions C into structure with a daily time step based on the supply and demand of carbohydrates across the entire day.

1.6 The role of crop models for decision support in horticulture

Horticultural companies are increasingly adopting a trend of providing decision-support tools that are based on predictions (Körner, 2019). The climate set points for the greenhouse are set by the grower, who is informed by the sensor data from indoor climate, weather forecasts, and output from the decision support system. The decision support system also uses sensor and weather forecast data, as well as a predictive model comprising crop, climate, and energy dynamics (Van Mourik et al., 2021). The quality of the models used is very important, that is why, models alone, are rarely used in greenhouse management (Körner, 2019). Current crop growth models lack processes that allow them to predict growth accurately in fluctuating environments (see Chapter 2). This thesis is situated in the decision support box highlighted in red in Figure 1.1, with the aim of developing a model that can predict growth under fluctuating environmental conditions. Having better and more robust models will enhance decision support and improve system performance.

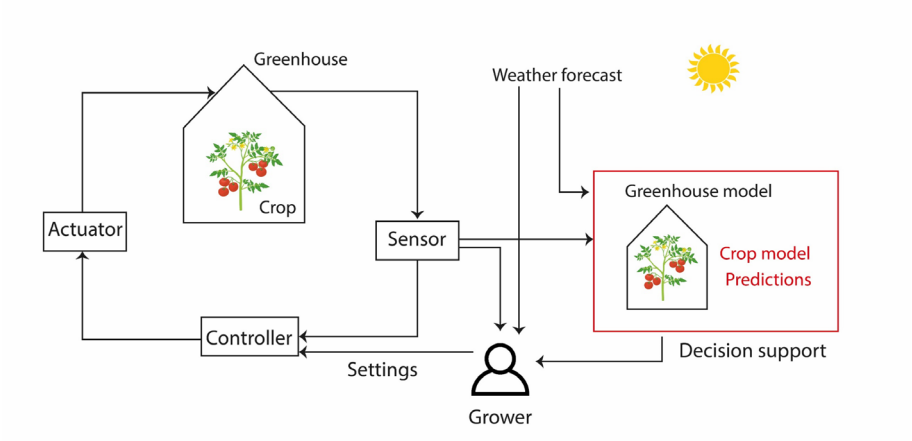

Figure 1.1. *Illustration of an operational management loop in high-tech greenhouse systems. The climate settings (like set points and constraints) are set by the grower, who is informed by sensor output (indoor climate and crop state), weather forecast, and output of a decision support system in the form of predictions, state estimations, and advice on control settings. The decision support system uses sensor and weather forecast data, and employs a predictive model comprising of crop, climate, and energy dynamics. The research within this thesis corresponds to the crop model predictions, highlighted in red, with the aim of improving predictions of dynamic crop processes under varying environmental conditions. Consequently, such an improvement might help improve decision support, and thereby improve system performance in terms of crop production and energy efficiency.*

1.7 Exploring crop flexibility to buffer environmental fluctuations: aim and approach of this thesis

The lack of quantitative information and a suitable crop model to simulate crop flexibility has hindered the implementation of energy-saving flexible climate control techniques in greenhouses. This is unfortunate, as numerous experimental and modelling studies over the past 40 years have demonstrated the potential for energy-saving using flexible climate control. Within this context, the aim of this thesis is to explore the crop flexibility to buffer environmental fluctuations. The hypothesis is that plants can achieve this through C storage and C remobilization. However, this flexibility might be constrained by the sensitivity of fruit set or seed set to low or high temperature stress. Understanding how the climate influence these processes is crucial for developing realistic dynamic climate control strategies. As a first step, a literature study was conducted to explore the physiological processes involved in the dynamic C storage **(Chapter 2).** Then, an experiment was conducted to study the vegetative

growth and NSC dynamics of plants grown under different light and temperature fluctuations **(Chapter 3).** A separate experiment was also conducted to investigate the impact of temperature stress and duration of the stress on pollen quality, seed set, fruit set, and individual fruit mass. Data from this experiment was used to develop a predictive model for seed set and fruit mass **(Chapter 4).** Finally, based on the literature review in **Chapter 2** and the data collected in **Chapter 3,** a dynamic model was developed that describes the crop's soluble sugar, starch, and structural mass **(Chapter 5)**. A schematic illustration of the outline of this thesis is presented in **Figure 1.2**.

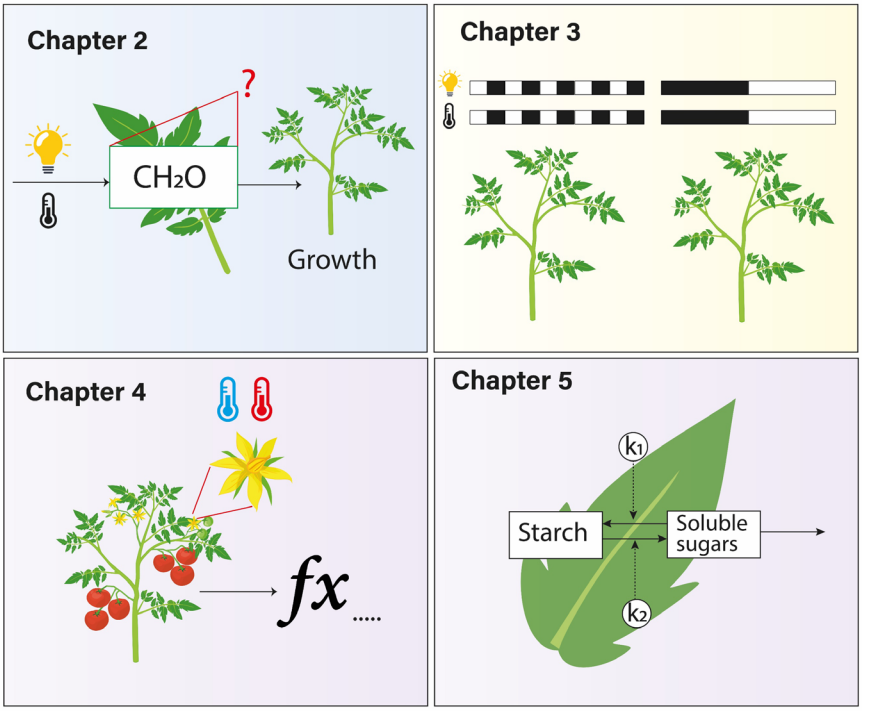

Figure 1.2. *Graphical abstract of the research done in this thesis, where the aim was to investigate the plant's ability to buffer environmental fluctuations. In* ***Chapter 2,*** *different processes that describe the C pool of the plant in response to environmental fluctuations was reviewed. In* ***Chapter 3****, the impact of temperature and light on plant growth, soluble sugar, and starch content was investigated. In* ***Chapter 4****, a predicitive model for seed set and fruit mass was developed. Experiments exposing plants to different temperature stress and duration of the stress were conducted and fruit set and pollen quality parameters were measured. Finally, in* ***Chapter 5,*** *a dynamic model that describes the crop soluble sugar, starch and structural mass was developed based on the literature review performed in* ***Chapter 2,*** *and data collected in* ***Chapter 3*** *was used to calibrate and evaluate the model.*

Chapter 2

Carbon storage in plants: a buffer for temporal light and temperature fluctuations

Ana Cristina Zepeda, Ep Heuvelink, Leo F.M. Marcelis

Published in In Silico Plants (2023), 5
DOI: https://doi.org/10.1093/insilicoplants/diac020

Abstract

Carbon (C) storage allows a plant to support growth whenever there is a temporal asynchrony between supply (source strength) and demand of C (sink strength). This asynchrony is strongly influenced by changes in light and temperature. In most crop models, C storage is included as a passive process that occurs whenever there is an excess of C from photosynthesis compared with the demand of C for metabolism. However, there are numerous studies that challenged this concept, and provided experimental evidence that C storage is an active process that allows buffering of environmental fluctuations and supports long-term plant growth. We propose that an active C pool needs to be included in simulation models for a better understanding of plant growth patterns under fluctuating environment. Specifically, we propose that the two main mechanisms actively regulating C storage in plants are the partitioning of assimilates between soluble sugars and starch and the degradation and remobilization of storage compounds. The insights gained here are important to optimize crop performance under fluctuating conditions and thus for developing more resource-efficient crop production systems.

2.1 Introduction

Storage is a fundamental process where plants build up resources that can be mobilized under future and less favourable conditions to support biosynthesis for growth or other plant functions (Chapin et al., 1990). Carbon (C) storage buffers temporal asynchrony between C supply by photosynthesis and C demand by the different plant organs. Plant C metabolism is often described as a relationship between autotrophic organs acting as 'source' (net producers of C) and heterotrophic organs acting as 'sinks' (net importers of C) (MacNeill et al., 2017). Within this context, the C status of the plant can be either source-limited or sink-limited. In source-limited plants, the net production of assimilates is less than the net demand of assimilates, therefore, plant growth is limited by C supply (Smith & Stitt, 2007). On the contrary, in sink-limited plants, the net production of assimilates exceeds the demand and growth is limited by assimilate usage (Palacio et al., 2014).

In nature, plants need to constantly cope with a rapidly changing environment. Plants are subject to diurnal variations in light, as the natural course of radiation during the day follows a sinusoidal pattern but temperature also changes diurnally, with higher temperatures during the light period and lower temperatures at night. Additionally, plants need to cope with unpredictable environmental fluctuations on a day-to-day basis, as natural light, ambient temperature, and water availability vary depending on the weather on a particular day and because of slower alterations due to seasonal effects (Parent et al., 2010). These fluctuations have a profound effect on C fluxes such as photosynthesis, respiration, growth, and storage (Fatichi et al., 2019). For example, during the light period, C is fixated by photosynthesis which is highly dependent on light (Farquhar et al., 1980) while respiration is mainly dependent on temperature. During the dark period, only mitochondrial respiration and growth take place and these processes are highly influenced by temperature and substrate availability. Upon a sudden increase in light intensity, photosynthesis is limited by enzyme activation in the Calvin-Benson cycle (Kaiser et al., 2018) or by energy dissipation (Kromdijk et al., 2016). Temperature, on the other hand, influences several metabolic processes that determine cell expansion and cell division, and thus the growth rate of organs (Parent et al., 2010).

The source-sink balance accounts for asynchronies between the supply of assimilates from photosynthesis and the demand of assimilates for respiration and growth. Within this context, the build-up of C storage through time is interpreted as a passive process that occurs only when C supply exceeds C demand by different sinks (Cannell & Dewar, 1994; Chapin et al., 1990; Dietze et al., 2014; Kozlowski, 1992; Sala et al., 2012). This interpretation, however, has been challenged several times in the past

(e.g., Cannell & Dewar, 1994; Dietze et al., 2014; Sala et al., 2012) and it is argued that C reserves cannot be treated as passive reservoirs or as an 'optional extra' (Da Silva et al., 2014). Instead, a more accurately view is that C storage is a constantly active process, where C storage is a sink that competes for carbohydrates to a greater or a leaser extend in specific instances, according to environmental conditions. (Chapin et al., 1990; Dietze et al., 2014). Active storage, therefore, involves metabolically regulated partitioning or synthesis of C to storage compounds from resources that would otherwise be used for growth (Gessler & Grossiord, 2019).

Despite the long list of studies on source-sink interactions (e.g., Sonnewald & Fernie, 2018), there is still a widely debated question: is C assimilation or rather C usage ultimately responsible for crop yield? There is a strong line of research that argues that C assimilation (source activity) ranks above any other process that drives plant growth (De Souza et al., 2017) while there are others that argue that both source and sink effects co-limit plant growth (Fatichi et al., 2014; Körner, 2015). For plants to grow they need resources and appropriate conditions so that these resources are converted into biomass. When conditions are temporarily unfavourable, resources are stored temporarily, and in this sense the C storage process also becomes an important process as well, although only partly understood (Dietze et al., 2014; Hartmann & Trumbore, 2016)

Although C has a central role in plants, there is no clear understanding about how allocation of C to storage and remobilization of C occurs in response to temporal environmental stresses. Moreover, an active C storage is rarely explicitly included in crop growth models (Dietze et al., 2014). Here, we propose that crop growth models should include an 'active' storage compartment based on biochemical processes in order to quantify plant responses to fluctuations in light and temperature. Incorporating a dynamic active C-storage pool would allow understanding plant strategies to cope with fluctuating environments as an integrated process: from fluctuations in environmental conditions to C-pool dynamics to growth of plants. We first discuss experimental evidence of the physiological mechanisms that drive C storage in plants. Specifically, we propose that the two main mechanisms actively regulating C storage in plants are the partitioning of assimilates between soluble sugars and starch and the degradation and remobilization of storage compounds. Second, we discuss the possibility of extrapolating insights gained from diel storage regulation to the long term (day to weeks) dynamics of C storage and its consequences for growth. Finally, we propose a modelling framework to simulate storage accumulation and remobilization based on biochemical processes. The insights gained here are important to optimize crop performance under fluctuating conditions and thus for developing more resource-efficient crop production systems.

2.2 The active regulation of C storage

We identify two mechanisms as key for the active regulation of C storage: 1) partitioning of assimilates between soluble sugars and starch and 2) degradation and remobilization of storage compounds. C is assimilated by plants via photosynthetic uptake of atmospheric CO_2, producing C-rich compounds such as glucose, fructose, sucrose, starch but in some herbs and grasses also fructans, oligosaccharides, polysaccharides other than starch (e.g., inuline), all referred to as non-structural carbohydrates (NSC) (Martínez-Vilalta et al., 2016). These are then partitioned among different processes such as respiration, structural growth, reproduction, storage, and defence (Chapin et al., 1990). Structural carbon (SC) is fixed in plant structure such as cell walls, composed of cellulose, hemicellulose, or lignin. These compounds cannot be re-used by the plant in the future because plants lack the enzymes for cellulose degradation (Furze et al., 2018). NSC, on the other hand, function as a source of stored energy and C for biosynthesis (Dietze et al., 2014). Sucrose synthesized during the day is either converted to starch or used to satisfy immediate respiratory requirements or is exported from the leaves to sink organs such as young leaves, reproductive organs, or fruits (MacNeill et al., 2017; Ruan, 2014). Other roles of sucrose are for cell osmoregulation (Talbott & Zeiger, 1998), as a signalling molecule to regulate gene expression, for crosstalk with hormonal, oxidative and defence signalling (Ruan, 2014) and as a transport sugar (Hartmann & Trumbore, 2016; Ruan, 2014). In contrast, starch is the most prevalent form of long-term carbohydrate reserve in trees (Da Silva et al., 2014), and in herbaceous plants can be transiently stored to fulfil C demand during the night (Thalmann & Santelia, 2017) or for later use in periods of low C supply like winter in perennial plants.

2.2.1 Assimilate partitioning: between sucrose and starch

One key process part of the active regulation of C storage is the partitioning of newly assimilated C between soluble sugars and starch during the day (Smith & Stitt, 2007). This is considered as an active response because assimilates are not immediately used, but rather partitioned into sucrose for the immediate demands during the day, but also partitioned into starch to fulfil C demand during the following night (Graf et al., 2010; Graf & Smith, 2011; Stitt & Zeeman, 2012). This mechanism is nicely demonstrated in starchless *Arabidopsis pgm* mutants which have much lower growth rates than the wild-type plants when grown at low light intensities or short days, however, their growth is normal in continuous light or very long days (Gibon et al., 2009; Graf et al., 2010). Partitioning of assimilates to starch is therefore strongly dependent on photoperiod, but weakly dependent on light intensity. For example, growing *Arabidopsis* in an 8 h photoperiod at 28 °C showed that when light intensity was

reduced from 160 to 40 μmol m^{-2} s^{-1} for one photoperiod, relative allocation fraction to starch was not changed (Pilkington et al., 2015). A similar response was also observed by (Mengin et al., 2017) as they showed that halving the duration of the light period (at a given light intensity) led to an increase of 41-61% in the fraction of assimilates allocated to starch, while halving the light intensity at a given photoperiod led to an increase of the relative partition to starch of only 7%. A higher partitioning into leaf starch was observed in different species such as corn, soybean, spinach, and sugar beet when plants were shifted from a long to a short photoperiod (Chatterton & Silvius, 1980).

Evidence of an active partitioning of C between immediate growth and storage has been also demonstrated in deciduous trees. Silpi et al. (2007) showed that, by tapping rubber trees to deplete the C reserves during the growing period (i.e., summer), the rate of C accumulation to storage increased to compensate for the depletion of the reserves caused by the latex production. They concluded that C storage appears to be an active sink that could compete with growth even in moments when growth rates are high. Similarly, although autumn is the main period for C accumulation in temperate trees, significant amounts of C were accumulated during active growth in the summer period (Barbaroux & Bréda, 2002; Landhäusser & Lieffers, 2003).

Assimilate partitioning between soluble sugars and starch at the gene and enzyme levels occur in response to sugars and is mediated by light and clock signalling (Stitt & Zeeman, n.d.). In the past, starch synthesis in leaves was explained by a simple overflow product synthesized when the rate of CO_2 fixation exceeds the rate of sucrose synthesis (see MacRae & Lunn, 2006) for detailed mechanism). Although this mechanism indeed occurs in plants, this model cannot explain how starch accumulation is regulated to guarantee an adequate supply of C at night in source-limited plants. An alternative (or complementary) mechanism is that C partitioning is programmed so that a fixed fraction of assimilates is allocated for starch synthesis. This occurs mediated by a central enzyme for starch synthesis, AGPase, which is redox-regulated by a light dependent signal leading to changes in trehalsoe-6-phosphate (T6P) levels (Kolbe et al., 2005). These changes in sucrose levels give feedback to the circadian clock, that in turn, synchronize circadian oscillators that affect the expression of the circadian genes allowing the plant to adapt to changes in daylength (Edwards et al., 2010; Feugier et al., 2013; Seki et al., 2017). Therefore, starch synthesis involves a complex interaction of regulatory mechanisms rather than only an overflow, although starch still can be synthesized via an overflow when sucrose levels are too high (Rasse & Tocquin, 2006).

Including this flexible partitioning of newly assimilated C between soluble sugars (for immediate use) and starch (for storage purposes) would be a first step towards representing the C storage pool in plants as an 'active' process. However, predicting partitioning quantitatively across different environmental fluctuations and/or across different species is still challenging. Assimilate partitioning may differ between species, according to their form of C storage (i.e., sucrose-accumulating species such as wheat and rice, starch-accumulating species such as *Arabidopsis* or tomato, or species that accumulate both such as maize or sorghum) (Liang et al., 2021). These differences can lead to alternative C balance strategies under changing environments among different species, which ultimately affects growth. For instance, Wiese-klinkenberg et al. (2010) showed that in the monocotyledon *Zea mays,* diel leaf elongation patterns followed changes in temperature. Contrary, in the dicotyledon *Nicotiana tabacum,* the effect of different temperatures is less obvious and leaf elongation followed a clear circadian oscillation. In deciduous trees, temperature play a key role in the carbohydrate metabolism, as energetic reserves are a requisite for trees to bloom. Dormant trees regulate structural C concentrations during winter through an increase in the starch synthase pathway when temperature is cold. Later on, when temperatures rise, starch synthase pathway is decreased and starch degradation pathway is promoted (Sperling et al., 2019).

2.2.2 Remobilization of storage

The second key process to explain the active regulation of storage in plants is the degradation of starch into sucrose at night, or in the long-term, the remobilization of previously stored NSC. On a diurnal basis, the starch degradation rate is set by a mechanism that sense the amount of starch in the leaves at the end of the day and anticipate the length of the night (Smith & Stitt, 2007). While the mechanisms in which the plant senses the amount of starch at the end of the day is not fully elucidated yet (although see Smith & Zeeman, 2020), there is evidence that the anticipation of the night is tightly coordinated with the circadian clock and sucrose sensing (Gibon et al., 2004, 2009; Pilkington et al., 2015; Scialdone et al., 2013). When plants are grown under very low light intensities or short daylengths, the stored starch during the day is almost completely remobilized precisely by dawn. Under these circumstances, plants can quickly adjust the rate of starch degradation to an unexpected shortening of the light period, as long as the 24h-periodicity of a diel cycle is kept. If the diel cycle is shorter or longer than 24h, the circadian clock cannot predict the change in periodicity and adjusts the rate on a 24h basis which results in incomplete or too rapid degradation (Graf et al., 2010).

An important observation here is that this 'near-to-complete' degradation of storage has been shown almost only in *Arabidopsis* plants grown under source-limiting conditions (light intensities between 90 to 170 µmol m^{-2} s^{-1}) (Gibon et al., 2004, 2009; Pilkington et al., 2015; Scialdone et al., 2013; Sulpice et al., 2014). There is very limited research done regarding starch degradation at night in plants grown at light intensities that are not limiting photosynthesis during the day. One of the few exceptions is work from Pilkington et al. (2015), where they compared starch degradation patterns between plants grown under low light intensities (140 µmol m^{-2} s^{-1}) and higher light intensities conditions (240 µmol m^{-2} s^{-1}). They concluded that under sink-limiting conditions, there is incomplete remobilization of starch at night, and that the rate of degradation of starch into sucrose can be then increased by increasing the temperature. These conclusions are very relevant for plants grown under in the field, as usually plants are exposed to higher light intensities, at least during spring and summer, or at the middle of the day. The incomplete remobilization of starch at night can lead to two situations. First, below a 'saturation' threshold, incomplete remobilization of starch can lead to a build of C reserves for plants to sudden changes C availability or sudden changes in the night temperatures. Second, the constant increase of starch content from day to day above a saturation threshold can ultimately cause feedback inhibition of starch breakdown by the sucrose signal trehalose 6-phosphate (Camara et al., 2013) and to a decrease in the expression of photosynthetic genes causing a downregulation in photosynthesis (Paul & Foyer, 2001). Both situations can have an effect at a whole-plant level and productivity.

In addition to the diurnal degradation of starch to soluble sugars in leaves to support growth, remobilization of stored NSC to the grains is maintained thorough the diurnal cycle in the grain filling stage in wheat and barley (Fisher & Gifford, 1986; Schnyder, 1993). Temporary NSC storage pools also are involved in supplying C to the grains during periods of fluctuating concurrent photosynthesis or when current photosynthesis is low at the beginning and end of the natural light period (Geiger et al., 2000).

To make progress in the prediction of diel starch remobilization in crops, it is necessary to have a better quantification of the starch usage at night under sink-limited conditions and a better quantification on the effect of temperature on the rate of degradation. Additionally, starch remobilization must be studied over a wider range of species, ideally with different metabolisms (i.e., C_3 and C_4 plants), with different life cycles (i.e., annual and perennial) and different responses to day length (short-day, neutral-day, and long-day plants). Finally, the fine limits between when do plants switch from source-limited conditions and sink-limited conditions, and when are they 'starch-saturated' is still needed.

2.2.3 Long-term accumulation and remobilization of storage

Although it is true that the circadian rhythm is in charge of the remobilization of storage on a diel basis, a remaining question is: how are NSC reserves remobilized in the longer term, for example, on a seasonal basis? C storage in other organs such as roots becomes crucial, for example in trees or in geophytes to resprout after winter (Clarke et al., 2013; Wiley et al., 2019), and in stems and other vegetative tissue in cereals (mostly as fructans) to satisfy their energy requirements during the annual life cycle (Pollock & Cairns, 1991; Pommerrenig et al., 2018). These storage pools are often considered as 'long-term' rather than a 'readily-available' storage pools because they act as sinks that store energy reserves in winter when aerial growth stops. Later, in spring, they become a source and remobilize the stored C to subsequent filling of the grain or the formation of new tillers or resprouting (Boscutti et al., 2018; Goudriaan & van Laar, 1992; Pollock & Cairns, 1991).

An interesting example that highlights the importance of seasonal C reserve pool and accumulation-depletion of NSC reserves on grasses is during the grain filling period. Two types of sources contribute with carbohydrates for grain filling: current photosynthesis but also the remobilization of NSC stored in vegetative tissue before the onset of grain filling (Serrago et al., 2013). NSC reserve pools provide the substrate needed to maintain transport and the supply of assimilates to grains during the dark period of the diurnal cycle, but also during the latter part of grain filling when growth rate of the ear is at its maximum (i.e., three weeks after anthesis) (Schnyder H., 1993). Therefore, cereals have the capacity to compensate for reductions in source-sink ratios based on the stored assimilates on the stem.

In addition to seasonal storage and remobilization of NSC, when plants are exposed to continuous environmental stress, C partitioning towards storage can increase, at the cost of the usage of C for immediate growth. For example, (Huang et al., 2018) observed that in spruce trees grown under source-limitations (120 ppm CO_2) growth and respiration was downregulated in a manner that maintained NSC concentration levels that were necessary to prevent C starvation ('operational NSC levels'). Using isotope labelling (Hartmann et al., 2015) showed that C was partitioned to storage pools independently of the net flux and even under severe C limitation. Similarly, in a study using isotope labelling, mint plants grown under low CO_2 and water deficit showed that newly assimilated C was used for monoterpenes production, a metabolite related to defence (Huang et al., 2019). These examples illustrate how in trees and herbaceous plants exposed to long-term abiotic stress, C is actively partitioned into storage and secondary metabolites at the expense of growth, which results in a reduced risk of starvation and can provide defence molecules to protect plant tissues.

From these examples we can conclude C allocation and remobilization in plants is continually changing in response to the C status of the plant, which is in turn highly dependent on the environment. In reality, most likely there are multiple C pools with different mean resident times (Dietze et al., 2014) and this represents a challenge for the characterization of the crop as a system.

2.2.4 The signalling role of carbohydrates in the regulation of plant growth

Plant growth depends largely on the availability of C as a substrate; however, carbohydrates can also drive plant growth acting as signalling molecules that interact with environmental cues that coordinate cell growth with storage and nutrient remobilization (L. Li & Sheen, 2016). For example, the conserved protein kinases SnRK1 (Snf1-related protein kinase 1) and TOR (target of rapamycin) are energy/sugar sensing molecules that have an essential role in the regulation of metabolism and gene expression of plants under unfavourable environmental conditions (Margalha et al., 2019; Rodriguez et al., 2019). SnRK1 is activated in response to declining energy supplies (e.g., unexpected darkness or extended night, herbicide feeding or hypoxia) (Baena-González et al., 2007) triggering the activation of catabolism and repressing energy-consuming anabolic processes and growth (Baena-González & Hanson, 2017). An increase in the levels of sucrose (Suc) increases the signalling sugar trehalose-6-phosphate (T6P) inhibiting the activity of SnRK1, therefore stimulating growth of cells and their metabolic activity (Lawlor & Paul, 2014; Nunes et al., 2013; Zhang et al., 2009). Conversely, TOR kinase is activated in favourable energy conditions (e.g. by light, sugars and inorganic nutrients) to promote growth and downregulated under stress conditions that restrict sugar availability (Rodriguez et al., 2019). Thus, plant energy/sugar also influences plant growth via activation or repression of SnRK1/TOR.

Growth depends also in the rate of protein synthesis, which occurs in the ribosomes (Lastdrager et al., 2014). It has been shown that ribosome abundance does not change between different photoperiods, but rather the plant optimizes for a better distribution of protein synthesis over a 24-hour cycle (Sulpice et al., 2014). This has an impact in the distribution of growth (as cell expansion) between day and night.

2.3 Modelling the C pool under light and temperature fluctuations: should an active C storage pool be included?

Quantifying changes in the C storage pool in response to light and temperature fluctuations at a whole-plant level can be challenging due to the complexity of the interactions between circadian signals, environmental cues, and metabolic signals. There is also complexity because light primarily affects source activity, while temperature primarily affect sink activity (Fatichi et al., 2014). Plants use most of the newly assimilated C for growth and respiration. However, under environmental stress, recently fixed C is allocated towards reserve formation at the cost of short-term growth (Dietze et al., 2014; Gessler & Grossiord, 2019; J. Huang et al., 2019; Mengin et al., 2017) . This entails complex feedback in which plants sense C storage level and according to day length and C status, plants induce changes in the partitioning and use of C, which in the end affects the growth pattern of the plant. Unravelling these dynamics requires a modelling approach that can accurately describe C storage metabolism and link it to plant growth.

There are still knowledge gaps that represent a challenge for model development. For example, it is still unclear what the metabolic costs of C storage are, which fraction of newly fixed C is partitioned to storage and which fraction is immediately used, what is the sink strength of C storage itself and implications of C storage over a long-term for herbaceous species or fruiting crops. In this section, we briefly review the way in which C storage is currently included in crop growth models and we discuss the role of the C storage pool affecting the response of the modelled system.

2.3.1 Approaches to simulate a dynamic storage C pool

Most crop production models are driven by the effect of shoot environment on gross photosynthesis and respiration over a day (Poorter et al., 2013). Growth over time is modelled as the net result of daily C input from gross photosynthesis minus C loss in respiration. However, this approach overlooks that in moments when supply exceeds demand, C should be temporarily stored. A more accurate analysis of gains and losses of C over the diel cycle should consider the asynchrony between the timing of acquisition of C and of the utilization of C for growth and respiration. At each time step, all C input from photosynthesis is directly placed in a temporary storage pool (NSC) and partitioned among different pools based on allometry, functional equilibrium or relative sink strengths of the plant organs (Marcelis et al., 1998). Allocation to storage occurs only if there is an excess of C from supply compared to

demand. Although these growth models have been developed a long time ago (e.g. (Goudriaan & van Laar, 1992; Marcelis et al., 1998; Thornley, 1976) they are still commonly used to model C source-sink relations (e.g. Cerasuolo et al., 2016; Gu et al., 2018; Schapendonk et al., 1998; Seginer & Gent, 2014; Vanthoor et al., 2011) The following three examples illustrate how a dynamic C storage pool was included in growth models. In each example, the storage pool is defined using different approaches.

In the first example, (Da Silva et al., 2014) updated the L-PEACH model to simulate annual long-term carbohydrate storage and mobilization. They modelled the sink strength of storage as a function of the total non-structural carbohydrate content. Storage sink strength was 0 as long as non-structural carbohydrate were below the minimum value. Then, storage sink strength increased along a logistic curve to reach 1 (so maximum sink strength capacity) when non-structural carbohydrate levels reached the maxim level. In this way, storage sink strength depended on the local carbohydrate conditions, and thus, non-structural carbohydrate concentration patterns appeared as a emergent property of the model. This approach requires the storage sink strength and the maximum carbohydrate available for remobilization to be experimentally determined. (Da Silva et al., 2014) determined the potential storage sink strength from the mean maximum trunk non-structural carbohydrate mass fractions. The carbohydrate storage source available for remobilization was estimated from the difference between the maximum mass fraction of carbohydrates in the sapwood and the minimum mass fraction under 'healthy' conditions (no water stress, severe pruning, or disease). With this approach, annual carbohydrate storage behaviour in trees was simulated accurately.

In a second example, (Jing et al., 2020) used a crop growth model to systematically analyse the response of perennial alfalfa under fluctuating environmental conditions and to evaluate potential adaptation options. In their model, C remobilization from storage organs to sinks was included as a function of non-structural carbohydrate content, nitrogen content and the residual leaf area after harvest in perennial forage. Mobilization was accelerated under low LAI until plants had sufficient leaves for maximum photosynthesis; only until then, C starts accumulating again.

In the third example, starch accumulation in wheat grains was modelled by focusing on the variations of plant C dynamics between pre- and post-anthesis stages. Assimilates for starch synthesis during grain filling can be obtained via remobilization of stored C in vegetative tissues during pre-anthesis stage or from ongoing photosynthesis (Schnyder, 1993). Pan et al. (2007) modelled the NSC dynamics by separating the C source between an instant pool (i.e., instantaneous translocation of

assimilates to wheat grains), and a long-term storage pool (i.e., remobilization of pre-stored C reserves). The remobilization the stored NSC was influenced by temperature, water, and nitrogen conditions. Additionally, they included a genetic parameter to describe the difference in starch synthesis ability among cultivars. This model was particularly useful to quantify grain starch concentration and starch yield of wheat under various growing conditions

2.3.2 Sucrose-starch dynamic models

As C storage ultimately depends on the rates of synthesis and degradation of starch, one way forward is to include the biochemical regulation of sugar-starch dynamics in growth models. Starch degradation has been described by two different models: arithmetic division (AD) and retrograde metabolic signalling models (RMS) (A. M. Smith & Zeeman, 2020). The AD model accounts for the rapid adjustment of the degradation rate to unexpected changes in the length of the night. In this model, the plant senses starch content and time until dawn and sets a rate of starch degradation that will deplete reserves at dawn (Scialdone et al., 2013). The RMS model assumes that a plant needs to maintain C homeostasis. The plant regulates the expression of the circadian clock genes via sugar signalling and adjusts the phase of the clock accordingly (Feugier et al., 2013; Seki et al., 2017; Webb et al., 2019). The main difference between these two models is that the RMS model accounts for mechanisms that control an integrated response between starch synthesis and degradation so that sugar homeostasis is maintained while the AD model simply sense starch content and time remaining until dawn.

There are a few models simulating crop growth that include sucrose synthesis and starch degradation. For example, (Rasse & Tocquin, 2006) used single rate modification of starch synthesis and breakdown in leaves to predict different growth patterns between wild-type and mutants of *Arabidopsis* at a high CO_2 concentration. Flis *et al.,* (2015) adopted a more complex approach by using integrated multiscale models that link gene expression dynamics, C partitioning to organ growth and development in response to environmental signals. In their model however, starch mobilization was underestimated in long-photoperiods. This might be attributed to the fact that in this case the plants were probably sink-limited (Poorter et al., 2013). Another limitation is that in both crop growth models (Flis et al., 2015; Rasse & Tocquin, 2006) a fixed ratio between sucrose synthesis and starch accumulation was assumed. This ratio was empirically parameterized based on measurements in controlled growth conditions. A fixed ratio between sucrose synthesis and starch accumulation assumes that different day lengths have no effect on C partitioning, which prevents the model to adapt to changes in daylength.

2.3.3 Simulating the effect of temperature and light fluctuations on growth

A pitfall in crop growth models to predict growth in a fluctuating environment is that they are mostly source driven (Marcelis et al., 1998), meaning that photosynthesis is the rate controlling factor for plant growth. Not surprisingly, the Calvin Benson cycle has been the most intensively modelled biochemical process. The development of a well calibrated and complete biochemical mathematical description of photosynthesis at leaf level has made it possible to obtain accurate predictions of photosynthesis under a wide range of conditions (Yin & Struik, 2009). A source-driven approach seems logical in highly controlled environments where no water, temperature or nutrient limitations occur. However, growth can also be limited by sink activity, for example at low temperature or high CO_2 concentrations. In these cases, there is a restriction in growth together with an accumulation of C (Körner, 2015).

Another limitation to accurately predict growth rate diurnally or in the short term (hourly) is that many plant growth models restrict growth only to the light periods and do not include knowledge on how C is used for metabolism and growth at night (e.g. (Henten, 1994a; Thornley, 1976; Vanthoor et al., 2011).When the C pool has no distinction between sucrose and starch, it is assumed that all carbohydrates are used immediately for daytime growth, or in case of an excess, stored transiently for the next light period. However, during the dark period, C is still being used for maintenance respiration and if the C pool is empty at the end of the light period (due to source-limited conditions), this can virtually lead to 'negative' growth at night. This raises two issues, first that without the distinction between sucrose and starch pools, it is unlikely to reproduce the critical mechanisms that drive the C cycle on an hourly basis. Second, it prevents understanding the effect of environmental fluctuations on growth in the day separately from the night. For example, if the goal is to study the effect of night temperature on night growth, with current models it is only possible to interpret the results as the effect of an average daily temperature or a temperature difference, rather than the effect of the night temperature itself on growth. Contrary, it the interest is only on the dynamics over a whole-day basis, the diurnal dynamics between soluble sugars and starch become less relevant.

2.3.4 Modelling growth with or without a C pool

In order to illustrate our argument that modelled growth patterns will be more realistic by including a C storage with the concepts discussed in the previous sections, we compared three models that differ only in the inclusion of a C pool. The first model features a static C allocation scheme and has no C storage pool. At each time-step, a

fixed proportion of the current assimilates is immediately lost through respiration and the remainder is allocated to growth (see Appendix A-Eq. A2.1).

In the second model (see Appendix B-Eq. A2.9, A2.10), C is first allocated to a dynamic storage pool from which it may be allocated to structural growth. The storage pool builds up when current assimilate production is greater than C allocation to respiration and structural growth and is depleted when the production of assimilates is smaller. This model divides respiration into growth and maintenance components. Growth respiration is proportional to structural growth and maintenance respiration is temperature-sensitive and proportional to biomass. In this model, relative growth rate (Eq. A2.12) depends on the concentration of NSC (Thornley & Hurd, 1974).

In the third model (See Appendix C-Eq. A2.15, A2.16, A2.17) there are two C pools: one for soluble sugars and one for starch. All assimilates produced by photosynthesis are partitioned between starch and soluble sugars depending on the photoperiod (Mengin et al., 2017; Pilkington et al., 2015). All assimilates allocated to the soluble sugar pool are used for structural growth and respiration. During the day the starch pool builds up and it is not used. During the night, the accumulated starch is degraded into soluble sugars at a constant rate according to the length of the night (Scialdone et al., 2013) until it is almost depleted at the end of the night (Gibon et al., 2004; Graf et al., 2010b). To avoid size-induced differences, in the models we considered a fixed crop size of 200 g m^{-2} and a leaf area index of 3. We compared the accumulated structural growth between the three models and the dynamics of the pools (when a pool is present). Detailed information about the models is provided in Appendix A, B and C.

As outlined in section 2, changes in light and temperature lead to temporal asynchronies between C supply by photosynthesis and C demand for growth. The source-sink ratio can be manipulated by light and temperature conditions. Following this logic, we initialize our simulation assuming a balanced source-sink ratio for 10 days (therefore, there is no accumulation or remobilization of C during this period) (Figure 2.1a). After 10 days, as light intensity increases and temperature decreases, the C supply is bigger than the demand, and the NSC pool starts building up in both models that include a C storage pool (Figure 2.1a). A similar dynamic pattern of the NSC has been observed previously under similar environmental conditions (Klopotek & Kläring, 2014). The main difference between the three models is that during this period of ‘accumulation’, the models with a C pool partitioned recently fixed C towards storage formation at the cost of short-term growth of structural mass (Figure 2.1a, b), compared to the model without C pool that has a higher growth because all assimilates are immediately used for growth. In both models with storage the stored

C is used later to give a higher growth rate for a few days once C-supply becomes more limiting (Figure 2.1c), (a high temperature and a low light intensity, from day 20 to 30). In the end, the accumulation of total dry weight (Figure 2.1d) (the sum of non-structural C and structural mass) is the same for the three models because C input from photosynthesis and loss by respiration is the same for all models.

In the present example, we illustrate that the inclusion of a dynamic C pool in growth models offers a more realistic representation of C allocation in abiotic stress conditions (for example, a higher allocation to storage during sink-limited conditions), and a more realistic effect on the growth patterns. This in principle can allow us to test hypotheses and different combinations of environmental conditions. The third model, which is built up on concepts discussed in this paper, represents in a very basic way the result of complex enzymatic interplay. This model approach provides a basis for further development and offers possibilities for targeted experimental studies on the rates of accumulation and depletion of C and their dependence on temperature. Subsequently, model-based studies may help us to understand the effect of temporal surplus of C on the specific growth rate of organs, which is a difficult task. We believe that this simple example highlights the potential effects of including these biochemical fine-tuning mechanisms on plants.

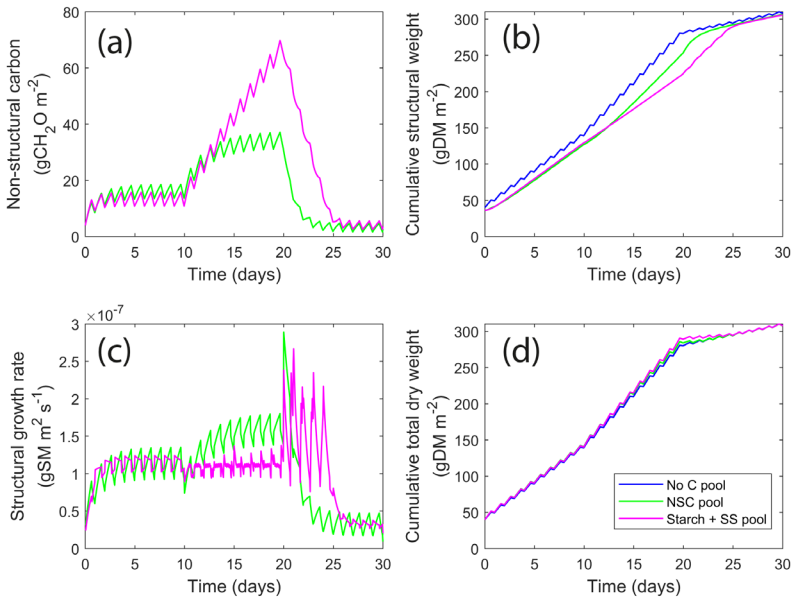

Figure 2.1. *Simulated (a) non-structural carbon (soluble sugars + starch), (b) cumulative structural mass, (c) structural growth rate and (d) cumulative total dry weight. Simulations were done using three models. Blue lines are simulations using a model with no C pool (Appendix A-Eq.* A2.1*). Green line are simulations using a model with only one common non-structural carbon pool (Appendix B-Eq.* A2.9, A2.10 *) and pink line is the model with separate soluble sugar and starch pool (Appendix C-Eq.* A2.15, A2.16, A2.17*). The environmental conditions used were: first 10 days 22 °C and 300 µmol m−2 s−1, from Day 10 to 20 average daily temperature of 15 °C and light intensity of 400 µmol* m^{-2} s^{-1} *and from Day 20 to 30 average daily temperature of 28 °C and light intensity of 200 µmol* m^{-2} s^{-1}*. The photoperiod was 16 h.*

2.4 Outlook

Here we identify four major knowledge gaps and propose concrete steps that can advance understanding of the regulation of C storage in plants. Filling these gaps would allow modelling these processes more accurately and to quantify growth of plants in environments with fluctuating light and temperature.

First, crop growth models should explicitly include a physiology-based dynamic C storage pool (Figure 2.2). This knowledge gap can be addressed by coupling biochemical models describing soluble sugars and starch metabolism e.g., (Millar et al., 2014; Nagele et al., 2010; Scialdone et al., 2013; Seki et al., 2017) to

plant growth models (e.g., Flis et al., 2015; Rasse & Tocquin, 2006). Primary C metabolism is highly influenced by temperature (Pilkington et al., 2015; Pyl et al., 2012), light and clock signalling (Scialdone et al., 2013) and these environmental factors affect C accumulation and remobilization differently. Including separated starch and sucrose pools can increase the resolution and robustness of crop growth models, specifically if the aim is to predict growth responses in short-time scales (within a day) or diurnally. This would allow testing specific hypotheses over a wider range of fluctuations; for example, the effect of alternating day lengths, extremes temperatures, or different day-night temperatures on growth and the C balance of the plant.

Second, detailed analysis of the relationship between C storage and growth across different species is needed. So far, diel starch turnover and its relationship with biomass has almost exclusively been investigated in *Arabidopsis* (Dietze et al., 2014; Stitt & Zeeman, 2012). However, it is relevant to question if the information gained from this model species is fully applicable to crops (Wiese-klinkenberg et al., 2010). For example, starch-less *Lotus japonicus*, did grow well in a 12-h photoperiod (Welham et al., 2010) whereas starch-less *Arabidopsis* showed a reduced growth (Rasse & Tocquin, 2006). Furthermore, Wiese-klinkenberg et al. (2010) showed differences in diel (24h) leaf growth between dicot and monocot plants, which points to differences in resource allocation strategies. In addition, the competition for C between an 'active' storage and other sinks change strongly according to the phenology of the plant (Li et al., 2015). Fruits are strong sinks that compete with C storage; therefore, a relevant question would be if the fruit 'active' competition for C affects the fine tuning of the diel sucrose-starch dynamics. These studies are important, especially if the goal would be to optimize resource use in crop production in an agricultural context.

Third, how is the information gained from diel starch turnover useful to predict C storage and acclimation of growth over a long-term? Biochemical models describing starch-sucrose dynamics address acclimation of sucrose-starch partitioning and degradation to a change in photoperiods and changing temperature (Seki et al., 2017). However, the consequences at a whole-plant level over longer term environmental fluctuations (e.g., over weeks or months) are still missing. To address this, better reference data for model evaluation at a whole plant level is needed, and these data set should include C assimilation (gas exchange measurements), quantification of primary metabolites, and growth rates. Additionally, conducting experiments with long-term temperature and light fluctuations would provide valuable information on longer term mechanisms of C storage and the consequences on growth.

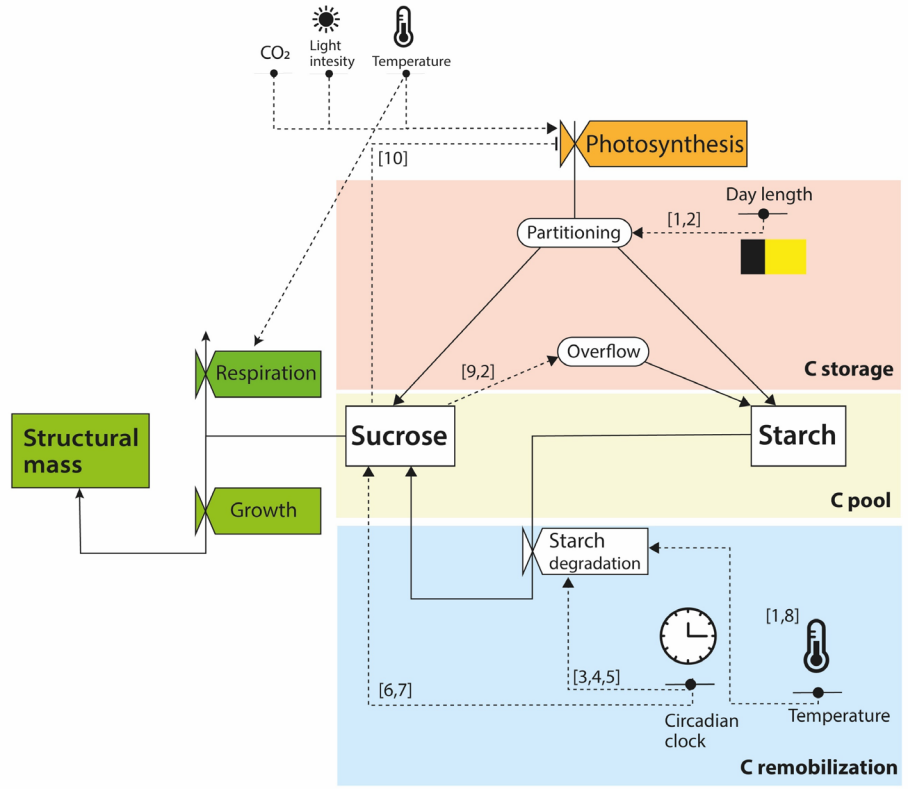

Figure 2.2. *Schematic diagram of the model of how the C pool is influenced by day length, circadian clock, and temperature. Partitioning to sucrose or starch is expressed as the proportion of fixed C that is accumulated during the light period. Starch degradation to sucrose at night is dependent on the circadian clock and is paced so that almost all starch is exhausted by dawn in source-limited conditions. Starch degradation at night can be influenced by temperature. Sucrose levels in both conditions (either source-limited or sink-limited) feedback to circadian clock to dynamically regulate the phase of the circadian oscillator. In sink-limited conditions there is less partitioning to starch. Feedback regulation decreases sucrose synthesis and triggers starch synthesis when sucrose accumulates on the leaf (overflow). Feedback downregulation of photosynthesis occurs when there is an excess accumulation of sucrose in the leaf. In sink-limited conditions not all the starch is completely remobilized at dawn and high temperature can accelerate the rate of starch degradation. Rectangles indicate states, valves indicate rates, solid lines indicate mass flows and dotted lines indicate flow of information. Numbers indicate references in support of the model as follows: [1]* (Pilkington et al., 2015)*; [2]* (Mengin et al., 2017)*; [3]* (Gibon et al., 2004)*; [4]* (Scialdone et al., 2013)*; [5]* (Graf et al., 2010a)*; [6] (Feugier & Satake, 2014); [7]* (Seki et al., 2017)*; [8] (Muller & Martre, 2019); [9]* (Horton, 1985)*; [10] (Paul & Foyer, 2001).*

Finally, if the goal is to increase productivity of crop plants while making a more efficient use of resources (e.g., water, nutrients, supplemental light, CO_2) a multiscale approach linking C-metabolism at cell level with whole-plant growth is needed. By using isotope labelling techniques, metabolic network fluxes can be estimated and incorporated into a model that would allow simulation of the effects of a dynamic environment on C metabolism in plants and plant growth (Sweetlove et al., 2017) or to determine differences between 'readily available' and long-term pools. A fundamental challenge in multiscale prediction is that the model becomes more complex when moving across molecular or biochemical scales to whole organisms due to the different timescale and finer granularity of the processes Hammer et al.,2004). This leads to difficulties related to parameter identification or computational time for optimization (Hammer et al., 2019). To successfully bridge across levels, the biochemical process (in this case the starch-sucrose dynamics) must have robust and quantitative measures of physiological responses. A balance between process details and predictability of the system in scales that are feasible to measure must also be achieved (Peng et al., 2020). A multiscale model that operates effectively across the biochemistry level and whole plant level would provide an important tool to rapidly assess different manipulation in the C partitioning or C storage and to explore different strategies for the control of the environmental conditions in which plants are growing.

2.5 Conclusions

The efficient management of C storage is essential for plant growth to be optimized, especially under fluctuating environmental conditions. As conducting experiments with many different light levels and temperatures is often not feasible, crop modelling can be used as a tool for hypothesis testing and scenario analysis under varied environmental conditions. To achieve this, crop growth models must extend beyond current scales and include a finer detail in essential processes like C storage and C usage and remobilization. Including separated starch and sucrose pools to represent an 'active' pool in growth models can increase the level of detail and robustness of the models. This is essential for predicting growth response on short-time scale in ever-fluctuating environments. Scenario-based model simulations can potentially guide manipulation and improvement of C allocation strategies (trade-off between C storage and other sinks) and can help to explore opportunities to optimize crop performance under temporal unfavourable environmental conditions and thus for developing more resource efficient crop-production systems.

2.6 Acknowledgements

The authors would like to thank the editor and anonymous reviewers for helpful remarks that greatly improved this manuscript. Also, thanks to Silvere Vialet-Chabrand and David Katzin for providing valuable feedback on earlier versions of the manuscript. Further thanks to Simon van Mourik for his help with the modelling work.

2.7 Appendices

2.7.1 Appendix A: Model 1: No C pool

The general structure of the model for calculating dry matter production is based on (Spitters et al., 1987a). Daily dry matter production is calculated according to:

$$\frac{dW}{dt} = c_\beta\left(c_\alpha \phi_{phot} - \phi_{resp}\right) \qquad A2.1$$

In which $\frac{dW}{dt}$ is the crop growth rate (kg DM m^{-2} s^{-1}), c_β is the conversion efficiency from assimilates to dry matter, ϕ_{phot} is the gross canopy photosynthesis rate (kg CO_2 m^{-2} s^{-1}) and c_α is the conversion factor from carbon dioxide into sugar equivalents ($kgCH_2O$ $kgCO_2^{-1}$). Gross canopy photosynthesis is calculated in accordance with the following empirical relation:

$$\phi_{phot} = \phi_{phot,max}(1 - e^{-c_k LAI}) \qquad A2.2$$

Where $\phi_{phot,max}$ is the response of canopy photosynthesis (kg CO_2 m^{-2}) response to the incident radiation and carbon dioxide concentration. This model account for photorespiration and temperature effects on the light use efficiency as well as temperature effects on the carboxylation conductance in the leaf:

$$\phi_{phot,max} = \frac{\epsilon U_i \sigma_{co_2}(U_c - \Gamma)}{\epsilon U_i + \sigma_{co_2}(U_c - \Gamma)} \qquad A2.3$$

in which ϵ (kg J^{-1}) is the light use efficiency, U_i (W m^{-1}) is the incident radiation, σ_{CO_2} (m s^{-1}) is the canopy conductance for carbon dioxide transport into the leaves, U_C (kg m^{-3}) is the carbon dioxide concentration and Γ (kg m^{-3}) is the carbon dioxide compensation point which accounts for photorespiration at high light levels.

The carbon dioxide compensation point Γ, (kg m^{-3}) is a function of temperature, U_T (◦C), described by:

$$\Gamma = c_\Gamma c_{q10,\Gamma}^{\frac{U_T - 20}{10}} \qquad A2.4$$

in which c_Γ (kg m^{-3}) is the carbon dioxide compensation point at 20°C. The temperature effects on Γ are accounted for by the Q10 factor $c_{Q10,\Gamma}$.

The effect of photorespiration on the light use efficiency ($kgCO_2$ J^{-1}) is described by:

$$\epsilon = c_\epsilon \frac{U_c - \Gamma}{U_c + 2\Gamma} \qquad A2.5$$

in which c_ϵ [kgCO$_2$ J^{-1}] is the light use efficiency at very high dioxide concentrations (Goudriaan et al., 1985).

The canopy conductance σ_{CO_2} [m s^{-1}] for carbon dioxide transport from the ambient air to chloroplast is determined by three series conductance

$$\frac{1}{\sigma_{co_2}} = \frac{1}{c_{bnd}} + \frac{1}{c_{stem}} + \frac{1}{\sigma_{car}} \qquad A2.6$$

where c_{bnd}, c_{stem} and σ_{car} (m s^{-1}) are the boundary layer conductance, the stomatal conductance, and the carboxylation conductance, respectively. The boundary layer and the stomatal conductance are assumed to be constant. The carboxylation conductance is described with by

$$\sigma_{car} = c_{car,1}{U_T}^2 + c_{car,2}U_T + c_{car,3} \qquad A2.7$$

for a temperature between 5°C and 40 °C, with the parameters $c_{car,1}$ (m s^{-1} °C^{-2}), $c_{car,2}$ (m s^{-1} ◦C^{-1}) and $c_{car,3}$ (m s^{-1}).

Maintenance respiration of the crop $\phi_{mainResp}$, (kgCH$_2$O m^{-2}) is described by

$$\phi_{mainResp} = c_{resp}X_s c_{Q10,resp}^{\left(\frac{U_T-25}{10}\right)} \qquad A2.8$$

where c_{resp} is the maintenance respiration rate for the shoot 25°C (kg CH$_2$O kgDM^{-1} s^{-1}) and $c_{Q10,resp}$ is the Q10 factor of the maintenance respiration.

2.7.2 Appendix B: Model 2, with only a NSC pool

The model divides the plant material into two state variables: non-structural dry weight (X_n, kgCH$_2$O m^{-2}) and structural dry weight (X_s, kgCH$_2$O m^{-2}), therefore total dry weight is $X_n + X_s$. Non-structural mass refers to sugars such as glucose, fructose and starch. Structural dry weight refers to structural components such as cell walls and cytoplasm. The dynamic model (eq. A2.9 and A2.10) is described by:

$$\frac{dX_n}{dt} = c_\alpha\phi_{phot} - \phi_{structGrowth} - \phi_{mainResp} - \phi_{growthResp} \qquad A2.9$$

$$\frac{dX_s}{dt} = \phi_{structGrowth} \qquad A2.10$$

where ϕ_{phot} (kgCO$_2$ m^{-2}) is the gross carbon dioxide uptake rate due to canopy photosynthesis and is calculated according to eq. A2.2 and A2.3, $\phi_{structGrowth}$

($kgCH_2O\ m^{-2}$) is the rate in which non-structural carbohydrates are being used for growth of the structural dry weight, $\phi_{mainResp}$ ($kgCH_2O\ m^{-2}$) is the maintenance respiration rate calculated according to eq. A2.8 and $\phi_{growthResp}$ ($kgCH_2O\ m^{-2}$) is the respiratory losses associated with growth.

Structural growth rate is calculated as

$$\phi_{structGrowth} = r_{gr} X_s \qquad A2.11$$

where the specific growth rate coefficient r_{gr} (s^{-1}) describes the transformation of non-structural carbohydrates to structural dry weight. It is assumed that the rate of utilization non-structural carbohydrates for the construction of structural material depends on the of NSC concentration in the plant tissue, following a Michaelis-Menten relation (Thornley & Hurd, 1976a) . The transformation of non-structural carbohydrates into structural material is also dependent on temperature. Therefore r_{gr} is calculated as

$$r_{gr} = c_{r,gr,max} \left(\frac{X_n}{X_s + X_n} \right) c_{Q10,gr}{}^{\frac{U_T - 20}{10}} \qquad A2.12$$

where $c_{r,gr,max}$ (s^{-1}) is the saturation growth rate at 20 ◦ and $c_{Q10,gr}$ (-) is the Q10 factor for growth.

Respiratory losses associated with growth ($\phi_{growthResp}$, $kgCH_2O\ m^{-2}\ s^{-1}$) are calculated as

$$\phi_{growthResp} = \frac{1 - c_\beta}{c_\beta} \phi_{structGrowth} \qquad A2.13$$

where c_β is a yield factor that accounts for respiratory and synthesis losses during the conversion of carbohydrates to structural material.

From eq. A2.9A2.9 A2.9 and A2.10 we can also describe other variables related to the state of the crop, for example, total crop dry weight (TDW, $kg\ m^{-2}$) is related to both states according to the relation:

$$TDW = X_n + X_s \qquad A2.14$$

2.7.3 Appendix C: Model 3, with a soluble sugar, starch and structural mass pool

This model has essentially the same structure as model 2, however, in this model X_n is divided into two pools: soluble sugars (X_{sol}, kgCH₂O m⁻²), and starch (X_{starch}, kgCH₂O m⁻²). The dynamic model (eq. A2.15, A2.16 and A2.17) is described by:

$$\frac{dX_{sol}}{dt} = a_1 + p_1\phi_{phot} - \phi_{structGrowth} - (1 - a_2)\phi_{mainResp} - \phi_{growthResp} \quad A2.15$$

$$\frac{dX_{starch}}{dt} = -a_1 + (1 - p_1)\phi_{phot} \quad A2.16$$

$$\frac{dX_s}{dt} = \phi_{structGrowth} - a_2\phi_{mainResp}. \quad A2.17$$

Where parameter a_1 denotes the degradation of starch into soluble sugars during the night, p_1 is the partition of assimilates, between soluble sugars and start during the day, ϕ_{phot} (kgCO₂ m⁻²) is the gross carbon dioxide uptake rate due to canopy photosynthesis and is calculated according to eq. A2.2 and A2.3, $\phi_{structGrowth}$ (kgCH₂O m⁻²) is the rate in which non-structural carbohydrates are being used for growth of the structural dry weight and is calculated according to eq. A2.11 and A2.12, $\phi_{mainResp}$ (kgCH₂O m⁻²) is the maintenance respiration rate calculated according to eq. A2.8 and $\phi_{growthResp}$ (kgCH₂O m⁻²) is the respiratory losses associated with growth calculated according to eq. A2.13.

The degradation of starch into soluble sugars during the night a_1 is based on literature and is described by:

$$a_1 = \frac{X^*_{sol}}{(24 - L_{light})3600} \quad A2.18$$

Here X^*_{sol} denotes the soluble sugar level at the end of the light period each day, and L_{light} (hours) denotes the length of the light period in a 24-hour day. The number 3600 is a conversion factor, from hours to seconds. The denominator equals the length of the dark period in a day. With this degradation rate, the starch level will be zero at the end of the night in case the degradation is not inhibited. Parameter a_2 denotes the rate of autophagy, in case there is not enough soluble sugar to satisfy the need of maintenance respiration:

$$a_2 = \mathbb{I}\_(X_{sol} < X_{sol,min}) \quad A2.19$$

Where $X_{sol,min} = 0.03X_s$ is the minimum level of soluble sugar before autophagy sets in.

Parameter p_1 denotes the partitioning of assimilates between soluble sugars and starch according to:

$$p_1 = \frac{L_{light}}{24} \qquad A2.20$$

Which means that a longer light period results in more partitioning of assimilates towards soluble sugars. Furthermore, when soluble sugar levels are too high ($X_{sol} > X_{sol,max}$), photosynthesis is inhibited (to 90% of the original rate) , assimilates are all partitioned to starch, and starch degradation is stopped:

$$\begin{aligned} &if\ X_{sol} > X_{sol,max} \\ &\quad \phi_{phot} = 0.9\phi_{phot} \\ &\quad p_1 = 0 \\ &\quad a_1 = 0 \end{aligned} \qquad A2.21$$

Non-structural carbohydrate dynamics and growth in tomato plants grown at fluctuating light and temperature

Ana Cristina Zepeda, Ep Heuvelink, Leo F.M. Marcelis

Published in Frontiers in Plant Science (2022), 13
DOI: https://doi.org/10.3389/fpls.2022.968881

Chapter 3

Abstract

Fluctuations in light intensity and temperature lead to periods of asynchrony between carbon (C) supply by photosynthesis and C demand by the plant organs. Storage and remobilization of non-structural carbohydrates (NSC) are important processes that allow plants to buffer these fluctuations. We aimed to test the hypothesis that C storage and remobilization can buffer the effects of temperature and light fluctuations on growth of tomato plants. Tomato plants were grown at temperature amplitudes of 3 °C or 10 °C (deviation around the mean of 22°C) combined with integration periods of 2 or 10 days. Temperature and light were applied in Phase (high temperature simultaneously with high light intensity, (400 µmol m^{-2} s^{-1}), low temperature simultaneously with low light intensity (200 µmol m^{-2} s^{-1}) or in Antiphase (high temperature with low light intensity, low temperature with high light intensity). A control treatment with constant temperature (22 °C) and a constant light intensity (300 µmol m^{-2} s^{-1}) was also applied. After 20 days all treatments had received the same temperature and light integral. Differences in final structural dry weight were relatively small, while NSC concentrations were highly dynamic and followed changes of light and temperature (a positive correlation with decreasing temperature and increasing light intensity). High temperature and low light intensity lead to depletion of the NSC pool, but NSC level never dropped below 8% of the plant weight and this fraction was not mobilizable. Our results suggest that growing plants under fluctuating conditions do not necessarily have detrimental effects on plant growth and may improve biomass production in plants. These findings highlight the importance in the NSC pool dynamics to buffer fluctuations of light and temperature on plant structural growth.

3.1 Introduction

In a natural environment, plants are exposed to strong fluctuations in light intensity and temperature which lead to periods of asynchrony between carbon (C) supply by photosynthesis and C demand by the plant organs (Palacio et al., 2014). The storage and remobilization of non-structural carbohydrates (NSC) are important processes that allow plants to buffer these fluctuations. Plants distribute recently assimilated C by the leaves (sources) into various C sinks such as growth, metabolic maintenance, storage and defence (Chapin et al., 1990). In many plant species, NSC are accumulated as soluble sugars and starch (Martínez-Vilalta et al., 2016) when the net production of carbohydrates exceeds the demand and growth is limited by assimilate usage (Palacio et al., 2014). The remobilization of stored C compounds is fundamental for plants to support growth and metabolism during periods of limited C supply (Chuste et al., 2020; Dietze et al., 2014), for example at higher latitudes in winter when short light periods and low light intensity are typical (Bours, 2014) or in perennial plants when there are no leaves that can do photosynthesis. Remobilization can occur across time scales: from diurnal (day-night) (Graf et al., 2010a; Smith & Stitt, 2007), over day-to-day (influenced by the weather on that specific day), up to seasonal remobilization (Furze et al., 2018). Despite the central role of storage and remobilization of C in response to fluctuations in light and temperature, plant responses to repeated changes in the C supply and demand, generated, for example, by repeatedly changing the light intensity or growth temperature are largely unknown.

On a time scale of weeks, plants can adjust rates of respiration (Atkin & Tjoelker, 2003a) or photosynthesis (Yamori et al., 2014) to compensate for changes in temperature or light environment through an adjustment in physiology, structure or biochemistry of the leaves (N. G. Smith & Dukes, 2013). These acclimation responses have been extensively studied, usually by growing plants at specific temperatures or light conditions and then exposing those plants to a new growth condition for several days. Under excess light and low temperatures, accumulation of NSC (mainly as starch and soluble sugars) is typical as an acclimation response in the long term (days) (Pommerrenig et al., 2018; Ruelland et al., 2009; Thalmann & Santelia, 2017). Lower temperatures also have an immediate effect on enzymatic activity which leads to a reduction in photosynthetic capacity (Huner et al., 1993; Ruelland et al., 2009) and respiration (Atkin & Tjoelker, 2003). Higher light levels may result in an increased accumulation of carbohydrates in the leaves, causing decreased expression of photosynthetic genes that lead to a downregulation in photosynthesis (Paul & Foyer, 2001b). At low light intensities, the net production of assimilates is less than the net demand of assimilates, making that plant growth is limited by C supply (A. M. Smith

& Stitt, 2007). If low light intensities coincide with higher temperatures, this may lead to a depletion of the NSC pool because of the increased energy requirements for respiration and growth (conversion into structural C) (Atkin & Tjoelker, 2003). So, while the effects of prolonged high supply or low demand of C on plant growth and development are well established, we know little of how much of the accumulated NSC pool is available for remobilization once the plants face more favourable environmental conditions and at what time scales accumulation and remobilization do occur (Dietze et al., 2014; Furze et al., 2018; Wiley et al., 2019). A change from warm to cool conditions and vice versa showed that tomato plants grown at low temperatures increased the NSC concentration over a week and then almost completely remobilized within 12 h exposure to warm temperatures (Klopotek & Kläring, 2014). Besides, the effect of dynamic light and temperature fluctuations at a scale of 1 to 2 days on the dynamic response of processes such as growth and storage are still largely unexplored.

Although C has a central role in plants, our understanding of its daily dynamics of storage and remobilization under short term (days) and long term (weeks) climate fluctuations is still limited. A quantitative understanding of C storage and remobilization is essential in order to explain plant responses to temporal suboptimal climate conditions. The overall aim of this paper was to evaluate how plants accumulate and remobilize C in response to short term (every other day) and long-term (every 10 days) temperature and light fluctuations and how these fluctuations affect growth and morphology. Plants can store carbohydrates under conditions where growth is demand-limited, and later on remobilize this C when temperature rises up to a certain limit. Consequently, we hypothesize that this C storage and remobilisation buffers the effects of temperature and light fluctuations on growth of tomato plants.

3.2 Materials and Methods

3.2.1 Plant materials and growth conditions

Tomato (*Solanum lycopersicum* 'Moneymaker') seeds were sown on stonewool plugs in a climate cabinet at 22 ◦C, relative humidity 70% and 200 µmol m^{-2} s^{-1} 16 h photoperiod. After 15 days, seedlings were transplanted to (7x7cm) stonewool cubes (Rockwool Grodan, Roermond, the Netherlands) and distributed over three climate cabinets with the same climate conditions as mentioned above. The growth surface of each climate cabinet was 0.84 m^2. Light was provided by white LED modules (GreenPower LED-TL-DR/W-MBVISN 0.16/0.24/0.59 blue/green/red fraction, Philips, Eindhoven, The Netherlands). The height of the LED lamps was adjusted weekly to maintain the desired photosynthetic photon flux density (PPFD) at the top of the canopy. Climate in the cabinet was controlled by a climate control computer.

Plants were watered with nutrient solution (electrical conductivity 2.1 dS m^{-1}, pH 5.5) containing 1.2mM NH_4^+, 7.2mM K^+, 4.0mM Ca^{2+}, 1.8mM Mg^{2+}, 12.4mM NO_3^-, 3.3mM SO_4^{2-}, 1.0mM PO_4^{2-}, 35µM Fe^{3+}, 8.0µM Mn^{2+}, 5.0µM Zn^{2+}, 20µM B, 0.5µM Cu^{2+}, 0.5µM MoO_4^{2-}. After 28 eight days after sowing (DAS) 6 plants were taken from each cabinet and destructively measured. Remaining plants were re-distributed over four cabinets. Treatments started in all four climate cabinets with a plant density of 59 plants m^{-2} and lasted 20 days.

3.2.2 Treatments and experimental set up

We distributed the plants in a multifactorial experiment with three factors with two levels each and a control treatment (hence nine treatments). The factor temperature amplitude (TA) had two levels:1) 10°C TA (day/night temperatures of 28/25°C or 18/15 °C) 2) and 3◦C (24.5/21.5 °C or 21.5/18.5 °C). Integration period (IP), meaning the period of time over which temperature and light was averaged, had two levels: 20 days (light and temperature levels were switched after 10 days) and 2 days (light and temperature levels were switched every day). Temperature was adjusted to light in two ways: in Phase, high temperature at high light intensity, low temperature at low light intensity; or Antiphase: low temperature at high light intensity, high temperature at low light intensity. High light intensity was 400 µmol m^{-2} s^{-1} and low light intensity was 200 µmol m^{-2} s^{-1} (at the top of the canopy) (Figure 3.1B, C, D, E). A ninth treatment with an average daily temperature of 22 °C (23/20 °C day/night) and constant light intensity of 300 µmol m^{-2} s^{-1} was also performed (Figure 3.1A). All treatments had received the same average light intensity (300 µmol m^{-2} s^{-1}) and the same average temperature (22°C) at the end of the experiment (day 20). In all treatments air humidity was 70%, photoperiod was 16 h and no CO_2 enrichment was applied.

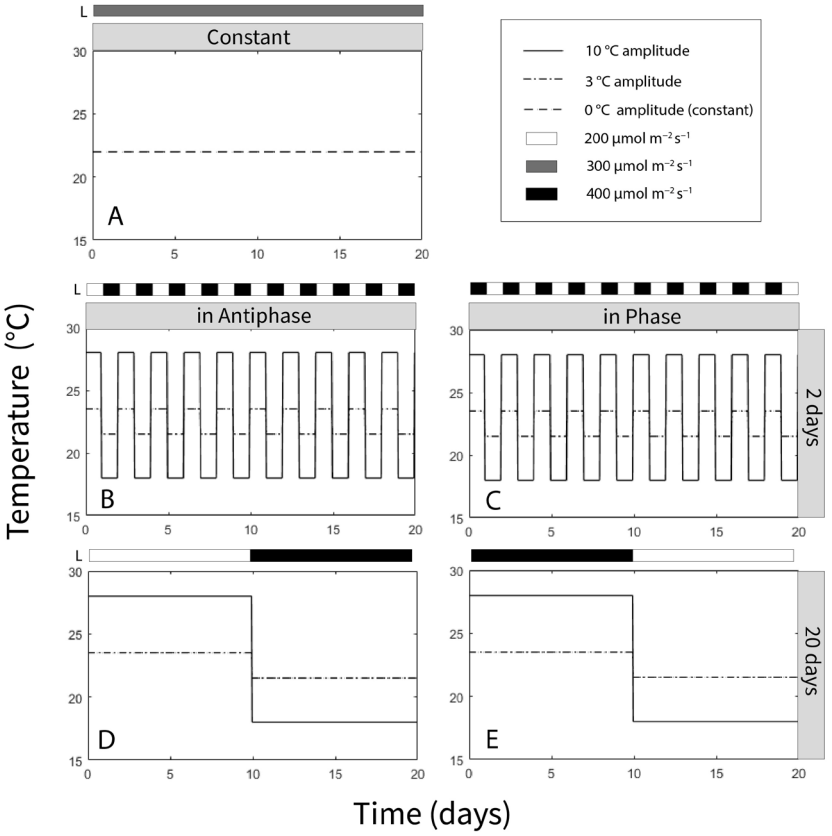

Figure 3.1. *Temperature and light regimes applied in nine treatments: (A) Average temperature 22°C (0°C temperature amplitude) and light intensity (300 µmol m^{-2} s^{-1}) were constantly maintained. (B) Antiphase treatments (low light with high temperature followed by high light with low temperature) in a 2-day integration period at two temperature amplitudes (3 or 10°C). (C) Phase treatments (high light with high temperature followed by low light with low temperature) in a 2-day integration period at two at two temperature amplitudes (3 or 10°C). (D) Antiphase treatments in a 20-day integration period at two temperature amplitudes (3 or 10°C). (E) Phase treatment in a 20-day integration period at two temperature amplitudes (3 or 10°C). All treatments received the same light intensity average (300 µmol m^{-2} s^{-1}) and same temperature average (22°C) at the end of the experiment after 20 days.*

3.2.3 Destructive measurements

For each cabinet, six plants were destructively measured to determine their leaf and stem dry mass (ventilated oven, 72h at 80ºC) and leaf area (LI-3100 area meter, LiCor) at days 0, 5, 10, 15 and 20. Because we wanted to investigate responses with a closed canopy, density was changed every five days: 59 plants m^{-2} from day 1 to 5, 50 plants m^{-2} from day 5 to 10, 38 plants m^{-2} from day 10 to day 15 and 26 plants m^{-2} from day 15 to day 20.

3.2.4 Starch and soluble sugar content

Leaf samples for total soluble sugars and starch content were taken on day 0 (before treatment started) and on days 5, 10, 15 and 20. Leaf samples were taken at the end of the light period. Sampling was done on every other leaf from the bottom to the top to obtain a 'canopy' sample. In each selected leaf, one leaflet adjacent to the terminal leaflet was collected. For every treatment (which was repeated 2 times) six replicate plants per cabinet were taken at each time point (therefore, each time point consisted of 18 samples). Samples were placed in vials, flash frozen in liquid nitrogen and stored at -80C for further analysis.

Approximately 15 mg of ground leaf material was mixed with 5 ml 80% EtOH (ethanol) in a shaking water bath at 80 °C for 20 min for the sugar extraction. After centrifugation at 8500 g for 5 min, 1ml of the supernatant containing soluble sugars was vacuum dried using a Savant SpeedVac rotary evaporator (SPD2010; Thermo Fisher Scientific, Waltham, MA, USA) and dissolved in 1 ml Mili-Q water and diluted 20x for analysis of soluble sugars. Sucrose, fructose and glucose quantification was done using a high-performance ion chromatograph (ICS-5000; Thermo Fisher Scientific) with an anion CarboPac 2 × 250 mm exchange column (PA1; Thermo Fisher Scientific) at 25°C with 100 nM NaOH as eluent at the flow rate of 0.25 ml min^{-1}. Pulsed amperometry was used for detection and Chromeleon (Thermo Fisher Scientific) was used for analysis of the chromatograms and quantification of sugar concentrations. The remaining pellet after sugar extraction was used for starch determination. After discarding the supernatant that contained the soluble sugars, the remaining pellet was washed three times with 80% ethanol, each time followed by 5 min centrifugation and removal of the supernatant. The remaining pellet was dried for 20 min in a SpeedVac rotary evaporator and resuspended in 2 ml 1 mg ml^{-1} thermostable α-amylase solution (Serva Electrophoresis, Heidelberg, Germany) and incubated for 30 min at 90°C. Then, 1 ml of 0.5 mg ml^{-1} amyloglucosidase (10115; Sigma-Aldrich) in 50 mM citrate buffer (pH 4.6) was added and the mixture incubated for 15 min at 60°C so that the starch in the

sample was converted into glucose. After centrifugation for 5 min at 8500 g, 1 ml of the supernatant was diluted 50× and was used for quantification of glucose content as described above. Glucose levels were analysed with the HPIC, which this time was eluted with is 100 mM $NaOH^+$ 25 mM sodium acetate.

3.2.5 Statistical analysis

The experiment was carried out in a complete randomized block design with 9 treatments. The complete experiment was conducted 3 times (3 blocks). The 9 treatments that were repeated 3 times (hence 27 treatments including repetitions) were randomized over four climate cabinets (experimental unit) making sure that no specific treatment was repeated on the same climate cabinet. Significance of the main effects and interactions at each time point was tested using a three-way ANOVA model for the complete factorial design so excluding the control treatment (constant conditions). The statistical tests were all conducted at a probability level of $\alpha = 0.05$ applying Fishers protected LSD test for mean separation. Differences between treatment means and constant conditions were tested using the LSD.

3.3 Results

3.3.1 Effect of light and temperature fluctuations on plant growth and morphology

The effect of adapting light to temperature in Phase (high light with high temperature followed by low light with low temperature) or in Antiphase (low light with high temperature followed by high light with low temperature) on total dry weight depended on the integration period (*P=0.05*, Table 3.1). For treatments with an integration period of 20 days, Antiphase resulted in 12% higher plant total dry weight (although not statistically significant), 35% higher stem dry weight and 28% longer stem, 4% lower leaf mass fraction compared to Phase (Table 3.1). For treatments with an integration period of 2 days, Antiphase resulted in 12 % lower plant total dry weight, 20% lower stem dry weight, and 15 % shorter stem compared to Antiphase (Table 3.1). Constant conditions had 11 - 12% less plant total dry weight, 26 % less stem dry weight, and 20 – 22% shorter stem compared to Antiphase 20 days and Phase 2 days respectively. Total plant dry weight, stem dry weight, stem length and leaf mass fraction were not statistically significantly different between Constant and Antiphase 2 days and Phase 20 days (Table 3.1). SLA and structural dry mass were not statistically different between treatments (Table 3.1).

Table 3.1. *Effect of adapting light to temperature in Phase (high light with high temperature followed by low light with low temperature) or in Antiphase (low light with high temperature followed by high light with low temperature) and Integration Period (either 2 or 20 days), averaged over 2 temperature amplitudes (3 or 10°C) on total dry weight, stem dry weight, structural dry weight, NSC, leaf dry weight, stem dry weight, stem length, LMF and SLA of tomato plants at day 20. In a fifth treatment (Constant) average daily temperature and light intensity were maintained constantly. Data are means of 3 blocks with 6 replicate plants per block an averaged over 2 temperature amplitudes (so each value based on 36 plants)*

Phase/Antiphase	Integration Period (days)	Total Dry Weight (g DM plant $^{-1}$)	Structural Dry Weight (g SDM plant $^{-1}$)	NSC (gCH_2O plant^{-1})	Leaf dry weight (g plant^{-1})	Stem Dry Weight (g plant^{-1})	Stem length (cm)	Leaf Mass Fraction (LMF)	Specific Leaf Area (SLA) (cm^2 g^{-1})
Phase	2	8.31 a	7.62	0.859 b	6.69	1.62 b	37.3 bc	0.805 ab	286
Antiphase	2	7.32 a	6.33	0.987 b	6.03	1.29 a	32.0 ab	0.825 bc	278
Phase	20	7.31 a	6.8	0.567 a	6.53	1.24 a	31.1 a	0.836 c	295
Antiphase	20	8.19 a	6.66	1.54 c	6.53	1.65 b	38.8 c	0.798 a	259
Constant	Constant	7.31 a	6.44	0.873 b	6.09	1.22 a	30.2 a	0.833 bc	269
F-probability interaction (Phase × Period)		0.05	0.201	0.011	0.19	<0.001	0.005	<0.001	0.321
Standard error of the mean (SEM)		0.626	0.611	0.194	0.56	0.114	2.78	0.009	18.8
LSD (P = 0.05)		1.36		0.205		0.22	5.9	0.009	

Plants grown in Phase had 11% higher leaf area compared to Antiphase (Table 3.2). Constant conditions had 13% less leaf area compared to Phase, but there was no difference with Antiphase (Table 3.2). Plants grown at lower temperature amplitudes (3°C) had 21% higher leaf area and 18% higher specific leaf area compared to plants grown at 10 °C amplitude (Table 3.3). Constant conditions had 17% less leaf area and specific leaf area compared to 3 °C amplitude but did not differ from Antiphase (Table 3.3).

For treatments with an integration period of 20 days, during the period from day 10 to 15, Antiphase had a 58% and 46% higher growth rate compared to Phase and Constant conditions respectively (Table 3.4). For treatments with an integration period of 2 days during the same time interval, Phase had 70% and 25 % higher growth rate compared to Antiphase and Constant conditions, respectively (Table 3.4). Constant conditions had a relatively constant growth rate at all time intervals (Table 3.4)

Table 3.2. *Effect of adapting light to temperature in Phase (high light with high temperature followed by low light with low temperature) or in Antiphase (low light with high temperature followed by high light with low temperature) on leaf area of young tomato plants at day 20. In a third treatment (Constant) average daily temperature and light intensity were constantly maintained. Data are means of 3 blocks with 6 replicate plants per block and averaged over two temperature amplitudes and 2 integration periods (so each value is based on 72 plants).*

Phase/Antiphase	**Leaf area (cm^2)**
Phase	1822 a
Antiphase	1635 b
Constant	1593 b
F-probability main effect (Phase/Antiphase)	0.032
Standard error of the means (SEM)	80.4
LSD (P = 0.05)	168

Table 3.3. *Effect of temperature amplitude (3 °C or 10 °C) on leaf area and specific leaf area of young tomato plants at day 20. In a third treatment (Constant) average daily temperature and light intensity were constantly maintained. Data are means of 3 blocks (n=3) with 6 replicate plants per block and averaged over Phase and Antiphase and 2 integration periods (so each value is based on 72 plants).*

Temperature amplitude (°C)	Leaf area (cm^2)	Specific leaf area ($cm^2\ g^{-1}$)
3	1899 a	303 a
10	1558 b	256 b
Constant	1593 b	269 b
F-probability main effect (Amplitude)	<0.001	0.005
Standard error of the means (SEM)	80.4	13.86
LSD (P = 0.05)	142	28

Table 3.4. *Effect of adapting light to temperature in Phase (high light with high temperature followed by low light with low temperature) or in Antiphase (low light with high temperature followed by high light with low temperature) and Integration Period (either 2 or 20 days), averaged over 2 temperature amplitudes (3 or 10 °C) on growth rate of tomato plants over time. In a fifth treatment (Constant) average daily temperature and light intensity were maintained constantly. Data are means of 3 blocks with 6 replicate plants per block and averaged over 2 temperature amplitudes (so each value based on 36 plants). Light intensity ($\mu mol\ m^{-2}\ s^{-1}$) and temperature (°C) are indicated in brackets.*

Phase/Antiphase	Integration Period	Growth rate ($gDM\ d^{-1}$) Day 0 to 5	Growth rate ($gDM\ d^{-1}$) Day 5 to 10	Growth rate ($gDM\ d^{-1}$) Day 10 to 15	Growth rate ($gDM\ d^{-1}$) Day 15 to 20
Phase	2	12.8 *(320/22.65)*	13.9 *(280/21.35)*	17.3 bc *(320/22.65)*	13.2 *(280/21.35)*
Antiphase	2	9.96 *(280/22.65)*	14.1 *(320/21.35)*	10.0 a *(280/22.65)*	13.4 *(320/21.35)*
Phase	20	14.8 *(400/25.3)*	13.6 *(400/25.3)*	12.7 ab *(200/18.8)*	10.8 *(200/18.8)*
Antiphase	20	9.15 *(200/25.3)*	13.9 *(200/25.3)*	20.1 c *(400/18.8)*	11.8 *(400/18.8)*
Constant	Constant	9.20 *(300/22)*	14.4 *(300/22)*	13.8 *(300/22)*	11.6 *(300/22)*
F-probability interaction (Phase × Period)		0.380	0.857	0.004	0.873
Standard error of the means (SEM)		2.21	1.68	3.01	3.36
LSD (P = 0.05)				6.46	

3.3.2 Non-structural carbohydrate dynamics

For treatments with an integration period of 20 days, Antiphase (low light with high temperature followed by high light with low temperature) showed a steep decline in NSC from about 0.25 g CH_2O g^{-1}DM on day 0 to about 0.10 g CH_2O g^{-1} DM on day 5 at both temperature amplitudes (3 °C and 10 °C). The NSC concentration remained constant from day 5 to day 10 (Figure 3.2D). From day 10 onwards, when light intensity increased and temperature decreased, NSC increased again to 0.25 g CH_2O g^{-1} DM for the 10 °C amplitude and to 0.14 g CH_2O g^{-1}DM for 3 °C amplitude (Figure 3.2D). Treatments in Phase (high light with high temperature followed by low light with low temperature) showed a linear decrease in the NSC from day 0 to day 10 in both temperature amplitudes (3 and 10 °C). When temperature amplitude was large (10 °C), the minimum NSC concentration (0.1 g CH_2O g^{-1}DM) was reached at day 10, and afterwards the concentration remained constant. The NSC decreased at a slower rate from day 0 to 10 in small temperature amplitudes (3 °C) and the minimum (0.1 g CH_2O g^{-1}DM) was reached on day 15 (Figure 3.2E). For treatments with an integration period of 2 days, Antiphase maintained almost a constant NSC concentration from day 0 to day 10. After day 10, the concentration decreased on days with high temperature and low light intensity and increased again at day 20 on a day with low temperature and high light intensity for both temperature amplitudes (Figure 3.2B). Treatments in Phase showed a general trend of a decline in the NSC pool (from 0.20 to 0.1 gCH_2O gDM^{-1}) throughout the experiment (Figure 3.2C). Plants grown under constant conditions showed a continuous decrease in NSC until day 15 (reaching a minimum of 0.14 gCH_2O gDM^{-1}) and afterwards, the NSC concentration remained constant (Figure 3.2).

3.3.3 Soluble sugar dynamics

For treatments with an integration period of 20 days Antiphase, at both temperature amplitudes, had on average lower SS concentration (0.015 g CH_2O g^{-1}DM) compared to Phase (Figure 3.3D,E). Antiphase treatment at a 20-day integration period showed a slight increase in the SS sugar at day 10 at 10 °C temperature amplitude once PPFD increased from 200 to 400 µmol $m^{-2}s^{-1}$ and temperature decreased from 28 °C to 18 °C (Figure 3.3D). For treatments with an integration period of 2 days, soluble sugars were on average twice as high at 10 °C amplitude, compared with 3 °C amplitude no matter whether in Phase of Antiphase (Figure 3.3B,C). Constant conditions resulted in constant SS concentration over time (0.03 g CH_2O g^{-1}DM) (Figure 3.3A). In all treatments, SS rarely were above 0.06 gCH_2O gDM^{-1}.

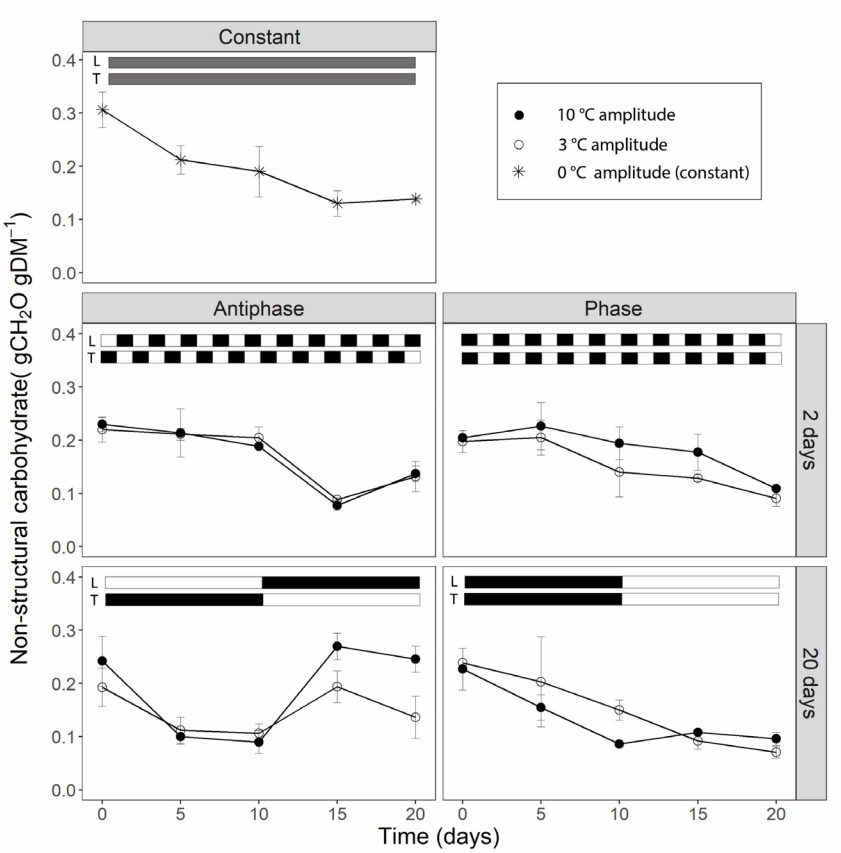

Figure 3.2. *Time course of non-structural carbohydrate content of tomato leaves (sum of glucose, fructose, sucrose and starch) for (A) constant light (300 µmol $m^{-2}s^{-1}$) and temperature (22 °C), (B) light and temperature in Antiphase and an integration period of 2 days (200 µmol $m^{-2}s^{-1}$ and 28 °C for 1 day followed by 400 µmol $m^{-2}s^{-1}$ and 18 °C for 1 day), (C) light and temperature in Phase and an integration period of 2 days (400 µmol $m^{-2}s^{-1}$and 28 °C for 1 days followed by 200 µmol $m^{-2}s^{-1}$ and 18 °C for 1 day), (D) light and temperature in Antiphase and an integration period of 20 days (200 µmol $m^{-2}s^{-1}$ and 28 °C for 10 days followed by 10 days at 400 µmol $m^{-2}s^{-1}$ and 18 °C) and e) light and temperature in Phase and an integration period of 20 days (400 µmol $m^{-2}s^{-1}$and 28 °C for 10 days followed by 10 days at 200 µmol $m^{-2}s^{-1}$and 18 °C). Closed symbols are treatments with a temperature amplitude of 10 °C and open symbols a temperature amplitude of 3 °C. White bars above the graphs indicate a low level of light intensity (L) and temperature (T) and black bars indicate a high level of light intensity (L) and temperature (T). Data are means of 3 blocks (n=3) with 6 replicate plants per block. Error bars are ±SEM.*

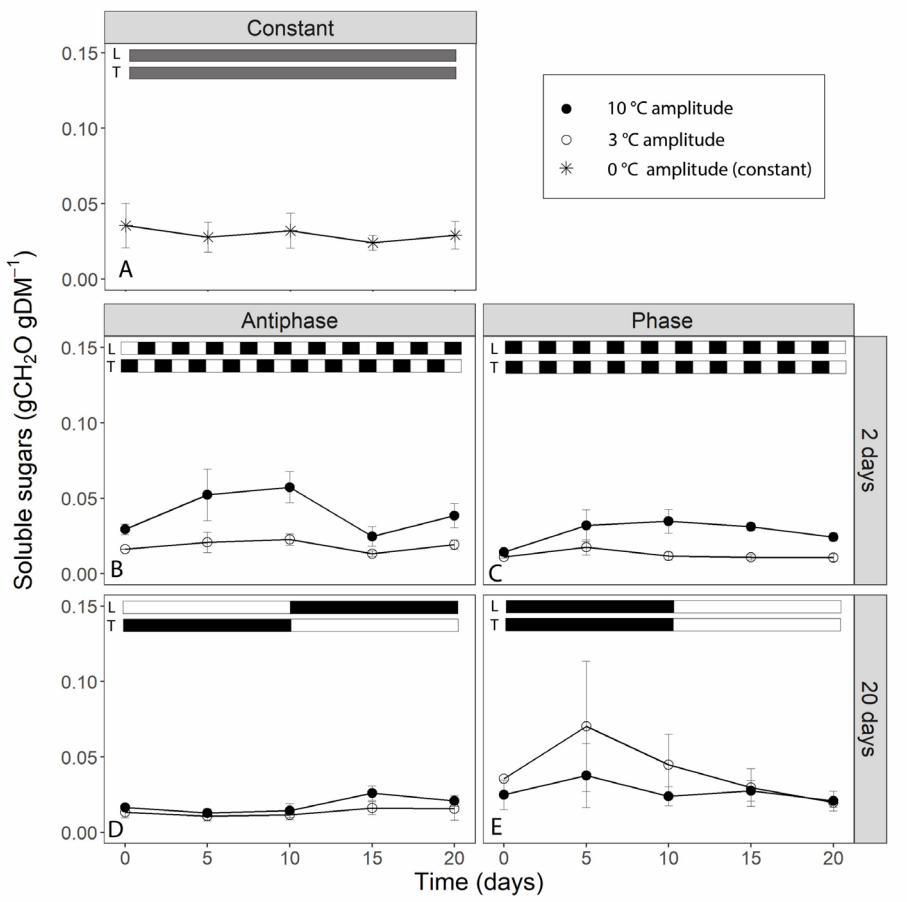

Figure 3.3. *Soluble sugar content of tomato leaves (sum of glucose, fructose, sucrose) over time for (A) constant light (300 µmol $m^{-2}s^{-1}$) and temperature (22 °C), (B) light and temperature in Antiphase and an integration period of 2 days (200 µmol $m^{-2}s^{-1}$ and 28 °C for 1 day followed by 400 µmol $m^{-2}s^{-1}$and 18 °C for 1 day), (C) light and temperature in Phase and an integration period of 2 days (400 µmol $m^{-2}s^{-1}$ and 28 °C for 1 days followed by 200 µmol m-2s-1 and 18 °C for 1 day), (D) light and temperature in Antiphase and an integration period of 20 days (200 µmol $m^{-2}s^{-1}$and 28 °C for 10 days followed by 10 days at 400 µmol $m^{-2}s^{-1}$ and 18 °C) and e) light and temperature in Phase and an integration period of 20 days (400 µmol $m^{-2}s^{-1}$ and 28 °C for 10 days followed by 10 days at 200 µmol $m^{-2}s^{-1}$and 18 °C). Closed symbols are treatments with a temperature amplitude of 10 °C and open symbols a temperature amplitude of 3 °C. White bars above the graphs indicate a low level of light intensity and temperature and black bars indicate a high level of light intensity and temperature. Data are means of 3 blocks (n=3) with 6 replicate plants per block. Error bars are ±SEM.*

3.4 Discussion

3.4.1 C storage and remobilization largely buffer the effects of temperature and light fluctuations on growth

C reserves are hypothesized to play a fundamental role in a plant's coping with environmental fluctuations, at different temporal scales from within a day to seasons (Dietze et al., 2014; Legros et al., 2009). Short-term temperature and light fluctuations (every other day) lead to a similar time course (both a depletion / decrease) of the NSC over 20 days independent from whether temperature and light intensity are in Phase or in Antiphase (Figure 3.2C). Constant conditions also lead to a depletion of the NSC over time, although in this case, the concentration of NSC start declining at a rate of ~0.012 gNSC day^{-1} from day 0 to 5, compared to Phase or Antiphase where during this time period, there is almost no depletion. This may indicate that plants in constant conditions were source-limited already from day 0 and had no C to allocate to storage. Surprisingly, differences in structural dry weight between these treatments were relatively small considering such contrasting temperature and light fluctuations (Table 3.1). Still, on the short-term, the dynamics of the NSC pools followed the patterns of light and temperature: plants reduced the amount of stored NSC on days with a low supply relative to the demand (i.e., days with low light intensity and high temperature) for example at day 15 (Figure 3.2B) and accumulated NSC carbohydrates over days with an excess supply (i.e. days with a high light intensity and a low temperature) for example at day 20 (Figure 3.2B). While on the short term we can see patterns of accumulation and depletion, on the long term we can see a continuous loss in the NSC pools indicating a net depletion of the storage pools, meaning that plants were source limited. If plants were grown at higher light intensities where source is higher than the sink, then gradual increases on NSC are expected up to the moment when the NSC pool reaches its limit, or until plants become source-limited again and NSC pool starts depleting.

3.4.2 Plants build up NSC reserves when supply exceeds demand up to a maximum

Fluctuations in the NSC pool are mainly driven by changes in assimilation vs. growth and respiration, which in turn are highly dependent on temperature and light environment. We hypothesize that a low light intensity results in reduced assimilation, and when this coincides with high growth and respiration demands due to high temperature, then C storage is quickly depleted. Conversely, a situation with increased assimilation rate due to high light intensity and low growth or respiration demand due to reduced temperature will result in a build-up of NSC storage. Our results show that

NSC storage pools were able to recover after 5 days (i.e., Figure 3.2D from day 10 to 15), (accumulation of 3 times more compared to the minimum NSC observed) from the C-limiting conditions after an increase in the light intensity. The rate of accumulation depended on temperature, for example, at 18 °C the accumulation rate was 0.038 gNSC day^{-1}, while at 21.5 °C the accumulation rate was lower with 0.014 gNSC day^{-1} (Figure 3.2D from day 10 to 15). Similarly, Klopotek & Kläring, (2014) showed that once plants were moved from 26 °C to 16 °C (at 400 µmol $m^{-2}s^{-1}$), in only 2 days, plants were able accumulate 3 times as much starch compared to the concentrations measured just before the temperature change. A similar behaviour has been long observed for *Arabidopsis* on a diurnal time scale (Gibon et al., 2009; Mengin et al., 2017; Smith & Stitt, 2007; Sulpice et al., 2014) for example, when during short days plant accumulate NSC (mainly in the form of starch) and these reserves are used during the C limiting conditions of 'darkness' (the night). The question remains: what are the limits for C storage in which growth then becomes negatively affected? Most likely conditions in the present experiment were not extreme enough compared to starvation conditions, which simply did not trigger or impair growth of the plants. In a more extreme case, Weber et al., (2018) showed that tissue concentrations of C reserves decreased in complete darkness, but seedlings were able to recover quickly after a few days of re-illumination. However, in this case, after re-illumination, the rebuilding of C reserves of seedlings was prioritized over other C-sink activities such as growth (Weber et al., (2018), see Fig 5 and 6).

An increased growth rate was observed at long integration periods (20 days), immediately after the increase in light intensity (Table 3.4) and coincides with a period of high accumulation of NSC. This suggests that the stored NSC is used to give a higher growth rate for a few days. This was previously observed by (Gent, 1986) in tomato plants, where RGR was 43% higher and NSC content was 41.5% higher at plants grown at high light intensity compared to low light intensity. However, in our experiment, after 5 days with a high NSC concentration, the NSC pool and growth rates started declining, indicating a possible feedback inhibition of photosynthesis, and suggesting that the NSC pool reached a 'limit' at ~0.28 gCH_2O gDM^{-1}. Altogether, this shows that NSC pools respond in a time scale of days to C source-sink asynchronies and that C storage and remobilization largely buffer the effects of temperature and light fluctuations on plant structural growth.

3.4.3 Stored NSC were not entirely remobilized even under source-limited conditions

Previous studies have shown that plants keep a relatively high minimum NSC concentration at all times (30 to 50% the percentage from the seasonal maximum)

(Martínez-Vilalta et al., 2016) unless they are under extreme conditions leading to death (Weber et al., 2018). From our results we can see that in all treatments, the NSC pool seems to reach a minimum, roughly 33% from the maximum NSC observed during the experiment which goes in line with previous research across different species and climates (Martínez-Vilalta et al., 2016). In our study, if light intensity and temperature remain the same, this 'minimum' level is maintained (Figure 3.2). This simply reflects that at this point, plants are not allocating any new C to storage, however, they are also not using any reserve although still 10% of the total plant mass is NSC (Figure 3.2). From the remaining NSC, only around 30% are soluble sugars (Figure 3.3) which denotes that there is still a fraction of starch that remains stored despite that the C flows for respiration and growth could be potentially higher than C assimilation (for example Figure 3.2D, day 5 to 10). Hence there is a fraction of the NSC that is non mobilizable, and that plants are likely keeping this level to prevent acute depletions of the NSC at all times, unless conditions are extreme.

3.4.4 Short-term fluctuations increase the concentration of soluble sugars when temperature fluctuations are large

Unexpectedly, short-term (days) fluctuations of light and temperature lead to constantly higher concentrations of soluble sugars in the leaves when temperature fluctuations were large (Figure 3.3B, C) (i.e. when mean daily temperature fluctuated between 18 and 28 °C) compared to a mean daily temperature fluctuating between 21.5°C and 23.5°C. Soluble sugars are involved in the response to a number of stresses, as they act as signalling molecules (Couée et al., 2006). Under low temperatures, accumulation of soluble sugars is typical as they contribute to the stabilization of the osmotic cell potential (Martínez-Vilalta et al., 2016; Pommerrenig et al., 2018a) and they have a protective role against ROS (Keunen et al., 2013). Perhaps those days with low temperatures triggered a 'cold acclimation' type of response in plants, or reduced respiration contributed to the accumulation of soluble sugars. However, in that case we would also observe such a response in treatments where plants were exposed to 18 °C constantly for 10 days (Figure 3.3D, E), but we did not observe this. Most likely temperatures were simply not sufficiently low to trigger a cold acclimation or to reduce respiration substantially. Another explanation is that plants perceived the 'repetitive sudden changes' in temperature as a sign of stress and triggered a response that led to an accumulation of soluble sugars. We conclude that daily abrupt changes in temperature lead to an accumulation of soluble sugars. Although extensive research has been conducted regarding accumulation of sugars as a response to low temperature (Ruelland et al., 2009) or excess light (Schmitz et al., 2014) there is limited research on the response of the soluble sugar

pool to dynamic fluctuations in light and temperature and its interaction which is relevant for plants exposed to naturally occurring environmental fluctuations.

Our findings also support the dual role of NS in plants: starch fluctuates and acts as a storage for future use under C-limiting conditions or drought, while soluble sugars stay relatively constant to perform immediate metabolic functions and are kept above some critical threshold (Dietze et al., 2014; Martínez-Vilalta et al., 2016; Sala et al., 2012).

3.4.5 Could temperature dependence of CO_2 assimilation explain higher growth in Phase treatments at short-term fluctuations?

The effect of adapting light to temperature in Phase or in Antiphase on total dry weight depends on the integration period (Table 3.1). When temperature and light changed every other day, adapting light to temperature in phase led to 14% higher total dry weight, compared to adapting light to temperature in Antiphase. These results could not be explained by changes in leaf morphology or allocation, as SLA, LA or LMF did not significantly differ between treatments (Table 3.1). As discussed earlier, the rate of depletion of the NSC was almost identical, so accumulation and remobilization of NSC could not explain the differences either. It is possible that the influence of temperature on CO_2 assimilation plays a significant role, as in many species, the optimal temperature that maximizes leaf photosynthetic rate increases with increasing growth temperature (Hikosaka et al., 2006). Most likely, C assimilation was temperature limited for Antiphase treatments, when plants were grown at days with high light intensity (400 μmol m^2 s^{-1}) and low temperature (18 °C), where according to (J. Thornley, 2016), temperature was below optimum for the given light intensity. The next day, when plants were exposed to a low PPFD (200 μmol m^2 s^{-1}) but a relatively high temperature (28 °C) C assimilation was simply reduced because of the lower PPFD but the higher temperatures lead to an increased respiration. If this pattern is then repeated over time (e.g., 20 days) this may have led to a disadvantage compared to fluctuations where the PPFD coincides paired with the optimal temperature for photosynthesis, which is the case in the Phase treatment.

A similar reasoning could be followed for the temperature dependence of CO_2 assimilation at different CO_2 levels, where there is a shift to a higher optimum temperature at elevated CO_2 levels (Körner et al., 2009). While in our study we maintained CO_2 at ambient concentrations, on a greenhouse where supplementing with CO_2 is a common practice, these interactions must be considered.

3.4.6 In long integration periods, ending with a high light intensity leads to a large total dry weight

When temperature and light changed every 10 days, adapting light to temperature in Antiphase led to 12% higher total dry weight, compared to adapting light to temperature in phase. When plants grown at low light intensities (200 µmol m^{-2} s^{-1}) were switched to a high light intensity (400 µmol m^{-2} s^{-2}), there is a 44% increased growth rate, compared with plants grown first at high light intensities and then switched to low light intensities (Table 3.4). This was expected, as an increase in the light intensity (and therefore in the photosynthesis rate) leads to an increase in the growth rate (Walters, 2005), however, the increased growth rate was only sustained for 5 days, and thereafter the growth rate was reduced from 20.1 to 11.8 gDM m^{-2}. The reduction in growth rate in day 15 to 20 was also accompanied by a reduction in the NSC pool (Figure 3.2D). A possible explanation is that initially, the increase in light intensity led to an increased growth rate, but after a while the NSC buffer was 'completely full' resulting in feedback inhibition of photosynthesis, which led to both, a decrease in the NSC reserves and also in the growth rate (Gent & Seginer, 2012; Paul & Foyer, 2001).

In both treatments (Phase and Antiphase), temperature changed equally (Figure 3.1E, D) (high temperature during the first 10 days and low temperature during the last 10 days), therefore we can exclude temperature as a factor explaining the increased growth rate. A remaining question is: would the growth rate be equally higher if the switch to higher light intensities would be paired with an increased temperature? Interestingly, in an additional experiment with an integration period of 14 days we observed similar increase in growth rate (2.2 and 2.8 times higher) for the treatment that ended high light intensity (400 µmol m^{-2} s^{-2}) and low temperature (18 °C) and treatment that ended with high light intensity but also high temperature (28 °C) (Table A. 3.1). The main differences were that at low temperatures, around 42% of the total dry weight was allocated to storage (starch and soluble sugars), while at high temperatures only 25% is allocated to storage (Table A. 3.2).

Accumulation of structural dry mass was not different between Antiphase and Phase at day 20 (differences less than 0.12 gSDM $plant^{-1}$), However, the absolute size of the non-structural carbohydrate pool is 3 times larger, compared to Phase (Table 3.1).The implications of these results are that the greater the mass of reserves, the higher the C availability is to build new tissue (Wiley et al., 2019). In this case, if these plants would then be exposed to an environmental stress such as high temperatures, drought, or high salinity, they would have more resources available to remobilize and release energy and sugars to help mitigate the stress (Thalmann & Santelia, 2017).

3.4.7 Fluctuating temperature led to higher leaf area and specific leaf area

In our study we observed changes in leaf morphology upon fluctuating temperature. Fluctuating temperature with an amplitude of 3 °C reduced leaf thickness and increased leaf area (Table 3) compared with larger temperature fluctuations (10 °C) or constant conditions. A similar response was observed in plants grown under fluctuating light regimes (Vialet-Chabrand et al., 2017; Zhang & Kaiser, 2020). Additionally, when plants are grown under fluctuating light and temperature, adjusting light to temperature in Phase (for example, high light levels together with high temperature levels) results in a larger leaf area compared to adjusting light to temperature in antiphase (high light levels together with low temperature levels) or with constant conditions (Table 3.2). This is a remarkable response, as an increase in leaf area or specific leaf area can lead to a larger light capture per unit biomass, ultimately leading to a higher dry weight accumulation. This implies that constant conditions (similar regimes used in greenhouse production or climate chambers) are not necessarily optimal, at least for tomatoes.

3.4.8 Future implications

Whereas much of the earlier research focused on seasonal patterns of C accumulation and remobilization (Huang et al., 2018; Sala et al., 2012; Tixier et al., 2013; Weber et al., 2019) or diurnal C remobilization (starch degradation pattern) (Gibon et al., 2004; Graf et al., 2010a; Pilkington et al., 2015; Scialdone et al., 2013), future studies should explore in more detail the day to day effect of fluctuations on the C pool dynamics and how these relate to growth. For example: what are the rates of accumulation and depletion of C and to what extent do these depend on temperature? Or where are the thresholds of minimum and maximum NSC before we can observe detrimental effects on growth or prioritization of C accumulation over growth? Future research should include gas exchange measurements, metabolic flux analysis, isotopic techniques and dynamic growth monitoring with the use of sensors (e.g. De Swaef et al., 2013), to have a better integration of the whole plant C economy over several days. As there is almost an infinite number of possible combinations of light and temperature fluctuations that lead to different source-sink relationships, parametrizing C accumulation and depletion rates and calibrating a model would allow us to test hypotheses over a larger range of environmental conditions.

Furthermore, we observed that short- and long-term fluctuations in light and temperature influence structural mass accumulation only slightly, and that C storage and remobilization plays a key role in buffering these fluctuations. These results raise

the following question: is there a reason to shift our paradigm about the way we grow crops in controlled environments? Throughout the years we have been growing plants in greenhouses and climate rooms highly focused on maintaining the 'perfect constant' climate and thus, reducing environmental fluctuations. It has now become increasingly questionable whether this may be the best practice, since plants in nature grow under highly variable conditions at all time scales (second to minutes, diurnally, day to day or seasonally) (Athanasiou et al., 2010; Poorter et al., 2016; Vialet-Chabrand et al., 2017). Rapid fluctuations in light (seconds to hours) (e.g.,Bhuiyan & Iersel, 2021; Zhang & Kaiser, 2020) or daily fluctuations in light and temperature (e.g., Dieleman & Meinen, 2007; Klopotek & Kläring, 2014) may not necessarily have detrimental effects on plant growth and may even improve physiological traits that lead to the same or improved biomass production in plants. Additionally, the fact that crops can buffer fluctuations in light and temperature allow a higher freedom in horticulture for allowing the climate to deviate from the set points. This has a profound impact on the energy use efficiency, as flexible climate set points can reduce energy consumption in greenhouse up to 20% (Körner & Challa, 2004; Van Beveren et al., 2015)

3.5 Conclusions

Differences in final structural dry weight were relatively small, while NSC concentrations were highly dynamic and followed changes of light and temperature (a positive correlation with decreasing temperature and increasing light intensity). High temperature and low light intensity lead to depletion of the NSC pool, but NSC level never dropped below 8% of the plant weight and this fraction was not mobilizable. Low temperatures lead to a faster accumulation of NSC and the NSC pool reached a 'limit' at ~0.28 $gCH_2O\ gDM^{-1}$. After 5 days with a constantly high NSC concentration, the NSC pool and growth rates started declining, indicating a possible feedback inhibition of photosynthesis. Our results suggest that growing plants under fluctuating conditions do not necessarily have detrimental effects on plant growth and may improve biomass production in plants. These findings highlight the importance in the NSC carbon pool dynamics to buffer fluctuations of light and temperature on plant structural growth.

3.6 Appendices

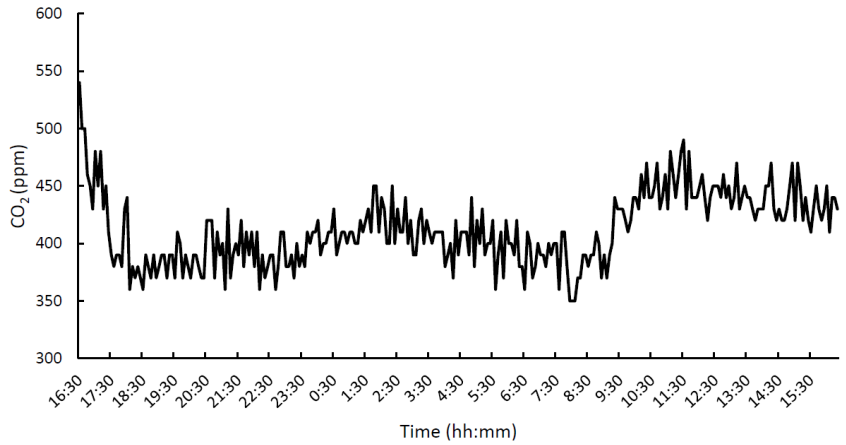

Figure A. 3.1. *Time course of CO_2 during a 24-hour measurement on experimental day 12 in growth cabinet 14. Average value over 24 hours is 412 ppm.*

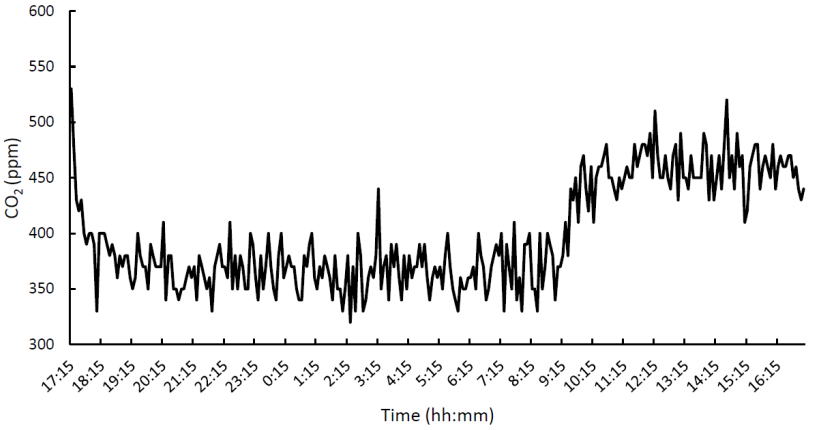

Figure A. 3.2. *Time course of CO_2 during a 24-hour measurement on experimental day 13 in growth cabinet 15. Average value over 24 hours is 399 ppm.*

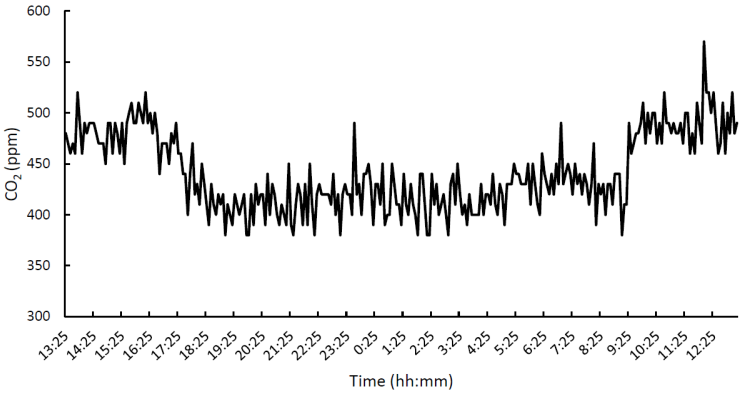

Figure A. 3.3. *Time course of CO_2 during a 24-hour measurement on experimental day 12 in growth cabinet 16. Average value over 24 hours is 441ppm*

Table A. 3.1. *Effect of adapting light to temperature in Phase (high light with high temperature followed by low light with low temperature) or in Antiphase (low light with high temperature followed by high light with low temperature) and Integration Period (either 2 or 20 days), averaged over 2 temperature amplitudes (3 or 10°C) on total dry weight, stem dry weight, NSC, leaf dry weight and stem dry weight. Data are means of 3 blocks with 6 replicate plants per block and averaged over 2 temperature amplitudes (so each value based on 36 plants).*

Phase/Antiphase	Integration Period (days)	Total Dry Weight (g DM m^{-2})	NSC (gCH_2O m^{-1})	Leaf dry weight (g m^{-1})	Stem Dry Weight (g m^{1})
Phase	2	216.1	22.34	173.9	42.12
Antiphase	2	190.3	25.66	156.8	33.54
Phase	20	190.1	14.74	169.8	32.24
Antiphase	20	213.0	40.04	169.8	42.9
Constant	Constant	190.1	22.69	158.34	31.72

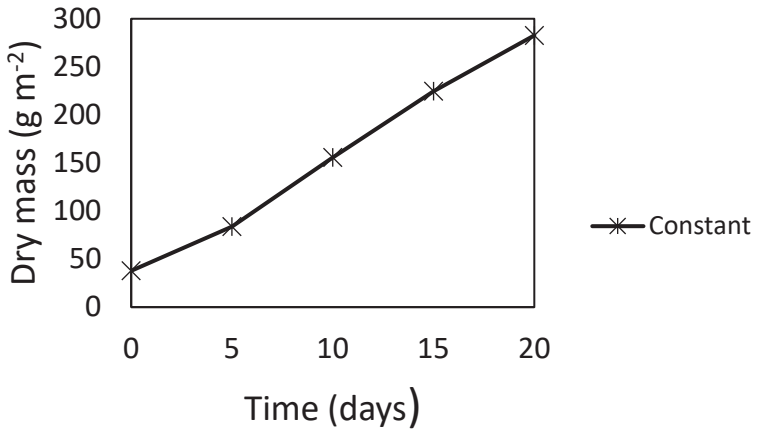

Figure A 3.4. *Total dry weight over time of tomato plants grown at 300 µmol m^{-2} s^{-1} and 22 °C constantly for 20 days. Symbols indicate the mean of two replications (n=2) and bars are SEM.*

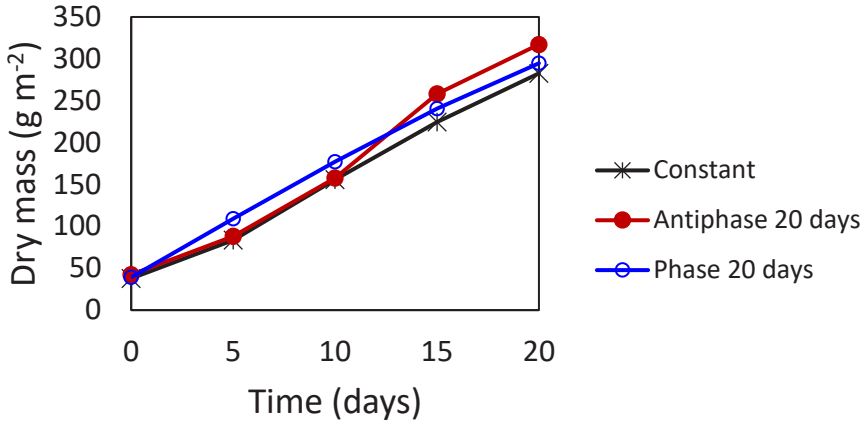

Figure A 3.5. *Cumulative dry mass of tomato plants over time. Star black symbols stand for constant conditions: constant light (300 µmol $m^{-2}s^{-1}$) and temperature (22 °C), red closed symbols are treatment in Antiphase light and temperature in Antiphase and an integration period of 20 days (200 µmol $m^{-2}s^{-1}$ and 28 °C for 10 days followed by 10 days at 400 µmol $m^{-2}s^{-1}$ and 18 °C and blue closed symbols is treatments in phase light and temperature in Phase and an integration period of 20 days (400 µmol $m^{-2}s^{-1}$ and 28 °C for 10 days followed by 10 days at 200 µmol $m^{-2}s^{-1}$ and 18 °C. Data are means of 3 blocks (n=3) with 6 replicate plants per block. Error bars are ±SEM.*

Table A. 3.2. *Growth rate of tomato plants grown in Phase (400 µmol m^{-2} s^{-1} and 28 °C for 7 days and then at 200 µmol m^{-2} s^{-1} and 18 °C for the last 7 day), Phase low (200 µmol m^{-2} s^{-1} and 18 °C for 7 days and then at 400 µmol m^{-2} s^{-1} and 28 °C for the last 7 day) or in Antiphase (200 µmol m^{-2} s^{-1} and 18 °C for 7 days and then at 400 µmol m^{-2} s^{-1} and 28 °C for the last 7 day).*

	Growth rate (gDM d^{-1}) Day 0 to 7	**Growth rate (gDM d^{-1}) Day 7 to 14**
Phase	9.17	8.91
Antiphase	6.33	14.2
Phase low	5.14	14.9

Table A. 3.3. *Plant dry mass, non-structural carbohydrate and structural dry mass of tomato plants grown in Phase low (200 µmol m^{-2} s^{-1} and 18 °C for 7 days and then at 400 µmol m^{-2} s^{-1} and 28 °C for the last 7 day) or in Antiphase (200 µmol m^{-2} s^{-1} and 18 °C for 7 days and then at 400 µmol m^{-2} s^{-1} and 28 °C for the last 7 day).*

	Plant dry mass (gDM m^{-2})	**Non-structural carbohydrate (gCH_2O m^{-2})**
Time	Phase low	Antiphase
0	40	40
7	76.0	84.3
14	180	183

Data are means of 3 blocks (n=3) with 6 replicate plants per block. Error bars are ±SEM.

Chapter 4

Too cold or too warm? Modelling seed set and fruit mass based on the effect of the temperature on pollen quality

Ana Cristina Zepeda, Stefan Vorage, Simon van Mourik, Ep Heuvelink, Leo F.M. Marcelis

Abstract

Temperature stress contributes considerably to yield losses by affecting various reproductive processes, yet many crop growth models do not explicitly incorporate these processes. The aim of this chapter was to develop a quantitative model to predict fruit mass, seed set, and fruit set based on the effects of temperature stress and duration of the stress on pollen quality (number of pollen, pollen viability and pollen germination). To develop the model, we conducted an experiment where we exposed dwarf tomato plants to 14°C for 4, 6, or 8 days, 30°C and 34°C for 1, 3, or 4 days, and a control treatment at 18°C. We quantified pollen number, pollen viability, pollen germination, fruit set, seed set, and fruit mass. Temperatures of 30°C and 34°C reduced pollen viability and germination, resulting in lower seed set and fruit mass. While fruit set remained unaffected at 30°C, both 14°C and 34°C led to reduced fruit set. No correlation was observed between fruit set and pollen number, germination, or viability. At low temperatures (14 °C) yield was predicted to decrease due to a lower number of fruits in the truss (as a consequence of low fruit set) and due to a reduced fruit mass compared to optimal temperatures (18 °C). At high temperatures (30 °C) yield was predicted to decrease mainly due to a reduced individual fruit mass (as a consequence of low seed set). Our model fits well the data for most of the treatments, however, it overestimates fruit mass at very high temperatures (34 °C) and long durations (3 or 4 days). By coupling this model with a crop growth model, a control algorithm could weight the presence of flowers and the impact of temperature fluctuations against the economic losses from harvesting smaller fruits or a reduced number of fruits, making it a valuable tool for optimizing greenhouse temperature strategies.

4.1 Introduction

The reproductive phase in flowering plants is highly sensitive to temperature, even more than the vegetative phase (Müller et al., 2016). As projected climate changes indicate a higher likelihood of extreme temperature fluctuations (Pereira et al., 2022), this could lead to significant yield losses in fruit-bearing crops. This is due to the reduced number of fruits resulting from poor fruit set or the decreased size of individual fruits, which affects quality (Bertin, 1995). Fruit set is the process of flowers developing into fruits, and this can occur independently of pollination (Ruan et al., 2012). The balance between supply and demand for assimilates, also known as the source-sink ratio, is often used to model fruit set (Bertin & Gary, 1993; Kang et al., 2010; Marcelis, 1994; Vanthoor et al., 2011; Wubs, 2010) with temperature playing an indirect role. Factors such as leaf area, radiation, and CO_2 levels can impact source strength, while sink strength can be influenced by factors such as fruit number, cultivar, and temperature (Li et al., 2015). The limited current understanding of fruit set poses a challenge in developing accurate models.

The success of fruit and seed crop production depends on the interplay of various processes such as pollen development, pollination, pollen tube growth, and fertilization of female gametes (Santiago & Sharkey, 2019) which are highly sensitive to temperature (Hedhly et al., 2005). The effect of temperature is a complex function of intensity, duration, and timing of exposure (Sato et al., 2002; Zinn et al., 2010). However, these processes are rarely included in crop simulation models, which can impact the accuracy and reliability of yield predictions under fluctuating temperature conditions. Improving our understanding of fruit set, seed set and fruit growth processes is crucial for improving the accuracy of yield predictions under changing climate.

An alternative to modelling fruit set based on the source sink-balance is the use of deterministic or probability models that link temperature with pollination, fruit set, or seed set failure. Coast et al. (2016) used a probability model based on optimum, minimum, and maximum temperature to describe pollen germination in response to temperature. Steduto et al. (2009) calculated the impact of pollination failure on harvest index (HI) using a probability function, while Challinor et al. (2005) calculated the flowering distribution and pod-set reduction coefficient based on high temperature episodes. However, research often focus on establishing a correlation between a single physiological process and fruit set, ignoring key intermediate processes that are critical to the overall fruit growth. These studies typically compared heat stress to optimum temperatures, providing limited information on the tomato's response over a broader range of temperatures. There is less research on the effect of

lower temperatures on reproductive processes in tomato and most of the research focus on grain crops (e.g., Kiran et al., 2021; Ohnishi et al., 2010; Thakur et al., 2010)

Temperature stress affects pollen development at early, middle, or late stages, which corresponds to 8-15 days before anthesis (Sato et al., 2002). At early stages, pollen develops in the anthers where microsporocytes undergo cell division until they become tricellular pollen with one nucleus and two sperm cells (Santiago & Sharkey, 2019). Exposure to high temperature (5 °C above optimum) at the early stage reduces pollen production in tomato up to 40% (Pham et al., 2020; Sato et al., 2000; Prasad et al., 1999). Temperature stress at the middle stage causes abnormal pollen wall formation which results in unviable pollen (Chaturvedi et al., 2021), reducing the probability of the ovule to be fertilized (Pham et al., 2020). High temperature at a later stage starves pollen grains, inhibition the germination of the tube, which is needed to fertilize the ovule (Santiago & Sharkey, 2019). Fruit set can occur without fertilization (Ruan et al., 2012), resulting in seedless (parthenocarpic) fruit. The absence of seeds is correlated with poor fruit shape and a lower fruit mass (Marcelis et al., 1997; Peet et al., 1998).

The aim of this study was to develop a quantitative model to predict fruit mass, seed set, and fruit set based on the effects of temperature stress and duration of the stress on pollen quality (number of pollen, pollen viability, and pollen germination). To develop the model, we conducted an experiment where we exposed dwarf tomato plants to 14°C for 4, 6, or 8 days, 30°C and 34°C for 1, 3, or 4 days, and a control treatment at 18°C.

4.2 Materials and methods

4.2.1 Plant material and growth conditions

Tomato (*Solanum Lycopersicum* cultivar F1 2414, Vreugdenhil, the Netherlands) seeds were sown in trays with potting soil mix covered with a thin layer of vermiculite and stored in a dark cold room at 4°C. After 24 hours, the trays with the seeds were moved to a climate cabinet (Weiss Technik, the Netherlands) and temperature was set at 18°C, relative humidity 70% and light intensity 230 µmol m^{-2} s^{-1} during a 16-hour photoperiod. Light was provided by white LED modules (Hettich Benelux B.V.). The desired photosynthetic photon flux density (PPFD) at canopy level was maintained by dimming the lamps. Seedlings were transplanted 25 days after sowing (DAS) to 11 x 11 x 12 cm plastic pots filled with the same potting soil and distributed over three climate cabinets with the same climate conditions as mentioned above. The growth surface of each climate cabinet was 0.84 m^2. Climate in the cabinet was controlled by a climate computer. Plants were watered with a nutrient solution (electrical

conductivity 2.1 dS m^{-1}, pH 5.5) containing 1.2mM NH_4^+, 7.2mM K^+, 4.0mM Ca^{2+}, 1.8mM Mg^{2+}, 12.4mM NO_3^-, 3.3mM SO_4^2, 1.0mM PO_4^{2-}, 35µM Fe^{3+}, 8.0µM Mn^{2+}, 5.0µM Zn^{2+}, 20µM B, 0.5µM Cu^{2+}, 0.5µM MoO_4^{2-}. The plant density inside the cabinets was 30 plants m^{-2}. Only the first three trusses on the main stem were kept, and all additional trusses were removed. The three trusses were numbered according to their order of appearance. All trusses were pruned to 9 flower buds per truss to eliminate potential treatment effects on flower initiation. Once the first flower was open, we gently shook the plant's stem every other morning to facilitate self-pollination of the flowers. In addition, throughout the experiment, emerging lateral shoots were removed weekly.

4.2.2 Treatments and experimental set up

We conducted and experiment with two factors (temperature and duration) and a control treatment (hence 10 treatments). The factor temperature had three levels: 14 ºC, 30 ºC or 34 º. The factor duration had five levels, but unbalanced: at 14 ºC duration was 4, 6, or 8 days and at 30 ºC and 34 ºC duration was 1, 3, or 4 days. The control treatment was continuous at 18 ºC, which in this study was considered the optimal growth temperature. The temperature treatments were applied just before the first flower of the first truss reached anthesis stage (approximately 49 DAS). At this moment the second and third truss were already present but were less developed. The same vapor pressure deficit (VPD) was maintained in all treatments resulting in 0.65 kPa. The relative humidity in the cabinets set at 34°C, 30°C, 14°C, and 18°C was set as 88%, 85%, 61%, and 70% respectively. The experiment was carried out using 5 available cabinets. For the treatments, 3 cabinets were set to 14°C, 30°C, or 34°C while the remaining 2 cabinets were set to 18°C. The plants were moved between cabinets according to duration of the temperature stress. After all treatments were completed, the temperature and humidity were reset to the standard conditions of 18°C and 70% relative humidity in all cabinets.

4.2.3 Pollen number and viability

To calculate the number of pollen produced, and to calculate viability, the first flower (position 1) of each truss (1, 2, or 3) was collected once it was fully open. The anther cone was removed from the flower, inserted to a 1.5 mL Eppendorf tube and a Carnoy's fixation solution (Kearns & Inouye, 1993) (6 Ethanol: 3 chloroform: 1 glacial acetic acid) was added to allow storage of the cone until measuring time. At measuring time, the anther cone was dried on tissue paper, dissected into four pieces with a sharp razor blade and inserted again inside a 1.5 mL Eppendorf tube. Pollen was stained by adding 200 µL of Alexander's dye (Alexander, 1969) to the Eppendorf

tube, vortexed for 20 s, and stored at room temperature for at least 24 h before observation. Alexander's dye consisted of 10 mL of 95% ethanol, 1 mL of malachite green (1% solution in 95% ethanol), 54.5 mL of distilled water, 25 mL of glycerol, 5 mL of acid fuchsin (1% solution in water), 0.5 mL of orange G (1% solution in water) and 4 mL of glacial acetic acid for a 100 mL solution (Kearns & Inouye, 1993). After 24h of staining, 10 µL of pollen suspension was loaded into a Fuchs-Rosenthal haemocytometer (4 x 4 x 0.2 mm grid, 3.2 mm^3). The counting chamber was observed under a LEICA MZ APO stereomicroscope equipped with an Axiocam 305 color camera controlled by Axio Vision 4.8.1.0 software. The counting chamber was divided into 16 large squares (1 x 1 mm, 1 mm^2), and each square was further divided into16 small squares (0.25 x 0.25 mm, 0.0625 mm^2). Two large squares (1 mm^2 each) were randomly selected per load, and pictures were made, to further count viable and unviable pollen with a cell counter plugin of Fiji - ImageJ (version 1.53c). For each sample (flower) the haemocytometer was loaded two times, (therefore the average viable, unviable, and total pollen number per flower is based on a total of 4 pictures) (Figure A 4.3). Pollen grains stained dark purple were classified as viable, and those that remained transparent were classified as dead (unviable). The fraction of viable pollen was calculated as the ratio of viable to total (viable and unviable) pollen grains on a 10 µL aliquot.

The total number of pollen per flower was calculated as:

$$pollen\ number\ per\ flower = \frac{pollen\ counted\ (in\ 10\ \mu L)}{volume\ of\ chamber\ (0.2\ mm^3)} * \frac{volume\ of\ the\ sample\ (200\ \mu L)}{} \quad 4.1$$

4.2.4 Pollen germination

For the germination test, the second flower (position 2) of each truss (1, 2 or 3) was collected once it was fully open. The anther cone was immediately dissected into four pieces inside a 1.5 ml Eppendorf tube were 200 µL germination solution was added and vortexed for 20 s to suspend the pollen into the solution. The germination solution consisted of 100 g L^{-1} sucrose, 2 mM boric acid, 2 mM calcium nitrate, 2 mM magnesium sulphate, and 1 mM potassium nitrate (Firon et al., 2006). The pollen suspension was added to a petri dish (3.5 cm) with 1 mL agar layer previously solidified (8 g of agar per L germination solution). This was left for 1 h to germinate. Germination was observed with a LEICA MZ APO stereomicroscope equipped with an Axiocam 305 color camera controlled by Axio Vision 4.8.1.0 software. Two random areas of 0.9 mm^2 were selected (therefore the average pollen germination is based in a total of 2 pictures) and pictures were made to further count pollen

germination with a cell counter plugin of Fiji - ImageJ (version 1.53c). Pollen was classified as germinated when the pollen tube exceeded the diameter of the pollen grain itself. The fraction of germinated pollen was calculated as the ratio of germinated to total (germinated and non-germinated) pollen grains on a 0.9 mm^2 area.

4.2.5 Fruit set, seed set, and fruit weight observations

All trusses were harvested around 100 DAS. The number of fruits and the total weight of all fruits larger than 1 cm in diameter (weight without sepal and pedicel) were recorded for each of the trusses. Furthermore, the individual weight of the second fruit (position 2) was determined and seeds from that fruit were counted. If the second fruit was not available, we used fruit 1 or 3.

4.2.6 Statistical design and analysis

The experiment was carried out in an incomplete randomized block design with 10 treatments. The complete experiment was conducted three times (three blocks). For each block, the four temperatures were randomized over four cabinets. All data was analysed in GenStat (22nd edition, 64-Bit) using a two-way unbalanced ANOVA model. Mean separation was conducted with Fisher's protected LSD test. The statistical tests were all conducted using a significance level of $\alpha = 0.05$.

4.2.7 Parameter estimation and model evaluation

The model consists of 5 main functions that each describe a process. The parameters p that describe each process are estimated from the experimental data, using a least squares regression. For each process j, the corresponding parameter vector $\hat{p}_j$ is estimated as

$$\hat{p}_j = argmin \sum_{i=1}^{n_j} (y_{ji}^{mes} - y_{ji}^{model}(p))^2. \quad 4.2$$

Here $p = (p_{np}, \theta_{v1}, \theta_{v2}, \theta_{v3}, \theta_{g1}, \theta_{g2}, \theta_{g3}, m_1, b_1, m_2)$ is a vector of all model parameters, $\hat{p}_j$ is the vector of parameters found to give the best fit, j is an index that denotes the process number from 1 to 5 (i.e. $y_1 = N_{pollen}$, $y_2 = f_{viablePollen}$, $y_3 = f_{germPollen}$, $y_4 = N_{seeds}$, $y_5 = M_{fruit}$). Index i denotes the data point over a range of temperature and durations for process j, y_{ji}^{mes} is the measured data for process j at data point i, and y_{ji}^{model} is the model predictions for process j at data point i. A list of estimated and measured parameters is given in Table 4.2.

The goodness of fit of the complete model (Eq. 4.13) to the measured data was evaluated using the root mean square error (RMSE), defined as

$$RMSE = \sqrt{\frac{1}{n}\sum_{i=1}^{n}\left(M_{fruit_i}^{mes} - M_{fruit_i}^{model}(\hat{p})\right)^2} \quad 4.3$$

where $M_{fruit_i}^{mes}$ is the measured fruit mass at treatment i; $M_{fruit_i}^{model}$ is the model predictions of fruit mass at treatment i, and n is the number of treatments (10).

4.2.8 The model

We developed a model that describes how temperature and duration of the temperature affects fruit mass. The model is composed by distinct processes. Firstly, it predicts the effect of temperature on the number of pollen per flower. Secondly, it predicts the effect of temperature and duration of the temperature on the number of viable pollen. Thirdly, it predicts the effect of temperature and duration of the temperature on the number of germinated pollen. The predicted values for the total, viable, and germinated pollen are then used to predict the seed number. Finally, the seed number is used to predict the fruit mass. A list of inputs and functions of the model is given in Table 4.1, and a graphical overview of the modelled processes is presented in Figure 4.1. In the model, N stands for number, and f for fraction. For unit consistency, we differentiate with {} between viable pollen (pollen grains that are capable of fertilization) and germinated pollen (pollen grains that can grow a pollen tube).

Pollen number (N_{pollen}, #pollen flower^{-1}) was modelled as a quadratic function of temperature (T, °C):

$$N_{pollen}(T) = \max\left[0, p_{np} + \frac{2(\alpha_{np} - p_{np})}{\beta}T - \frac{(\alpha_{np} - p_{np})}{\beta^2}T^2\right] \quad 4.4$$

where p_{np} (#pollen flower^{-1}) is a parameter estimated from the regression between T and N_{pollen}, α_{np} (#pollen flower^{-1}) is the maximum amount of pollen measured at optimal temperature, and β (°C) is the optimum temperature. For a derivation of the function see Appendix A, section 4.7.1.

Fraction of viable pollen $f_{viablePollen}$ was modelled as a function of T and duration (D, days):

$$f_{viablePollen}(T, D) = \max\left[0, p_v(D) + \frac{2(\alpha_v - p_v(D))}{\beta}T - \frac{(\alpha - p_v(D))}{\beta^2}T^2\right] \quad 4.5$$

where α_v, (-) is the maximum viability fraction measured at optimal temperature and β (°C) is the optimal temperature.

$p_v(D)$ (-) is a function describing the relationship between duration of stress D and the associated derived parameter p_v:

$$p_v(D) = \theta_{v1} + \theta_{v2}D + \theta_{v3}D^2 \quad 4.6$$

Where θ_{v1} (-), θ_{v2} (days^{-1}), and θ_{v3} (days^{-2}) are parameters estimated from the regression between p_v and D. For a derivation of the complete function see Appendix B, section 4.7.2.

Number of viable pollen ($N_{viablePollen}$, #pollen{viable} flower^{-1}) was calculated as

$$N_{viablePollen} = f_{viablePollen}N_{pollen} \quad 4.7$$

The fraction of germinated pollen ($f_{germPollen}$, -) was modelled as a function of T and D:

$$f_{germPollen}(T,D) = \max\left[0, p_g(D) + \frac{2\left(\alpha_g - p_g(D)\right)}{\beta}T - \frac{\left(\alpha - p_g(D)\right)}{\beta^2}T^2\right] \quad 4.8$$

where α_g, (-) is the maximum germination fraction measured at optimal temperature and β (°C) is the optimum temperature.

$p_g(D)$ (-) is a function describing the relationship between the stress duration D and the associated derived parameter p_g:

$$p_g(D) = \theta_{g1} + \theta_{g2}D + \theta_{g3}D^2 \quad 4.9$$

Where θ_{g1} (-), θ_{g2} (days^{-1}), and θ_{g3} (days^{-2}) are parameters estimated from the regression between p_g and D. For a derivation of the function see Appendix C, section 4.7.3

Number of germinated pollen ($N_{germPollen}$, #pollen{germinated} flower^{-1}) was calculated as

$$N_{germPollen} = f_{germPollen}N_{viablePollen} \quad 4.10$$

The number of seeds N_{seeds} (#seeds fruit^{-1}) was modelled as function of number of germinated pollen $N_{germPollen}$

$$N_{seeds} = m_1 N_{germPollen} c_{flowertofruit} + b_1 \quad 4.11$$

where m_1 is the slope (#seeds #pollen^{-1}{germinated}), b_1 (#seeds fruit^{-1}) is a coefficient estimated from the regression between N_{seeds} and $N_{germPollen}$, and $c_{flowertofruit}$ (flower fruit^{-1}) is a conversion factor that assumes that 1 flower is equivalent to 1 fruit.

Finally, fruit mass (M_{fruit}, gDM fruit^{-1}) was modelled as a function of number of seeds (N_{seeds}):

$$M_{fruit} = m_2 N_{seeds} + b_2 \quad 4.12$$

where m_2 is the slope (gDM #seeds^{-1}) and b_2 (gDM fruit^{-1}) is a coefficient estimated from the regression between N_{seeds} and M_{fruit}.

Combining all of the above results in the following:

$$M_{fruit}(T,D) = m_2\left(m_1 N_{pollen}(T) f_{viablePollen}(T,D) f_{germPollen}(T,D) + b_1\right) + b_2 \quad 4.13$$

Table 4.1. *List of functions and inputs*

Nomenclature	Unit	Definition	Equation no.
Functions			
N_{pollen}	#pollen flower^{-1}	Number of pollen grains per flower as a function of temperature	4.4
$f_{viablePollen}$	-	Fraction of viable pollen as a function of temperature and duration of the stress	4.5
$p_v(D)$	-	Function describing the relationship between duration of stress and the related estimated coefficient p_v	4.6
$N_{viablePollen}$	#pollen{viable} flower^{-1}	Number of viable pollen, the product of the total number of pollen and the fraction of viable pollen	4.7
$f_{germPollen}$	-	Fraction of germinated pollen as a function of temperature and duration of the stress	4.8
$p_g(D)$	-	Function describing the relationship between duration of stress and the related estimated coefficient p_g	4.9
$N_{germPollen}$	#pollen{germinated} flower^{-1}	Number of germinated pollen, the product of the number of viable pollen and the fraction of pollen germination	4.10
N_{seeds}	#seeds fruit^{-1}	Number of seeds per fruit	4.11

M_{fruit}	gDM fruit^{-1}	Fruit mass	4.12, 4.13
Inputs			
T	°C	Temperature	
D	days	Duration of the temperature	

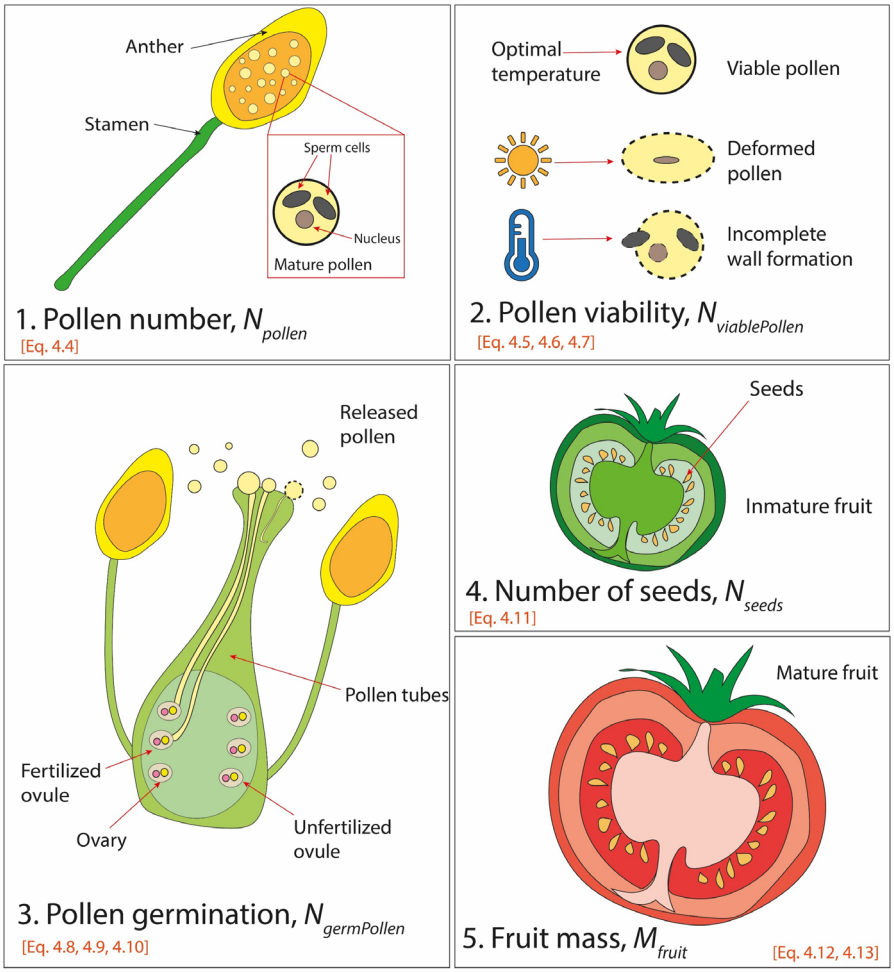

Figure 4.1. *Schematic illustration of the modelled processes (1) Pollen is developed in the anthers where microsporocytes undergo cell division until they become tricellular pollen with one nucleus and two sperm cells. (2) Exposure high or low temperatures causes abnormal pollen formation, or an incomplete wall formation leading to unviable pollen. (3) For successful fertilization to occur, mature pollen grains must land on the stigma and germinate and produce a pollen tube. High or low temperatures prevent pollen tube to germinate due to a lack of soluble sugars and starch reserves. During pollen germination, the pollen tube grows through the style until it reaches the ovule. (4) Successful fertilization of an ovule leads to the formation of seeds (seed set). (5) Developing seeds in the fruit trigger auxin and gibberellin signalling pathways that promote fruit growth.*

***Table 4.2**. List of model parameters*

Parameter symbol	Value	Unit	Meaning
p_{np}	1.24x10^{-4}	#pollen flower^{-1}	Parameter estimated from the regression between pollen number and temperature
α_{np}	63,856	#pollen flower^{-1}	Measured number of pollen at optimal temperature (18 °C)
β	18	°C	Optimal temperature
α_v	0.94	-	Measured fraction of viable pollen at optimal temperature (18 °C)
θ_{v1}	-2.53x10^{-1}	-	Parameter estimated from the regression between p_v and duration D
θ_{v2}	1.03	days^{-1}	Parameter estimated from the regression between p_v and duration D
θ_{v3}	6.71x10^{-1}	days^{-2}	Parameter estimated from the regression between p_v and duration D
α_g	0.31	-	Measured fraction of germinated pollen at optimal temperature (18 °C)
θ_{g1}	-1.14x10^{-1}	-	Parameter estimated from the regression between p_g and duration D
θ_{g2}	4.35x10^{-1}	days^{-1}	Parameter estimated from the regression between p_g and duration D
θ_{g3}	-2.69x10^{-1}	days^{-2}	Parameter estimated from the regression between p_g and duration D
m_1	1.60x10^{-3}	#seeds #pollen^{-1} {germinated}	Slope of the regression between y_{Nseeds} and $y_{NgermPollen}$
b_1	2.23	#seeds fruit^{-1}	Intercept of the regression between y_{Nseeds} and $y_{NgermPollen}$
$c_{flowertofruit}$	1	flower fruit^{-1}	Conversion factor that assumes that 1 flower is equivalent to 1 fruit
m_2	7.80x10^{-2}	gDM #seeds^{-1}	Slope of the regression between y_{Mfruit} and y_{Nseeds}
b_2	2.06	gDM #fruit^{-1}	Intercept of the regression between y_{Mfruit} and y_{Nseeds}

4.3 Results

4.3.1 Pollen production

Low and high temperatures significantly reduced the number of pollen grains produced per flower by 45%, 38%, and 30% at 14 °C, 30 °C and 34 °C respectively compared to the temperature of 18 °C ($P < 0.001$, Table A 4.1). The relationship between pollen number and temperature was accurately described by a quadratic

function (Eq. 4.4) at high temperatures, but with a large overestimation of pollen number produced per flower at low temperatures (Figure 4.2).

4.3.2 Pollen viability

Compared to conditions at 18 °C, pollen viability was reduced at 30 C by 17%, 49%, and 60% when 30 °C was applied for 1, 3, and 4 days respectively (Table A 4.1). For 34 °C the reduction was much more pronounced with 75%, 88%, and 98% less pollen viability respectively compared to 18 °C. In contrast, a lower temperature (14 °C) had a milder effect on pollen viability. Only at longer durations (6 or 8 days) we observed a reduction of ~ 24%, although not statistically significant (Table A 4.1). The relationship between pollen viability, temperature and duration was accurately described by Eq. 4.5**Error! Reference source not found.** and Eq. 4.6 (Figure 4.3, RMSE = 0.09 [-]). However, there is still a significant underestimation of the fraction of viable pollen at short durations (1 day) around 30 °C (Table A 4.1).

4.3.3 Pollen germination

Temperature reduced the fraction of pollen germination depending on the duration of the temperature stress (*P = 0.018*, Table A 4.1). Overall, germination fraction across treatments was low and the maximum germination fraction observed for the control treatment (18 °C) was 0.3 (Table A 4.1). A temperature of 30 °C for 1 day did not reduce germination fraction, but for 3 and 4 days there was a reduction of 54% and 77% respectively compared to 18 °C (Table A 4.1). After 3 days under 34 °C, germination fraction was reduced drastically to ~ 99% compared to 18 °C. Low temperatures had a less pronounced effect compared with high temperatures and germination was reduced by 30%, 32%, and 50% at 4, 6, and 8 days duration (Table A 4.1). The relationship between pollen germination, temperature, and duration was described accurately by Eq. 4.8 and Eq. 4.9 (Figure 4.4, RMSE = 0.04 [-]).

4.3.4 Fruit set, number of seeds and fruit size

Very high temperatures (34 °C) or low temperatures (14 °C) decreased the fraction of fruit set, however, temperature duration did not play a significant role (Table A 4.1). Fruit set was reduced by 16% and 19% at 14 °C and 34 °C respectively (Table A 4.1). Temperature reduced the number of seeds by 47%, 73%, and 85 % at 14 °C, 30 °C and 34 °C respectively ($P < 0.001$, Table A 4.1). Similarly, temperature reduced fruit mass by 38%, 35% and 42% at 14 °C, 30 °C and 34 °C respectively ($P < 0.001$, Table A 4.1, Figure 4.6). Number of seeds increased linearly with increased number of germinated pollen ($R^2 = 0.56$, Figure 4.5). Similarly, fruit mass increased linearly with an increased number of seeds ($R^2 = 0.62$, Figure 4.6).

4.3.5 Sensitive stage for pollen failure

The stage at which temperature was applied did not influence pollen production per flower. Only at very high temperatures (> 34 °C) when temperature is applied 8 days before anthesis, pollen production is reduced by 72% compared to applying temperature 4 days before anthesis or at anthesis (Table A 4.3). The sensitive period for pollen viability was 4 to 8 days before anthesis (Table A 4.3), as in all cases, applying temperature at anthesis resulted in a higher viability, although the response was more pronounced at 30 °C and 34 °C compared to 14 °C. Surprisingly, we did not find a specific sensitive stage for pollen germination. However, high and low temperatures resulted in lower germination percentage compared to optimal temperatures (18 °C).

4.3.6 Measured vs simulated fruit mass

The model predicts accurately almost all treatments (RMSE = 0.95 g). Most model predictions fall within the middle 50% of the data (Figure 4.7), indicating a good fit of the model to the data. Some exceptions are treatments with very high temperatures (34 °C) at either 3 or 4 days, where the model overestimates the fruit mass. Additionally, the model slightly overestimates fruit mass at 14 °C for 4 days, although predictions still fall within the range of observed data.

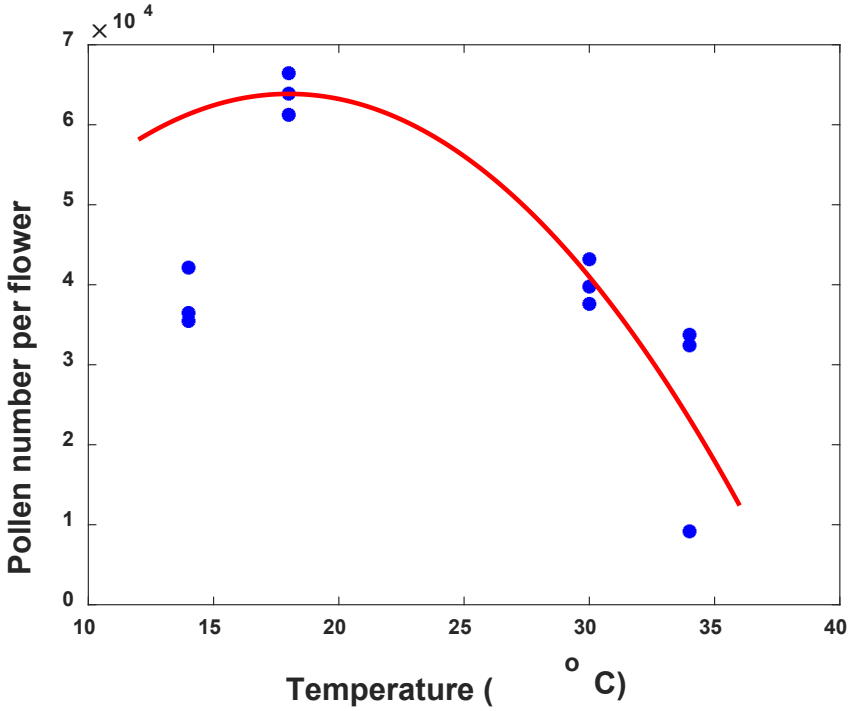

Figure 4.2. *Relationship between temperature and pollen number per flower. Dots are measured data from flowers where stress was applied at anthesis and 4 and 8 days before anthesis. Data are means of 3 blocks with 4 replicate plants per block and averaged over truss 2 and truss 3 (so each value is based on 24 plants). Line is the model prediction. Model is described by the regression function* $N_{pollen}(T) = max\left[0, p_{np} + \frac{2(\alpha_{np} - p_{np})}{\beta} T - \frac{(\alpha_{np} - p_{np})}{\beta^2} T^2\right]$, *where* $\beta = 18$, $\alpha = 6.39 \times 10^4$ *and* $p_{np} = 1.24 \times 10^4$. $RMSE = 1.16 \times 10^4$ *(pollen flower*$^{-1}$*).*

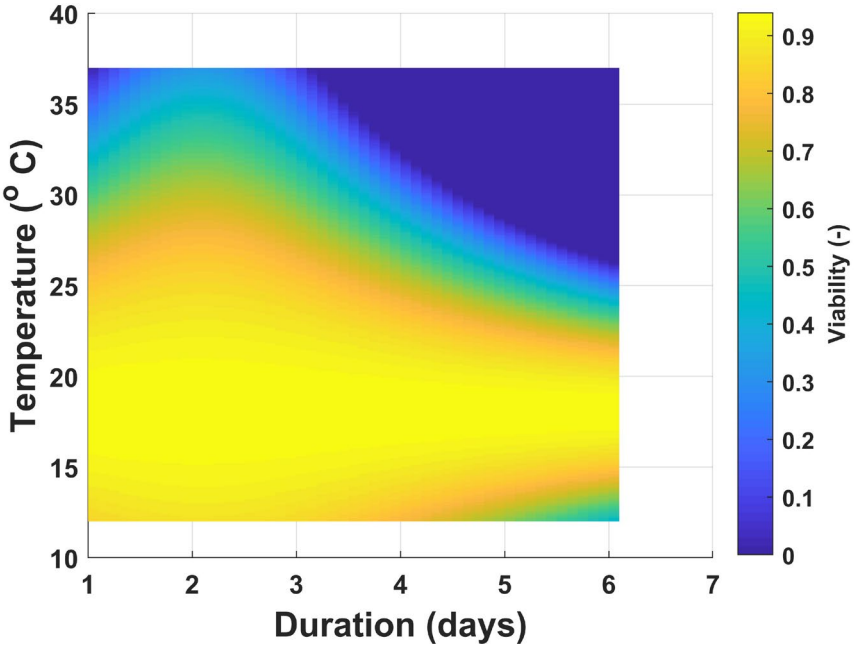

Figure 4.3. *Response surface of the predicted pollen viability values of plants grown at different temperature stress (14, 18, 30, 34 °C) and different durations (0, 1, 3,4, or 6 days). Model is described by the regression line:* $f_{viablePollen}(T, D) = max\left[0, p_v(D) + \frac{2(\alpha_v - p_v(D)}{\beta}T - \frac{(\alpha_v - p_v(D))}{\beta^2}T^2\right]$ *where* $\beta = 18, \alpha_v = 0.94,$ *and* $p_v(D) = -0.2527 + 1.0308D - 0.6706D^2$. *RMSE = 0.09 (-).*

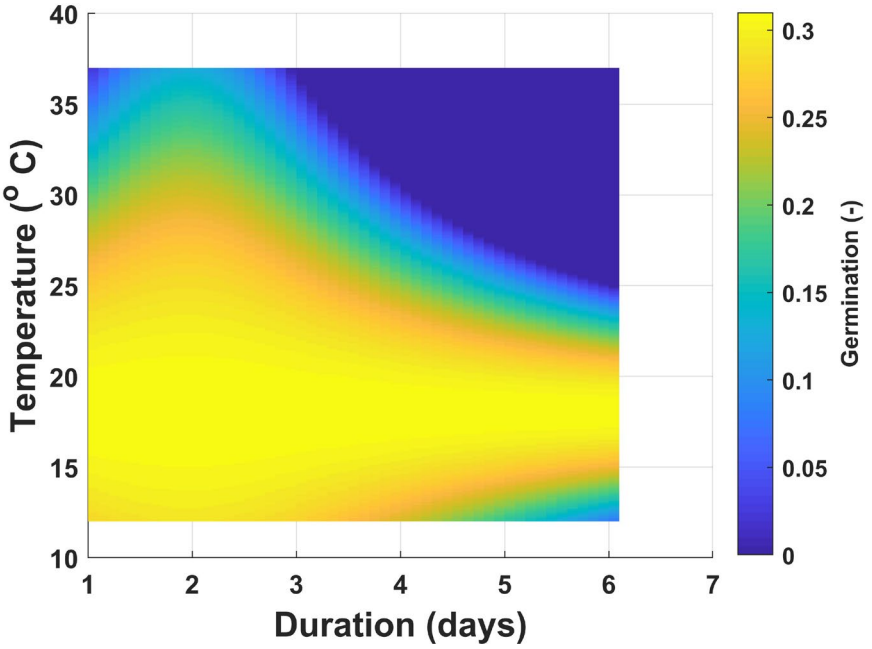

Figure 4.4. *Response surface of the predicted pollen germination values of plants grown at different temperature stress (14, 18, 30, 34 °C) and different durations (0, 1, 3, 4 or 6 days). Model is described by the regression line:* $f_{germPollen}(T, D) = max\left[0, p_g(D) + \frac{2(\alpha_g - p_g(D))}{\beta}T - \frac{(\alpha_g - p_g(D))}{\beta^2}T^2\right]$ *where* $\beta = 18$, $\alpha_g = 0.31$, *and* $p_g(D) = -0.1144 + 0.4354D - 0.2694D^2$. *RMSE = 0.04(-).*

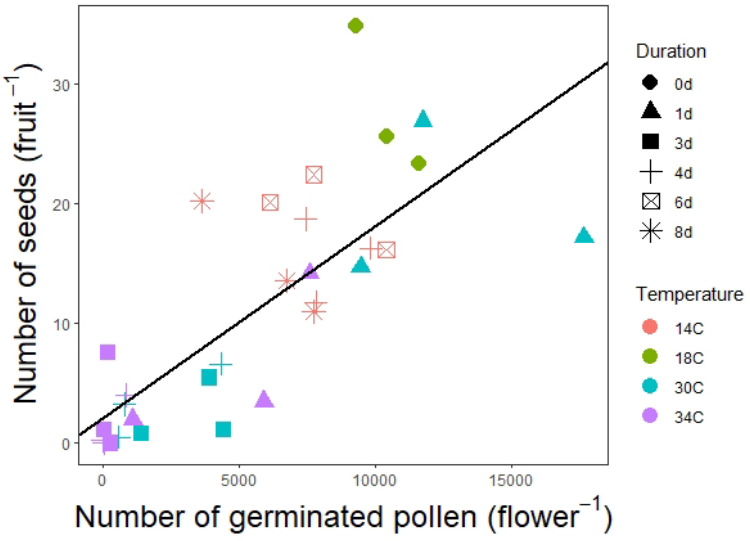

***Figure 4.5**. Relationship between number of seeds and number of germinated pollen for 4 temperatures and different durations. Data are symbols and regression line:* $N_{seeds} = 0.0016 \cdot N_{germPollen} + 2.2351$. $R^2 = 0.56$. *Data are means of 3 blocks with 4 or 6 replicate plants per block and averaged over truss 2 and truss 3 (so each value is based on 36 plants).*

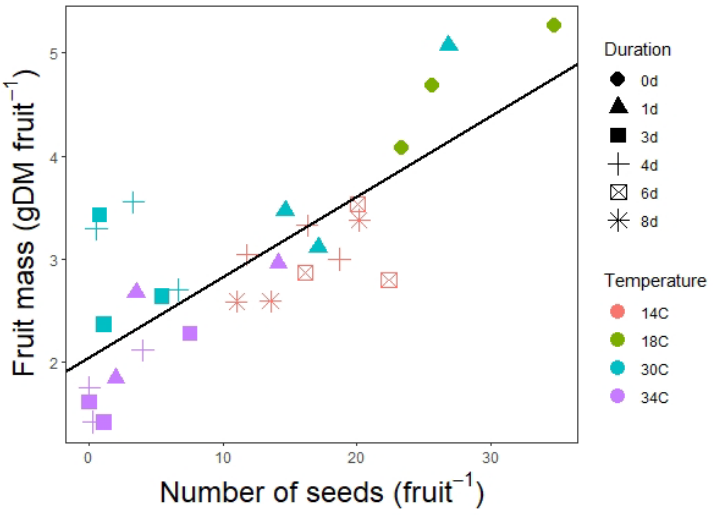

***Figure 4.6.** Relationship between number of seeds and fruit mass for 4 temperatures and different durations. Data are symbols and regression line:* $M_{fruit} = 0.078 \cdot N_{seeds} + 2.06$. $R^2 = 0.62$. *Data are means of 3 blocks with 6 replicate plants per block and averaged over truss 2 and truss 3 (so each value is based on 36 plants).*

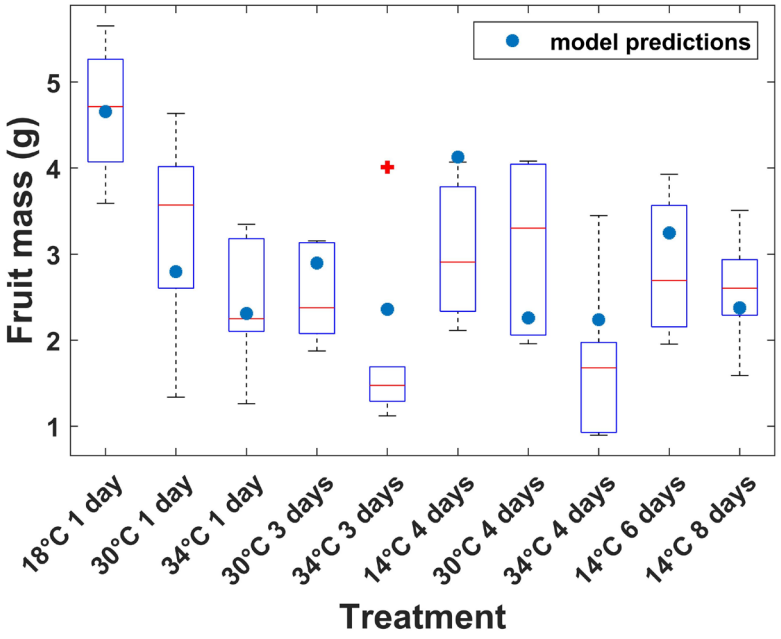

Figure 4.7*. Measured and predicted fruit mass in tomato plants. Fruit mass was simulated as a function of temperature and duration according to Eq. 4.13. Box plots are data from 3 blocks with 6 replicate plants per block and averaged over truss 2 and truss 3 (so each box plot represents 36 data points). RMSE = 0.95 g. The + sign indicates an outlier in the data.*

4.4 Discussion

4.4.1 Pollen formation is more sensitive to cold temperatures than warm temperatures

Exposure to low temperatures (14 °C) produced a similar amount of pollen compared to exposure to high temperatures (30 °C), suggesting that pollen formation is more sensitive to cold stress than heat stress. This could be attributed to the fact that low temperatures slow down metabolic processes and cellular activity, including cell division (Chaturvedi et al., 2021; Ohnishi et al., 2010). However, a reduction of pollen at low temperatures did not correlate to number of seeds, fruit set or fruit mass (Figure A 4.5, Figure A 4.6). This suggest that the number of pollen does not play a crucial role in determining yield. Sato et al. (2000) also found a reduced number of pollen at high temperatures and no correlation between total number of pollen and fruit set. However, this response may be species dependant as Prasad et al., (1999) found a positive correlation between pollen production and fruit set in groundnut.

4.4.2 Pollen viability and germination can explain the variation observed in number of seeds and fruit mass, but not in fruit set

Temperature stress reduced pollen viability and germination. This agrees with observations in tomato (Pham et al., 2020; Sato et al., 2001), groundnut (Prasad et al., 1999), cowpea (Ahmed et al., 1992), and wheat (Bheemanahalli et al., 2019; Osman et al., 2021). The reduction in viability and germination increased with duration of the temperature stress. Heat stress might cause early tapetum degradation, which is a layer of nutritive cells vital for the nutrition of pollen (Chaturvedi et al., 2021). Premature tapetum degradation leads to reduced nutrient translocation and ultimately, sterility (Ahmed et al., 1992). Heat stress can negatively impact pollen germination by reducing the starch content of the pollen, causing a shortage of energy resources needed for germination (Firon et al., 2006; Pressman, 2002). Cold stress can also result in decreased starch content (Kiran et al., 2021) and interfere with cell expansion and cell wall formation during meiosis, leading to a decreased fertility (Chaturvedi et al., 2021; Ohnishi et al., 2010).

Pollen germination is considered a critical factor in determining fruit set (Sato et al., 2000a). However, our results did not show a correlation between pollen germination and fruit set (Figure A 4.7). A positive correlation was found between the number of seeds and the number of pollen germinated (Figure 4.5). These results suggest that heat stress lowers the probability of obtaining seeded fruits due to fewer viable pollen

capable of fertilizing the ovules, rather than through a reduction in pollen number. This result is logical because if pollen grains are unable to germinate, ovule fertilization will be prevented, leading to impaired seed development (Thakur et al., 2010). Hence, we conclude that pollen quality (i.e., viability and germination) rather than the amount of pollen produced per flower, determines number of seeds in this tomato genotype.

4.4.3 Number of seeds and fruit mass

Number of seeds (as a function of number of germinated pollen) can explain the observed variation in fruit mass (Figure 4.6). A linear relationship between number of seeds and fruit mass has been previously observed in sweet pepper (Marcelis et al., 1997) and tomato (Sato et al., 2001). The developing seeds have two functions in the early developmental stages of fruit growth: first, they favour assimilate supply to fruit acting as 'sinks' (Bangerth & Ho, 1984; Varga & Bruinsma, 1976) and second, they trigger the fruit developmental program through the activation of auxin and gibberellin signalling pathways (De Jong et al., 2009; Peet et al., 1997). Although fruit mass positively correlates with the number of seeds, this relationship can reach a saturation at high seed numbers (e.g. Bakker 1989, Table 5) because of different factors such as competition between fruits or sink strength of the fruit itself. However, in our case, we were still within the linear range of the relationship between seed number and fruit mass, and saturation was not reached. Marcelis et al., (1997) found that at low seed numbers, fruit set is positively correlated with seed number. However, our results did not align with this, as no correlation was found between fruit set and the number of seeds (Figure A 4.8).

4.4.4 The effect of temperature on fruit set is independent to the effect of temperature on pollen quality

Fruit set can be described as a quadratic function of temperature (Figure A 4.4) however, there is only a weak association between fruit set and both number of seeds and fruit mass (Figure A 4.8, Figure A 4.9). Thus, we can conclude that for our cultivar, the effect of temperature on fruit set is independent to the temperature effect on pollen quality. This is in line with the understanding that fruit set and fruit growth can occur without pollination (parthenocarpy) through hormonal regulation triggered during flowering (Pandolfini et al., 2009), while seed development requires successful fertilization, which includes formation of viable pollen, germination of the pollen tube, and the delivery of sperm cells (Ruan et al., 2012). Since the temperature effect on fruit set was independent from the effect on pollen quality, this process was not considered in our model to predict number of seeds and fruit mass. Instead, we

modelled fruit set only as a function or temperature (Figure A 4.4) independent of pollen quality, in order to estimate yield per truss. This approach can be useful for tomato cultivars where fruit set and pollen quality are affected differently, and where a reduction in yield can result from decreased fruit set, smaller individual fruit size, or a combination of both factors.

As an example, our model predicts that exposing plants to 30°C for 4 days will result in an individual fruit mass of 2.9 g and to a relatively high fruit set fraction of 0.9. Given that trusses can have a maximum of 9 flowers per truss, this would yield ~ 23.2 gDM per truss. Contrary, model predictions of plants exposed to 14 °C for 4 days, will result in a higher individual fruit mass of ~ 3.2g, compared to heat stress. However, the fruit set prediction for this plants is 0.7, this yields 20.1 gDM per truss. This example demonstrates that when plants are exposed to heat stress or cold stress for four days, their yield per truss is similar. However, under heat stress (30 °C), the reduction in truss yield is due to lower individual fruit mass, while under cold stress conditions (14 °C), the truss yield reduction is caused by both reduced fruit set and individual fruit mass, compared to optimal temperature. Our results suggest that relying solely on temperature effects on fruit set to predict yield can be inaccurate. Other factors such as reduced fruit size, due to lower number of seeds per fruit, should also be considered to improve the accuracy of yield predictions.

4.4.5 Sensitive period for fruit set and pollen development during temperature stress

Sato et al., (2002) found that tomato flowers were the most susceptible to elevated temperature stress 8 to 13 days before anthesis, which corresponds with the stage of pollen formation. Surprisingly, only pollen viability was affected by the stage at which temperature stress was applied (Table A 4.3). High temperature applied 4 to 8 days prior to anthesis resulted in a larger reduction in pollen viability compared to applying high temperature at anthesis. Neither pollen production nor pollen germination were influenced by the stage at which temperature stress was applied (Table A 4.3), although they were much lower compared to control conditions (18 °C). The only remarkable exception was at very high temperatures (34 °C) applied at 8 days before anthesis, which reduced pollen production by almost 72%. In a commercial tomato production, there are multiple trusses on a plant and each of these is in a different developmental stage. Therefore, it is important to identify which trusses are in the most sensitive stage when a short period of high temperature stress occurs to determine and predict accurately the fate of a flower and the impact on yield (Kang et al., 2010).

4.4.6 Towards prediction of fruit-set, seed set and fruit mass in crop models

Quantifying the effects of temperature and other environmental factors on fruit set is critical for accurate yield prediction in fruit crops (Liu et al., 2020). However, the limited research on the effects of temperature over a broad range of non-optimal temperatures and duration of these non-optimal temperatures has limited the potential of simulation models. To bridge this gap, our research synthesizes the results into a simple quantitative model that includes different of pollen development and links them to seed set and fruit growth. Currently, the model overestimates fruit mass under prolonged exposure (4 days) to very high temperatures (34 °C). Although there is not a large variation in the data at that specific treatment (Figure 4.7), a better estimation of the relationship between seed number and fruit mass is needed at very low or zero seed count (see Figure 4.6). Furthermore, to evaluate the predictive power of the model, we need independent data for validation, which would enable us to assess how well the model generalizes to new data beyond the calibration dataset.

In the context of greenhouse climate control, it has been long recognized that flexible climate control can lead up to a reduction in the greenhouse energy consumption by up to 20% (Körner & Challa, 2003; Van Beveren et al., 2015). However, these studies frequently neglect the effect on crop yield itself or lack explicit simulation of fruit and seed set. This raises questions: how realistic is in practice the suggested energy reduction? For example, in **Chapter 3** of this thesis we found that vegetative tomato plants can integrate temperature fluctuations of ± 10 ºC over a period of 20 days without major reductions in growth. However, fruiting plants are predicted to show a decrease in the number of seeds of 40% according to our model which would lead to a reduction in yield per truss of ~33 % compared with optimal temperature. This highlights the relevance of incorporating the impact of temperature on the processes that determine successful fruit and seed set and growth into crop models for an accurate prediction of yield, specially under temperature stress. To optimally determine the temperature boundaries in the greenhouse, the control algorithm must weigh the presence of flowers and the impact of temperature fluctuations against economic losses from harvesting smaller fruits or a reduced number of fruits. A model that accurately predicts the number and mass of the fruits is crucial for the control algorithm to make informed decisions while balancing the costs of maintaining optimal temperature conditions against deviating from it.

4.5 Conclusions

The aim of this chapter was to develop a quantitative model to predict fruit mass, seed and fruit set based on the effects of temperature stress and duration of the stress on pollen quality. Number of seeds, influenced by pollen quality was a major factor in determining fruit mass. However, as fruit set did not correlate with pollen quality, it was not included in the fruit mass prediction model. Instead, fruit set was modelled independently as a function of temperature. At low temperatures, yield reduction was a result of both reduced fruit set and smaller fruit size, whereas at high temperatures (30°C), reductions in yield were primarily due to lower seed number, although this response might be cultivar dependent. Our model provides valuable insights into the effects of temperature stress and duration of the stress on seed set and fruit mass, can inform decisions regarding temperature control to maximize yields or to improve energy use.

4.6 Acknowledgements

We are grateful to Gerrit Stunnenberg, David Brink, and Jannick Verstegen for their help with crop management and technical support. Thanks to David Katzin for the feedback on the Materials and Methods section. We also thank Pinglin Zhang and Marloes Rodewijk for their help with growth and pollen measurements, and to Julieta Zepeda for her help with pollen counting.

4.7 Appendices

4.7.1 Appendix A: Derivation of the N_{pollen} function

Because we did not observe a clear effect of duration of the temperature stress on the number of pollen, we modelled the effect of temperature on pollen number with the following quadratic function:

$$N_{pollen} = p_1 + p_2 T + p_3 T^2 \quad \text{A4.1}$$

Where $y_{Npollen}$ is the number of pollen in a flower and T is temperature (°C). We have 3 boundary conditions:

1. Number of pollen is maximal at $\beta = 18$ °C.
2. The maximum number of pollen in a flower is $\alpha_{np} = 63853$ (determined experimentally)
3. The number of pollen cannot be negative

Condition 1 results in the requirement that $\frac{dN_{pollen}}{dT}(\beta) = 0$, whereas condition 2 is associated with the requirement that $N_{pollen}(\beta) = \alpha_{np} = 63853$.

Derivation of Eq. A4.1 results in

$$p_3 = -\frac{1}{2\beta} p_2 \quad \text{A4.2}$$

And condition 2, combined with Eq. A4.2, results in

$$p_2 = \frac{2(\alpha_{np} - p_1)}{\beta} \quad A4.3$$

Inclusion of condition 3, treating β as fixed at 18°C, and denoting $p_1 = p_{np}$, yields a model with one degree of freedom (parameter p_{np} to be fitted to the data):

$$N_{pollen}(T) = \max\left[0, p_{np} + \frac{2(\alpha_{np} - p_{np})}{\beta} T - \frac{(\alpha_{np} - p_{np})}{\beta^2} T^2\right] \quad A4.4$$

4.7.2 Appendix B: Derivation of the $f_{viablePollen}$ and $f_{germPollen}$

To model pollen viability, we first followed the steps described above (Eq. A4.1, Eq. A4.2, and Eq. A4.3) for each duration to obtain parameter p at durations 1, 3, 4 and 6 days.

The 3 boundary conditions for$f_{viablePollen}$ were:

1. Fraction of viable pollen is maximal at $\beta = 18$ °C.
2. The maximum fraction of viable pollen is $\alpha_v = 0.94$ (determined experimentally)
3. The fraction of viable pollen cannot be negative

Next, the quadratic function (Eq. A4.4) was fitted to 4 data sets separately, where each data set contained measured viability fractions under different temperatures while keeping the duration of the temperature stress fixed. Altogether this resulted in 4 curves, each associated with a different parameter value p (Figure A4.1).

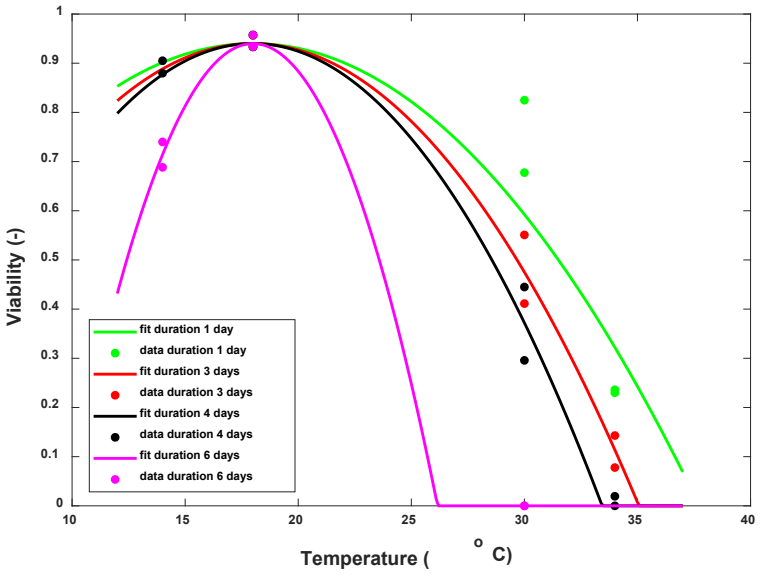

Figure A4.1. *Relationship between temperature and viability of tomato flowers grown at different durations of stress. Dots are measured data from flowers where stress was applied 4 and 8 days before anthesis. Model is described by the regression function* $f_{viablePollen}(T) = max\left[0, p_v + \frac{2(\alpha_v - p_v)}{\beta}T - \frac{(\alpha_v - p_v)}{\beta^2}T^2\right]$..

Next, the model was extended to describe viability as a function of duration of the temperature stress. For this, the relationship between the duration of the stress D and the derived parameter p was stablished by fitting a quadratic expression through the 4 values of D and the related estimated value for p. This relationship between parameter p and the stress duration D was denoted $p_v(D)$. Here, v stands for viability, as p is a parameter for the curve representing the relationship between temperature and pollen viability

$$p_v = \theta_{v1} + \theta_{v2}D + \theta_{v3}D^2 \qquad A4.5$$

where D denotes duration in days.

The fit is shown in Figure A4.2.

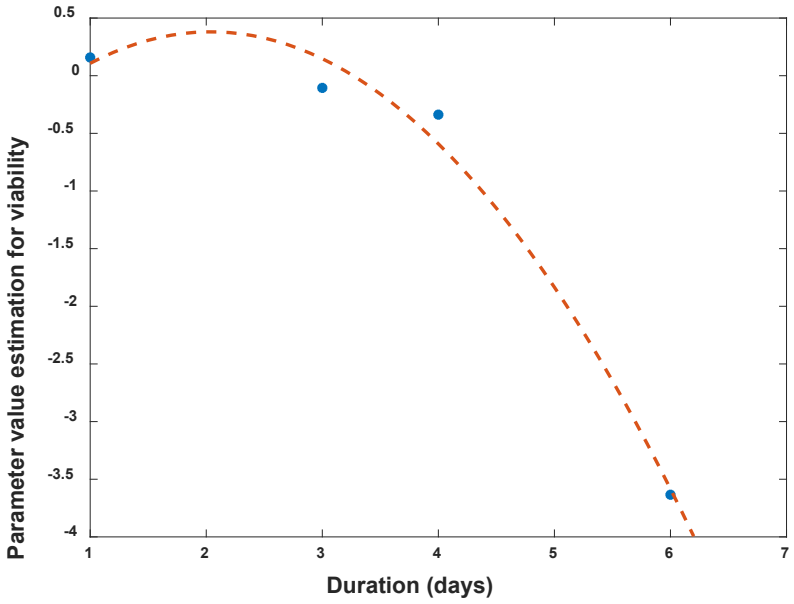

Figure A4.2. *Parameter (p) estimation for viability at different durations. Red dotted line is the polynomial function:* $p_v(D) = -0.2527 + 1.0308D - 0.6706D^2$. *Blue dots are data measured for viability at durations 1, 3,4 and 6 days.*

Combining Eq. A4.4 and Eq. A4.5 gives the final model for viability as function of temperature T and duration D:

$$f_{viablePollen}(T, D) = \max\left[0, p_v(D) + \frac{2(\alpha_v - p_v(D))}{\beta}T - \frac{(\alpha_v - p_v(D))}{\beta^2}T^2\right] \quad A4.6$$

$$p_v = \theta_{v1} + \theta_{v2}D + \theta_{v3}D^2 \quad A4.7$$

4.7.3 Appendix C: Derivation of the $f_{germPollen}$

To model pollen viability fraction $f_{germPollen}$, we followed the same procedure as for $f_{viablePollen}$ but following 3 boundary conditions:

1. Fraction of pollen germination maximal at $\beta = 18$ °C.
2. The maximum fraction of pollen germination is $\alpha_g = 0.31$ (determined experimentally)
3. The fraction of pollen germination cannot be negative

Here the subscript g for parameters p and θ which stands for germination.

4.7.4 Appendix D: Additional figures and tables

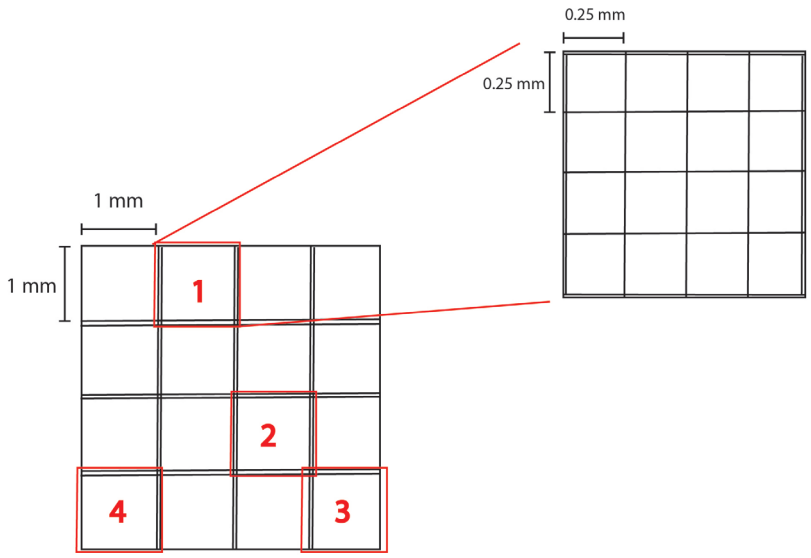

Figure A 4.3. *Schematic representation of the Fuchs-Rosenthal haemocytometer (4 x 4 x 0.4 mm grid, 3.2 mm3). The counting chamber was divided into 16 large squares (1 x 1 mm, 1 mm^2), and each square was further divided into16 small squares (0.25 x 0.25 mm, 0.0625 mm^2). Two large squares (1 mm^2) were randomly selected per load, and pictures were made, to further count the pollen with a cell counter plugin of Fiji - ImageJ (version 1.53c). For each sample (each flower), the haemocytometer was loaded two times, (therefore the average pollen number per sample is based in a total of 4 pictures)*

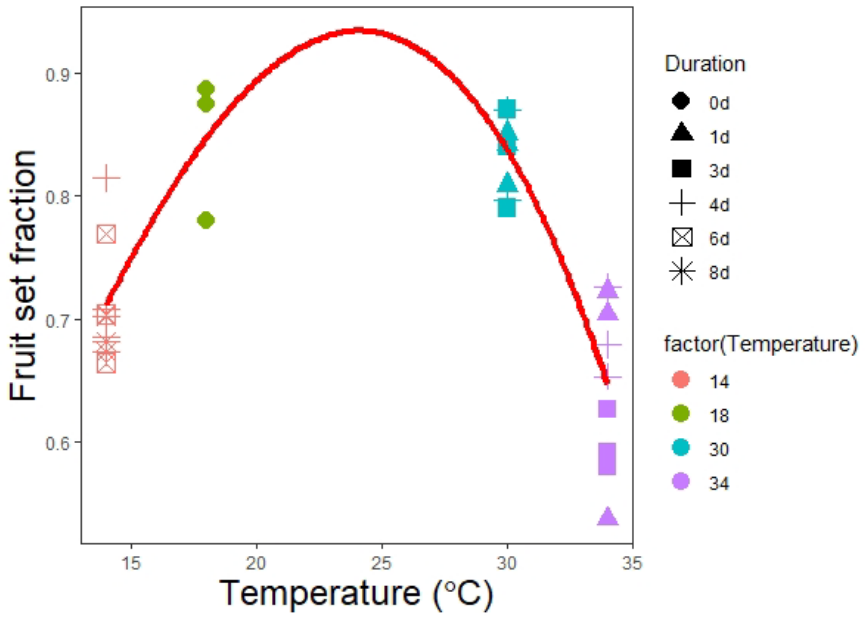

Figure A 4.4. *Relationship between temperature and fruit set fraction. Dots are measured data from flowers where stress was applied at anthesis and 4 and 8 days before anthesis. Data are means of 3 blocks with 4 replicate plants per block and averaged over truss 2 and truss 3 (so each value is based on 24 plants). Line is the model prediction. Line is described by the regression function* $y = -2.65 \times 10^{-3}T^2 + 1.24 \times 10^{-1} - 5.14 \times 10^{-1}$.

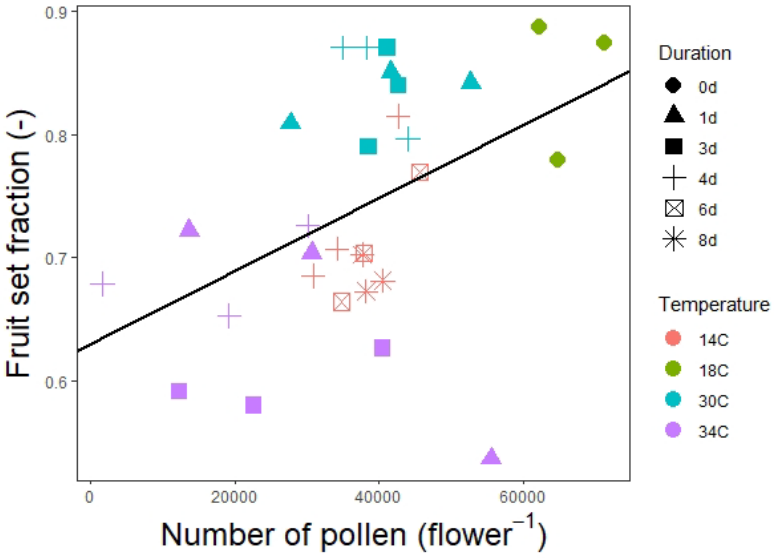

***Figure A 4.5**. Relationship between fruit set fraction and number of pollen per flower for 4 temperatures and different durations. Data are symbols and regression line:* $y = 2.96 \times 10^{-6} \cdot m + 0.6318$. $R^2 = 0.181$.

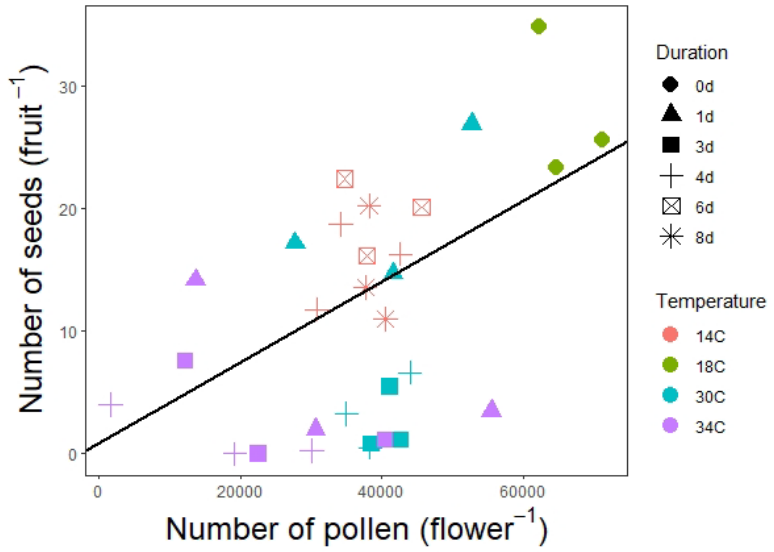

***Figure A 4.6.** Relationship between number of seeds and number of pollen per flower for 4 temperatures and different durations. Data are symbols and regression line:* $y = 3.29 \times 10^{-4}x - 0.95$. $R^2 = 0.23$.

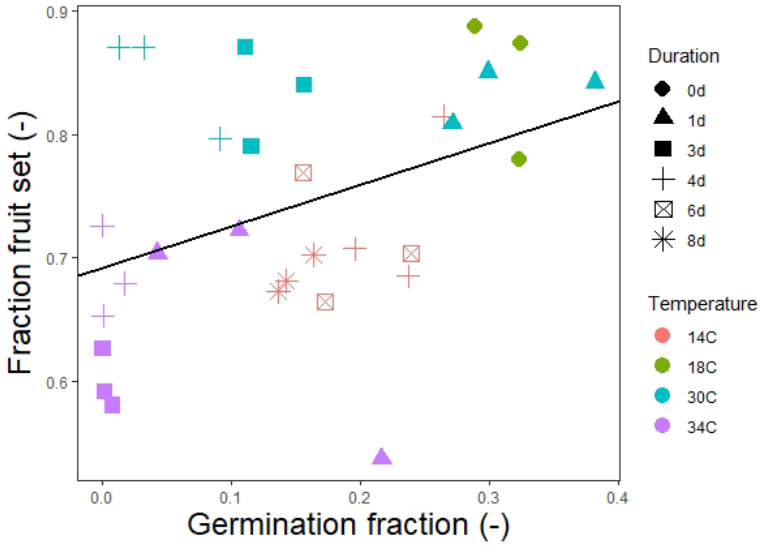

***Figure A 4.7**. Relationship between fruit set fraction and germination fraction for 4 temperatures and different durations. Data are symbols and regression line:* $y = 0.3386x + 0.6923$. $R^2 = 0.13$.

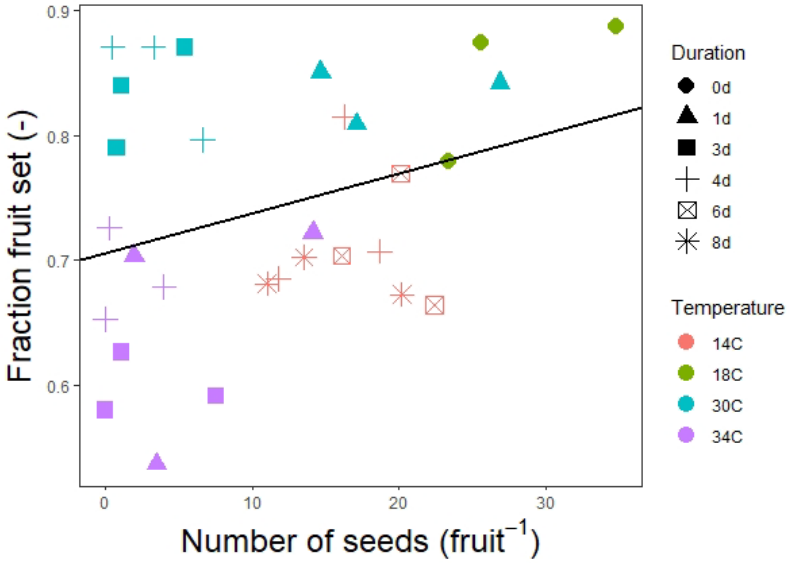

***Figure A 4.8**. Relationship between fruit set fraction and number of seeds for 4 temperatures and different durations. Data are symbols and regression line:* $y = 0.0032x + 0.7063$. $R^2 = 0.07$.

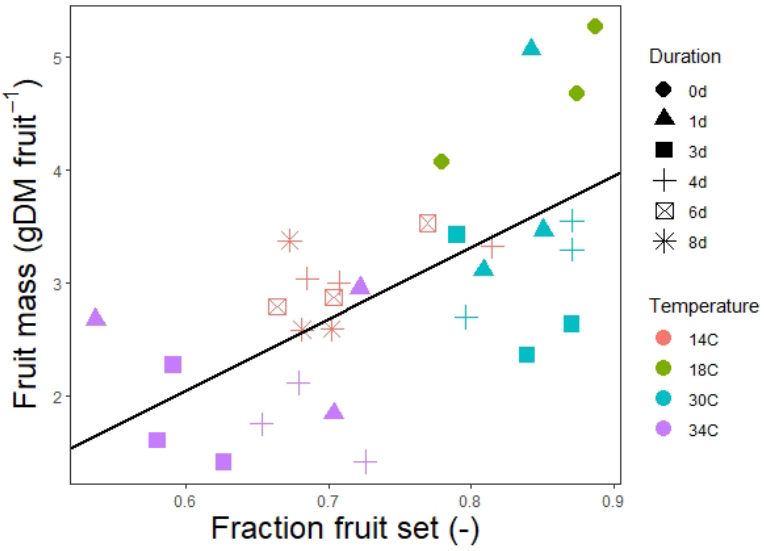

Figure A 4.9. *Relationship between fruit mass and fruit set fraction for 4 temperatures and different durations. Data are symbols and regression line:* $y = 6.346x - 1.75$. $R^2 = 0.39$.

Table A 4.1. *Interaction effect of temperature × duration on pollen number per flower, pollen viability fraction, pollen germination fraction, fraction of fruit set, fruit weight and number of seeds per fruit. Data are means of 3 blocks with 4 or 6 replicate plants per block and averaged over truss 2 and truss 3 (so each value is based on 24 plants).*

Duration	Temperature (ºC)	Pollen number	Viability fraction	Germination fraction	Fruit set fraction	Fruit weight	Number of seeds
Constant	18	63,467	0.95	0.31 d	0.83	4.7	29
1 day	30	34,661	0.75	0.29 d	0.83	3.3	16
	34	22,151	0.23	0.07 ab	0.71	2.398	8.0
3 days	30	41,922	0.48	0.13 bc	0.85	2.5	3.2
	34	26,365	0.11	0.001 a	0.61	1.8	4.3
4 days	14	32,484	0.89	0.22 cd	0.70	3.0	15
	30	39,474	0.37	0.07 ab	0.83	3.1	4.9
	34	15,854	0.009	0.01 a	0.70	1.8	2.1
6 days	14	36,344	0.74	0.21 cd	0.68	2.8	19
8 days	14	39,078	0.73	0.15 bc	0.69	2.6	12
F-probability interaction (temperature × duration)		0.596	0.235	0.018	0.378	0.609	0.341
Standard error of the mean (SEM)		6,691	0.0521	0.0279	0.07	0.400	4.352

Table A 4.2. *Temperature effect on pollen number per flower, pollen viability fraction, pollen germination fraction, fraction of fruit set, fruit weight and number of seeds per fruit. Data are means of 3 blocks with 4 or 6 replicate plants per block and averaged over truss 2 and truss 3 (so each value is based on 24 plants).*

Temperature (ºC)	Pollen number	Viability fraction	Germination fraction	Fruit set fraction	Fruit weight	Number of seeds
14	34,575 b	0.82 c	0.20	0.69 ab	2.90 b	15.4 b
18	63,467 c	0.95 c	0.31	0.83 bc	4.67 c	29.0 c
30	38,798 b	0.51 b	0.13	0.83 c	2.99 b	7.60 a
34	20,656 a	0.10 a	0.02	0.67 a	1.97 a	4.45 a
F-probability main effect (temperature)	<0.001	<0.001		<0.001	<0.001	<0.001
Standard error of the mean (SEM)	4,204	0.05	0.023	0.05	0.40	3.36

Table A 4.3. *Effect of the stage at which temperature is applied (30 °C, 34 °C or 14 °C) on pollen number, viability, and germination. Data are means of 3 blocks with 4 replicate plants per block and averaged over all durations (so each value is based on 36 plants except for the control which is 12).*

Pollen number				
Period	**18 °C**	**30 °C**	**34 °C**	**14 °C**
Anthesis	71,236	43,188	32,417 b	42,139
4 days before anthesis	62,187	39,767	33,743 b	35,465
8 days before anthesis	64,747	37,604	9,170 a	36,472
F-probability period	0.93	0.683	0.007	0.558
Standard error of the means (SEM)	24,265	6,398	7,841	6576
Viability				
Period	**18 °C**	**30 °C**	**34 °C**	**14 °C**
Anthesis	0.93	0.80 b	0.52 b	0.87 b
4 days before anthesis	0.94	0.56 a	0.13 a	0.80 ab
8 days before anthesis	0.96	0.51 a	0.10 a	0.76 a
F-probability	0.467	0.012	0.002	0.091
Standard error of the mean (SEM)	0.0204	0.095	0.1133	0.0510
Germination				
Period	**18 °C**	**30 °C**	**34 °C**	**14 °C**
Anthesis	0.32	0.20	0.09	0.19
4 days before anthesis	0.29	0.16	0.01	0.21
8 days before anthesis	0.32	0.14	0.04	0.17
F-probability	0.249	0.828	0.322	0.309
Standard error of the mean (SEM)	0.0211	0.0874	0.0544	0.0278

Modelling soluble sugars and starch dynamics in plants under fluctuating light and temperature conditions

Ana Cristina Zepeda, Stefan Vorage, Simon van Mourik, Ep Heuvelink, Leo F.M. Marcelis

Chapter 5

Abstract

The storage and remobilization of non-structural carbohydrate (NSC) allow plants to support growth during periods of asynchrony between carbon (C) supply (source strength) and C demand (sink strength). This asynchrony is strongly influenced by changes in light and temperature. NSC consists of starch, which serves as a long-term reserve of C, and soluble sugars, which are used either to satisfy immediate respiratory needs or are transported to sink organs. Because starch and sugars have distinct functions and respond differently to environmental conditions, it is crucial to explicitly differentiate between these two pools in models to accurately predict the effect of NSC on growth. The aim of this study is to develop a plant growth model that can explain the day-to-day variations in starch, soluble sugars, and structural growth of vegetative plants under fluctuating conditions of light and temperature. To achieve this, we extended the existing crop growth model by separating the non-structural carbohydrate pool into a soluble sugar and starch pool. The interconversion between starch and soluble sugars was described by a kinetic reversible reaction. The simple structure of the model, consisting of only three states and 19 parameters, makes it suitable to be used in optimal control. The model accurately predicted growth in all conditions except for high light intensities and low temperatures. Under these sink-limited conditions, the model overestimated structural dry mass and underestimated starch concentration. The model can be improved by incorporating the direct influence of temperature on meristem activity or also consider the rate of starch degradation into soluble sugars.

5.1 Introduction

Non-structural carbohydrate (NSC) storage plays an essential role in productivity of plants (Dietze et al., 2014). As there is no perfect match in timing of NSC acquisition and their utilization for growth and respiration, NSC must be temporarily stored (Goudriaan & van Laar, 1992). Therefore, the NSC pool acts as a 'buffer' whenever there is asynchrony between source activity (i.e., photosynthesis) and sink activity (i.e., utilization of NSC). NSC—including glucose, fructose, sucrose, and starch—are produced via photosynthesis, then partitioned among processes such as respiration, structural growth, reproduction, storage and defence (Chapin et al., 1990; Huang et al., 2019). Structural carbon (SC) is fixed in plant structure and cannot be reused in the future (Furze et al., 2018; Hilty et al., 2021). Furthermore, soluble sugars and starch serve different functions in the plants (MacNeill et al., 2017). The allocation of newly assimilated NSC between starch and soluble sugars are key processes in the dynamic process of NSC storage (Smith & Stitt, 2007; Chapter 2 of this thesis). Annual crops commonly store C in the form of starch, utilizing the stored energy to support resprouting in spring (Clarke et al., 2013; Wiley et al., 2019) or to fill grains in cereals (Pollock & Cairns, 1991). Starch is also an important diurnal C reserve in herbaceous plants as a fraction of starch is stored during the day to meet the C demand during the following night (Graf & Smith, 2011; Stitt & Zeeman, 2012). Another fraction of C is allocated to soluble sugars for the immediate respiratory and growth needs (MacNeill et al., 2017b; Ruan, 2014). Soluble sugars also contribute to sustaining osmotic balances (Talbott & Zeiger, 1998), act as signalling molecules for regulating gene expression, for crosstalk with hormones (Ruan, 2014), and are also used as transport sugar (sucrose) (Hartmann & Trumbore, 2016).

The relative fraction of NSC partitioned into starch is strongly dependent on photoperiod but weakly dependent on light intensity (Chatterton & Silvius, 1980; Mengin et al., 2017; Pilkington et al., 2015). Therefore, in shorter days, a larger fraction of C is allocated into starch to anticipate the long night (Graf & Smith, 2011). This process is regulated via the circadian clock (Seki et al., 2017). Starch accumulation can also occur via the overflow mechanisms that is triggered when soluble sugar levels are too high (Stitt, 1996), for example under high light intensities and low temperatures (Pommerrenig et al., 2018; Ruelland et al., 2009; Thalmann & Santelia, 2017). When the supply of carbohydrates from photosynthesis is greater than the demand for growth, the surplus can be stored as NSC, adding to total biomass but not to structural mass (Gent & Seginer, 2012). High starch levels in leaves can further lead to an inhibition of photosynthesis through a decrease in the phoptosynthetic gene expression (Paul & Foyer, 2001). At low light intensities, the net production of

assimilates might not meet the net demand of assimilates, thereby limiting plant growth (Smith & Stitt, 2007). When low light intensities coincide with high temperatures, there can be a depletion in NSC due to an increased demand for energy for respiration and growth, coupled with low assimilate supply under low light intensity (Atkin & Tjoelker, 2003).

Crop growth models are essential in decision support systems, greenhouse climate control and prediction and planning of production (Marcelis et al., 1998). Most crop production models are driven by the effect of shoot environment on gross photosynthesis and respiration over a day (Poorter et al., 2013). Growth is then modelled as the net result of daily C input from photosynthesis minus C lost in respiration (Spitters et al., 1987). However, this approach assumes that all carbohydrates are immediately used for growth and maintenance, ignoring the temporary storage of C when supply exceeds demand. This oversimplification may not accurately capture growth patterns on a day-to-day basis.

A more accurate analysis of C gain and losses over the diurnal cycle should consider the asynchrony between the timing of acquisition and utilization of NSC (Goudriaan & Van Laar, 1992). Van Henten (1994) separated the NSC pool from structural growth in his lettuce model. A limitation of this model is that growth is restricted to the light periods and does not include knowledge in how C is used for metabolism and growth at night. Only in cases of excess daytime NSC accumulation assimilates are stored transiently for the next light period. Additionally, this model has only been partially validated it with respect to total dry weight, but not for the NSC. This raises questions about the validity of the model to predict NSC content in plants. Although, Gent & Seginer (2012) explicitly included a NSC pool in their growth model and successfully validated it for predicting total dry weight and NSC in tomato, sunflower, and wheat under constant environmental conditions, it falls short in predicting diurnal growth patterns. This is because in their model, there is no conservation of carbohydrates until dawn. Instead, their model partitions C into structure with a daily time step based on the supply and demand of carbohydrate for the entire day.

Environmental stress can lead to a shift in C allocation towards starch at the expense of structural growth (Dietze et al., 2014; Gessler & Grosser, 2019; Huang et al., 2019; Mengin et al., 2017). To the best of our knowledge, no crop model has yet separated the NSC pool into a starch pool and a soluble sugar pool, despite their distinct functions. An exception is the model developed by Rasse & Tocquin, (2006a) which predicts structural growth, soluble sugars, and starch concentrations of *Arabidopsis* grown at high CO_2 levels. However, it relies on several parameters (i.e., baseline starch production coefficient, minimum sugar in leaves, proportion of night-time

starch breakdown) determined in their own study using *Arabidopsis* plants, which may not be applicable to other plant species. Additionally, the previous model's assumption of a fixed proportion of night-time starch breakdown limits the applicability of the model, not being able to consider fluctuating environments such as different daylengths.

The aim of this paper was to develop a plant growth model that can explain the day-to-day variations in observed starch, soluble sugars, and structural mass of vegetative plants grown under day-to-day fluctuations in light and temperature. To achieve this, we extended the existing crop growth model published by Van Henten (1994) by separating the NSC pool into a starch pool and a soluble sugar pool. The interconversion between starch and soluble sugars was described by a kinetic reversible reaction. We evaluate to what extent the model can explain the dynamics of these three states (starch, soluble sugars, and structural mass) observed for plants grown at different temperature and light fluctuations.

5.2 Materials and methods

5.2.1 Model description (3 state model)

To describe the dynamics between starch and soluble sugars dynamics in the leaf, we propose a kinetic reversible reaction where soluble sugars (X_{Sol}, $gCH_2O\ m^{-2}$) turns into starch (X_{Starch}, $gCH_2O\ m^{-2}$) with a rate constant k_1 (s^{-1}) and the reversible conversion (from starch to soluble sugars) has a rate constant of k_2 (s^{-1}), so that parameters k_1 and k_2 characterize the interconversion between soluble sugars and starch based on (Luo et al., 2020):

$$X_{Sol} \underset{k_2}{\overset{k_1}{\rightleftharpoons}} X_{Starch}$$

In this model, plant dry mass is divided in three states: soluble sugars (X_{Sol}, $gCH_2O\ m^{-2}$), starch (X_{Starch}, $gCH_2O\ m^{-2}$), and structural dry mass (X_{Struct}, $gCH_2O\ m^{-2}$). The dynamic model (Eq. 5.1, Eq. 5.2, and Eq. 5.3) is described by

$$\frac{dX_{Sol}}{dt} = (-k_1 \cdot X_{Sol} + k_2 \cdot X_{Starch}) + c_\alpha \phi_{phot} - \phi_{MainResp} - \phi_{StructGrowth} - \phi_{GrowthResp} \quad 5.1$$

$$\frac{dX_{Starch}}{dt} = -k_2 . X_{starch} + k_1 . X_{Sol} \quad 5.2$$

$$\frac{dX_{Struct}}{dt} = \phi_{structGrowth} \quad 5.3$$

where ϕ_{phot} is the gross canopy photosynthesis rate (gCO_2 m^{-2} s^{-1}) and c_α is the conversion factor from carbon dioxide into sugar equivalents (gCH_2O gCO_2^{-1}). Gross canopy photosynthesis is calculated in accordance with (Goudriaan & Van Laar, 1978) with the following empirical relation:

$$\phi_{phot} = \phi_{phot,max}(1 - e^{-c_k LAI}) \quad 5.4$$

where c_k is the light extinction coefficient (-), and LAI is the leaf area index (m^2 [leaf] m^{-2} [soil]) and is calculated as

$$LAI = c_{LAR} \cdot X_{Struct} \quad 5.5$$

where c_{LAR} is the 'structural' leaf area ratio (m^2 [leaf] $gSDM^{-1}$) and X_{Struct} (gCH_2O m^{-2}) is the structural crop dry mass.

Maximum canopy photosynthesis $Phot_{max}$ (gCO_2 m^{-2}) is a function of photosynthetically active radiation PAR (µmol[photons] m^{-2} s^{-1}) and carbon dioxide concentration (gCO_2 m^{-3}). This model accounts for photorespiration and temperature effects on the light use efficiency as well as temperature effects on the carboxylation conductance in the leaf:

$$Phot_{max} = \frac{\varepsilon L \sigma_{CO_2}(C_a - \Gamma)}{\varepsilon L + \sigma_{co_2}(C_a - \Gamma)} \quad 5.6$$

in which ε (gCO_2 µmol[photons]$^{-1}$) is the light use efficiency, L (µmol[photons] m^{-2} s^{-1}) is PAR, σ_{CO_2} (m s^{-1}) is the canopy conductance for carbon dioxide transport into the leaves, C_a (g m^{-3}) is the carbon dioxide concentration, and Γ (g m^{-3}) is the carbon dioxide compensation point which accounts for photorespiration at high light levels.

The carbon dioxide compensation point Γ, (g m^{-3}) is a function of air temperature, T (◦C), described by:

$$\Gamma = c_\Gamma c_{q10,\Gamma}^{\frac{T-20}{10}} \quad 5.7$$

in which c_Γ (g m^{-3}) is the carbon dioxide compensation point at 20°C. The temperature effects on Γ are accounted for by a Q10 factor $c_{Q10,\Gamma}$.

The effect of photorespiration on the light use efficiency (gCO_2 µmol[photons]$^{-1}$) is described by:

$$\varepsilon = c_\varepsilon \frac{C_a - \Gamma}{C_a - 2\Gamma} \quad 5.8$$

in which c_ϵ [gCO_2 µmol[photons]$^{-1}$] is the light use efficiency at very high carbon dioxide concentrations (Goudriaan et al., 1985).

The canopy conductance σ_{CO_2} [m s^{-1}] for carbon dioxide transport from the ambient air to chloroplast is determined by three conductance in series

$$\frac{1}{\sigma_{co_2}} = \frac{1}{c_{bnd}} + \frac{1}{c_{stoem}} + \frac{1}{\sigma_{car}} \quad 5.9$$

where c_{bnd}, c_{stoem} and σ_{car} (m s^{-1}) are the boundary layer conductance, the stomatal conductance, and the carboxylation conductance, respectively. The boundary layer and the stomatal conductance are assumed to be constant. The carboxylation conductance is described with by

$$\sigma_{car} = c_{car,1}T^2 + c_{car,2}T + c_{car,3} \quad 5.10$$

Maintenance respiration of the crop $\phi_{mainResp}$, (gCH_2O m^{-2}) is described by

$$\phi_{mainResp} = c_{resp} X_{Struct} c_{Q10,resp}^{\left(\frac{T-25}{10}\right)} \quad 5.11$$

where c_{resp} is the maintenance respiration rate for the shoot 25°C (g CH_2O gDM^{-1} s^{-1}) and $c_{Q10,resp}$ is the Q10 factor of the maintenance respiration.

Structural growth $\phi_{structGrowth}$ (gCH_2O m^{-2} s^{-1}) is the rate in which sugars (Eq. 1) are being used for growth of the structural dry mass. It is calculated as

$$\phi_{structGrowth} = r_{gr} X_{Struct} \quad 5.12$$

where the specific growth rate coefficient r_{gr} (s^{-1}) describes the transformation of soluble sugars to structural dry mass following a Michaelis-Menten relation (Thornley & Hurd, 1976b)

$$r_{gr} = c_{r,gr,max} \left(\frac{X_{sol}}{X_{Sol} + X_{Starch} + X_{Struct}} \right) c_{Q10,gr}^{\frac{T-20}{10}} \quad 5.13$$

where $c_{r,gr,max}$ (s^{-1}) is the saturation growth rate at 20 ºC and $c_{Q10,gr}$ (-) is the Q_{10} factor for growth. The main difference with respect to the two state-model is that here, structural growth rate is dependent to the soluble sugar level, while in the two-state model according to Van Henten (1994), structural growth rate is dependent on the non-structural carbohydrate concentration.

Growth respiration of the crop $\phi_{GrowthResp}$ (gCH$_2$O m^{-2} s^{-1}) is described by:

$$\phi_{GrowthResp} = \frac{1 - c_\beta}{c_\beta} \phi_{StructGrowth} \quad 5.14$$

Where c_β (-) account for the respiratory and synthesis losses during the conversion of carbohydrates to structural material (De Vries et al., 1974).

Total crop dry mass (TDW, gDM m^{-2}) is related to the three states according to the relation:

$$TDW = X_{Sol} + X_{Starch} + X_{Struct} \quad 5.15$$

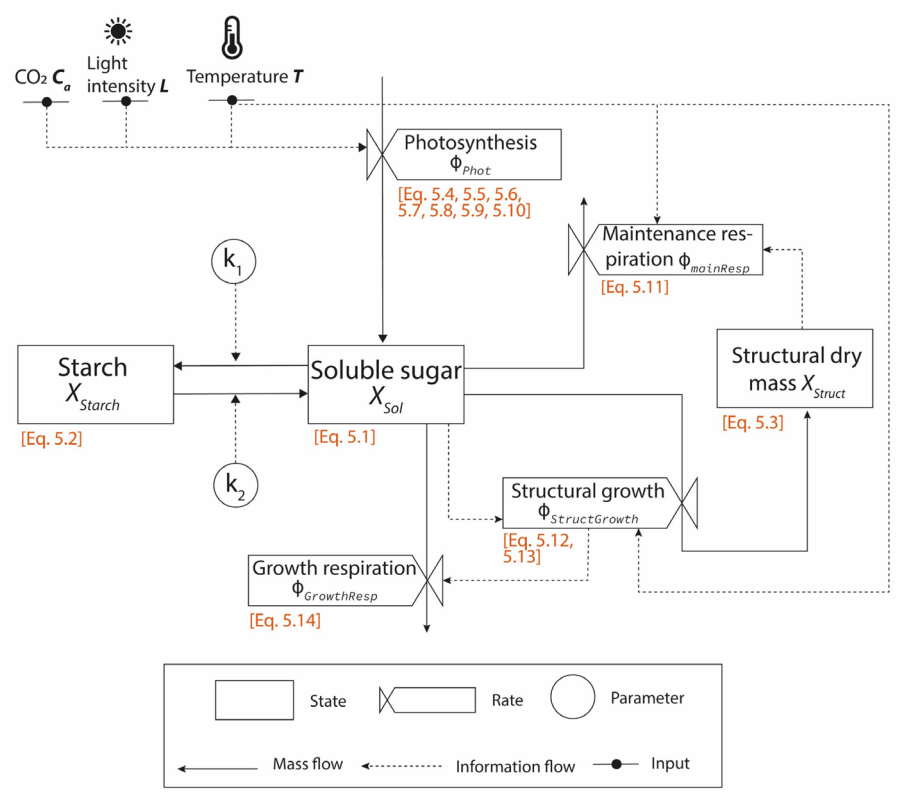

Figure 5.1. *Forrester diagram of the growth of a vegetative plant. Boxes are state variables. Circles are parameters and valves are rate variables. Solid lines represent carbon flow and dashed lines represent information flow.*

5.2.2 Parameter estimation and calibration

The two-state model and the parameters describing plant growth in Van Henten (1994) were used as a basis for model evaluation (nominal parameters). However, this model was originally calibrated for simulation of a lettuce crop. We modified two parameters to describe the growth of a vegetative tomato crop: light extinction coefficient c_k (-) based on (Heuvelink, 1996), and the 'structural' leaf area ratio (c_{LAR}, m^2[leaf]·gSDM^{-1}). Additionally, six parameters (**Table A 5.1**) were calibrated (optimal parameters) based on time series data of vegetative tomato plants grown under different light and temperature fluctuations (in total 9 treatments; for a detailed description of the experiments see **Chapter 3**). The uncertainty ranges for the parameter value are know from literature. We limited the number to 6 to avoid overfitting. These parameters were calibrated via parameter optimization using a local search algorithm (*fmincon,* MATLAB, 2017). The admissible range for the parameter optimization was based on literature research and is summarized in (Table A 5.1).

The optimal parameters estimated from this procedure were fitted to the experimental data. This calibrated model served as a basis for the development of the three-state model (Eq. 5.1, Eq. 5.2, and Eq. 5.3). The three-state model resulted in 2 additional parameters, k_1 (s^{-1}) describing the rate constant from soluble sugars to starch, and k_2 (s^{-1}) describing the rate constant degradation of starch to soluble sugars. Additionally, as in the three-state model growth depends on the soluble sugar and not the NSC concentration, parameter $c_{r,gr,max}$ was calibrated. These three parameters were calibrated based on time series data of total dry weight, starch and soluble sugar concentrations based on experiments from **Chapter 2,** using a local search algorithm (*fmincon*). Optimal values for the three-state model are given in (Table A 5.1).

5.2.3 Evaluation of predicted structural dry weight, soluble sugar and starch concentration

In order to evaluate how well the three states of the model (starch, soluble sugars, and structural dry weight) are predicted, the environmental conditions light intensity $L, (\mu mol\ m^2 s^{-1})$ and temperature $T, (°C)$ for the 9 treatments (see **Chapter 3**) were used as inputs and optimal parameters from the calibration were used. The CO_2 concentration was assumed to be 400 ppm. Simulations were performed using MATLAB, 2017b environment. Ordinary differential equations (ODEs) were solved using Forward Euler integration, using 1 hour time steps. Initial values used for the simulation $X_{Sol(0)}$ (gCH_2O m^{-2}), $X_{Starch(0)}$ (gCH_2O m^{-2}), and $X_{Struct(0)}$ (gCH_2O m^{-2}) were the initial values measured in **Chapter 3**. Simulated $X_{Sol,}$ X_{Starch}, and X_{Struct} were compared against the measured values by calculating the relative root mean

squared error (RMSE). Because the same data sets were used for calibration and evaluation, a leave-one-out cross validation was performed. This means that the model parameters were calibrated using data from 8 treatments, then the optimal parameters were used to evaluate model performance on the 9th treatment (Table A 5.2)

The root mean square error was defined as

$$\mathrm{RMSE} = \sqrt{\frac{1}{n}\,\Sigma_{i=1}^{n}(y_i^{mes} - y_i^{model})^2} \qquad 5.16$$

where y_i^{mes} is the measured value at time i; y_i^{model} is the model predictions at time i; and n is the number of measurements. Measured data was always at the beginning of the light period. The measured and modelled data were sampled at every 5 days. The RMSE provides a measure of prediction error, in the same unit as the measured variable y^{mes}. An RMSE close to zero indicates good model prediction.

Table 5.1*. List of rate variables, states, auxiliary states and inputs*

Nomenclature	Definition	Unit
Rates		
ϕ_{phot}	Rate of photosynthesis	$gCO_2\ m^{-2}\ s^{-1}$
$\phi_{mainResp}$	Maintenance respiration rate	$gCH_2O\ m^{-2}s^{-1}$
$\phi_{growthResp}$	Growth respiration rate	$gCH_2O\ m^{-2}s^{-1}$
$\phi_{StructGrowth}$	Structural growth rate	$gCH_2O\ m^{-2}s^{-1}$
States		
X_{Sol}	Soluble sugar content	$gCH_2O\ m^{-2}$
X_{Starch}	Starch content	$gCH_2O\ m^{-2}$
X_{Struct}	Structural mass	$gCH_2O\ m^{-2}$
Auxiliary states		
LAI	Leaf area index	m^{-2}[leaf] m^{-2}[soil]
$Phot_{max}$	Maximum canopy photosynthesis	$gCO_2\ m^{-2}$
Γ	Carbon dioxide compensation point	$g\ m^{-3}$
ϵ	Effect of photorespiration on light use efficiency	gCO_2 µmol[photons]$^{-1}$
σ_{CO_2}	Canopy conductance	$m\ s^{-1}$
σ_{car}	Carboxylation conductance	$m\ s^{-1}$
r_{gr}	Relative growth rate	s^{-1}
Inputs		
T	Temperature	°C
L	Photosynthetically active radiation, wavelength of 400 to 700 nm	µmol(photons) $m^{-2}s^{-1}$
Ca	Carbon dioxide concentration	$gCO2\ m^{-3}$

Table 5.2. *List of model parameters and symbols.*

Parameter symbol	Value	Meaning	Unit	Reference
c_{α}	0.68	Conversion of assimilated CO_2 into sugars (CH_2O) (molecular weight of CH_2O/CO_2 30/44)	g mol^{-1} / g mol^{-1}	Physical constant
c_{β}	0.8	Factor accounting for respiratory and synthesis losses during the conversion of CH_2O to structural material	-	(Penning De Vries et al., 1974)
c_{bnd}	0.004	Boundary layer conductance	m s^{-1}	Stanghellini 1993
$c_{car,1}$	-1.32x10^{-5}	Parameters from polynomial regression	m s^{-1} $^{\circ}C^{-2}$	Estimation from Goudriaan (1987)
$c_{car,2}$	5.94x10-4	Parameters from polynomial regression	m s^{-1} $^{\circ}C^{-1}$	Estimation from Goudriaan (1987)
$c_{car,3}$	-2.64x10^{-3}	Parameters from polynomial regression	m s^{-1}	Estimation from Goudriaan (1987)
c_{ϵ}	3.69*	Light use efficiency (LUE) at very high CO_2 concentrations.	gCO_2 mol[photons]$^{-1}$	Goudriaan et al. (1985)
c_{Γ}	0.0732	Carbon dioxide compensation point at 20 °C	gCO_2 m^{-3}	Goudriaan et al. (1985)
c_k	0.72	Leaf extinction coefficient	-	Heuvelink
c_{lar}	2.6x10^{-2}	Structural leaf area ratio	m^2[leaf] g[SDM]$^{-1}$	Measurements (Zepeda et al., 2022b)
$c_{q10,\Gamma}$	2	Temperature effects on the carbon dioxide compensation point	-	Goudriaan et al. (1985)
$c_{q10,gr}$	1.6	Temperature effects on structural growth	-	Sweeney et al. 1981
$c_{q10,resp}$	2	Temperature effects on respiration	-	Van Keulen et al. (1982)
$c_{r,gr,max}$	6.8x10^{-5}	Saturation growth rate at 20 °C	-	Estimation from this study
c_{resp}	3.47x10^{-7}	Maintenance respiration rate at 25 °C (mass of glucose consumed)	s^{-1}	Van Keulen et al. (1982)
c_{stm}	0.007	Stomatal conductance	m s^{-1}	Stanghellini 1993
k_1	1.2x10^{-4}	Rate constant conversion of soluble sugars to starch	s^{-1}	Estimation from this study
k_2	2.20x10^{-1}	Rate constant conversion from starch to soluble sugars	s^{-1}	Estimation from this study

c_{C_DM}	1	Conversion factor for expressing plant mass in CH_2O to express it as dry mass	g[DM] g[CH_2O]$^{-1}$

*Original parameter value was 17x10^{-9} kgCO_2 J[PAR from sunlight]$^{-1}$ and was converted to gCO_2 mol[photons]$^{-1}$ using the conversion factor 4.6mol[photons] = 1 MJ.

5.3 Results

5.3.1 Starch concentration

Measured starch concentrations declined over time in all treatments (Figure 5.2 A-F, H) except in antiphase treatments (low light with high temperature followed by high light with low temperature) with an integration periods of 20 days (Figure 5.2 G, I). The model accurately predicted these starch patterns over time, except in constant conditions (300 µmol m^{-2}s^{-1} and 22 °C) where starch concentrations were slightly underestimated at all time points (Figure 5.2 A). The model underestimates starch accumulation at high PPFD (400 µmol m^{-2} s^{-2}) combined with low temperature (18 °C) (Figure 5.2 I, day 10 onwards). A less severe underestimation was also observed when temperature decreased to 20.5°C (Figure 5.2 G, day 10 onwards), although the underestimations were less severe in this case. In all treatments, the starch pool reached a minimum level of approximately 0.09 gCH_2O gDM^{-1}. The model also predicted a similar minimum level of approximately 0.07gCH_2OgDM. The main difference was for constant conditions (300 µmol m^{-2}s^{-1} and 22 °C) where the model underestimates the minimum starch concentration by 40% (Figure 5.2 A).

5.3.2 Soluble sugar concentrations

The model accurately predicted trends in soluble sugar concentration across the treatments (Figure 5.3). Antiphase treatments ending with 10 days of high light intensity and low temperature resulted in an increased soluble sugar concentration after the change in temperature (Figure 5.3 G, I), which was correctly captured by the model. The main discrepancy between measurements and simulations was for the antiphase treatment 10 °C 2 days (Figure 5.3 E), where the model consistently underestimated the soluble sugar concentrations at all time points.

5.3.3 Structural dry mass

The model overestimated structural mass accumulation by ~40% in the Antiphase 10 °C 20 days treatment (Figure 5.4 I), when plants are exposed for the last 10 days to high light intensity (400 µmol m^{-2} s^{-2}) and low temperature (18 °C). Furthermore, in constant conditions (300 µmol m^{-2} s^{-2} and 22 °C), the model also overestimated the structural dry mass during the last 10 days of growth (Figure 5.4 A). The model

consistently underestimated structural growth at short integration periods (2 days, as seen in Figure 5.4 C, E). In contrast, in long integration periods (Figure 5.4 G, H, I), the model initially underestimated structural growth but then quickly overestimated it steeply from day 10.

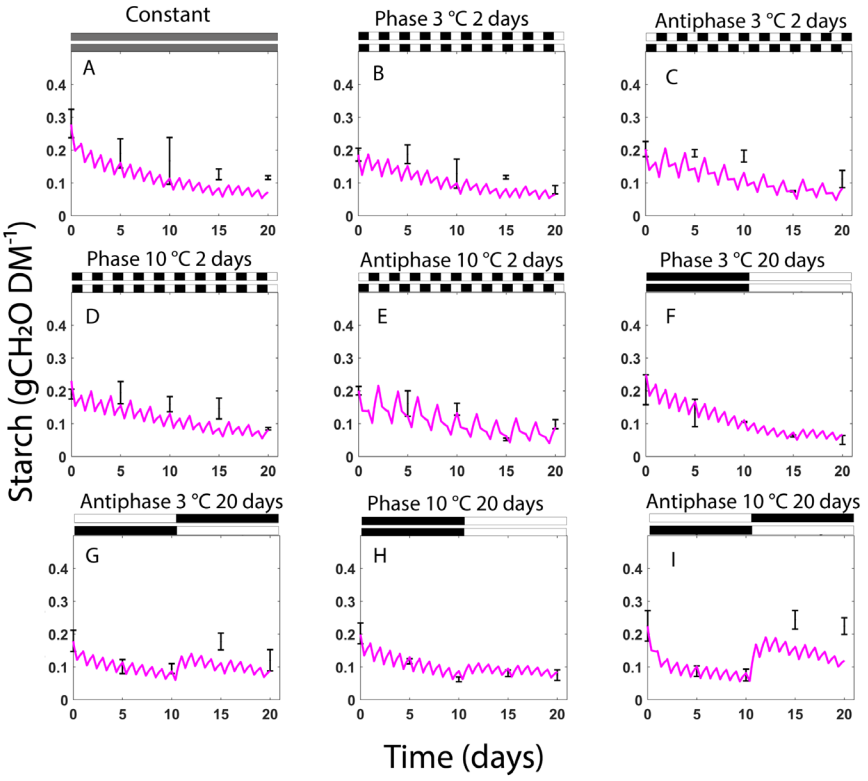

***Figure 5.2**. Measured (error bars) and simulated (lines) starch concentration as a function of time as described in Eq. 5.1, 5.2 and 5.3. Treatments are (A) constant light (300 µmol m^{-2} s^{-1}) and temperature (22 °C), (B) light and temperature in phase, integration period of 2 days and 3 °C amplitude (400 µmol m^{-2} s^{-1} and 23.5 °C for 1 day followed by 200 µmol m^{-2} s-1 and 20.5 °C for 1 day), (C) light and temperature in antiphase, integration period of 2 days and 3 °C amplitude (200 µmol m-2 s-1 and 23.5 °C for 1 day followed by 400 µmol m^{-2} $s^{-1}$and 20.5 °C for 1 day), (D) light and temperature in phase, integration period of 2 days and 10 °C amplitude (400 µmol m^{-2} s^{-1}1 and 27 °C for 1 day followed by 200 µmol m^{-2} s^{-1} and 18 °C for 1 day), (E) light and temperature in antiphase, integration period of 2 days and 10 °C amplitude (200 µmol µmol m^{-2} s^{-1} and 27 °C for 1 day followed by 400 µmol m^{-2} s^{-1} and 18 °C for 1 day), (F) light and temperature in phase, integration period of 20 days and 3 °C amplitude (400 µmol m^{-2} s^{-1}*

and 23.5 °C for 10 days followed by 200 µmol m^{-2} s^{-1} and 20.5 °C for 10 days) (G) light and temperature in antiphase, integration period of 20 days and 3 °C amplitude (200 µmol m^{-2} s^{-1} and 23.5 °C for 10 days followed by 400 µmol m^{-2} s^{-1} and 20.5 °C for 10 days), (H) light and temperature in phase, integration period of 20 days and 10 °C amplitude (400 µmol m^{-2} s^{-1} and 27 °C for 10 days followed by 200 µmol m^{-2} s^{-1} and 18 °C for 10 days), (I) light and temperature in antiphase, integration period of 20 days and 10 °C amplitude (200 µmol m^{-2} s^{-1} and 27 °C for 10 days followed by 400 µmol m^{-2} s^{-1} and 18 °C for 10 days). White bars above the graphs indicate a low light intensity or temperature and black bars indicate a high light intensity or temperature. Data are means of three blocks (n=3) with 6 replicate plants per block.

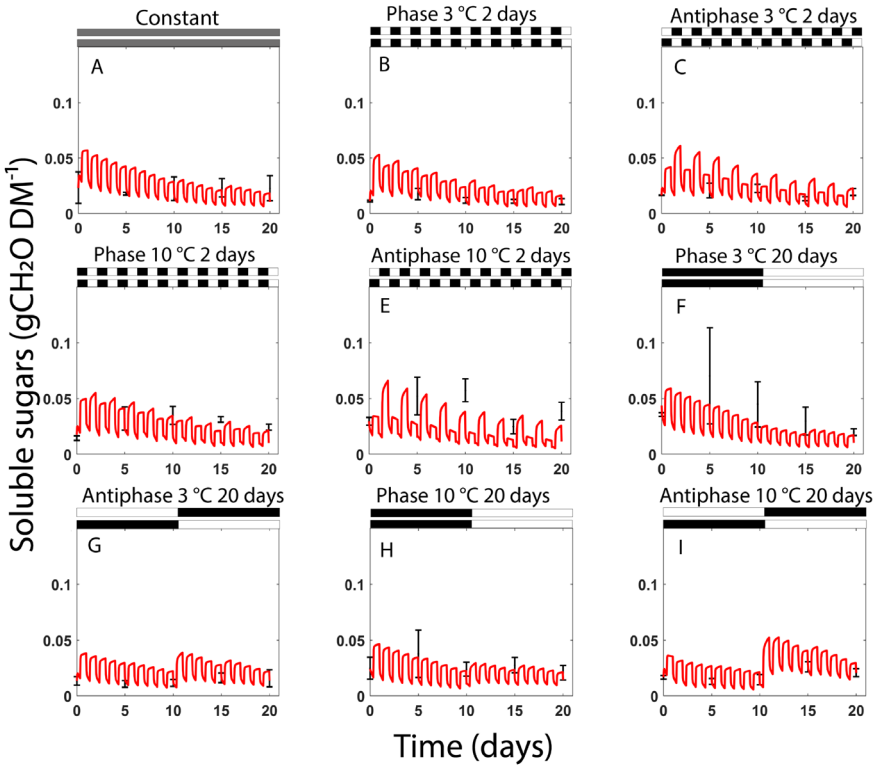

Figure 5.3. *Measured (error bars) and simulated (lines) soluble sugar (glucose, fructose, sucrose) concentration as a function of time as described in Eq. 5.1, 5.2 and 5.3. Treatments are as described in Figure 2. White bars above the graphs indicate a low light and temperature level and black bars indicate a high level of light intensity and temperature. Data are means of three blocks (n = 3) with 6 replicate plants per block.*

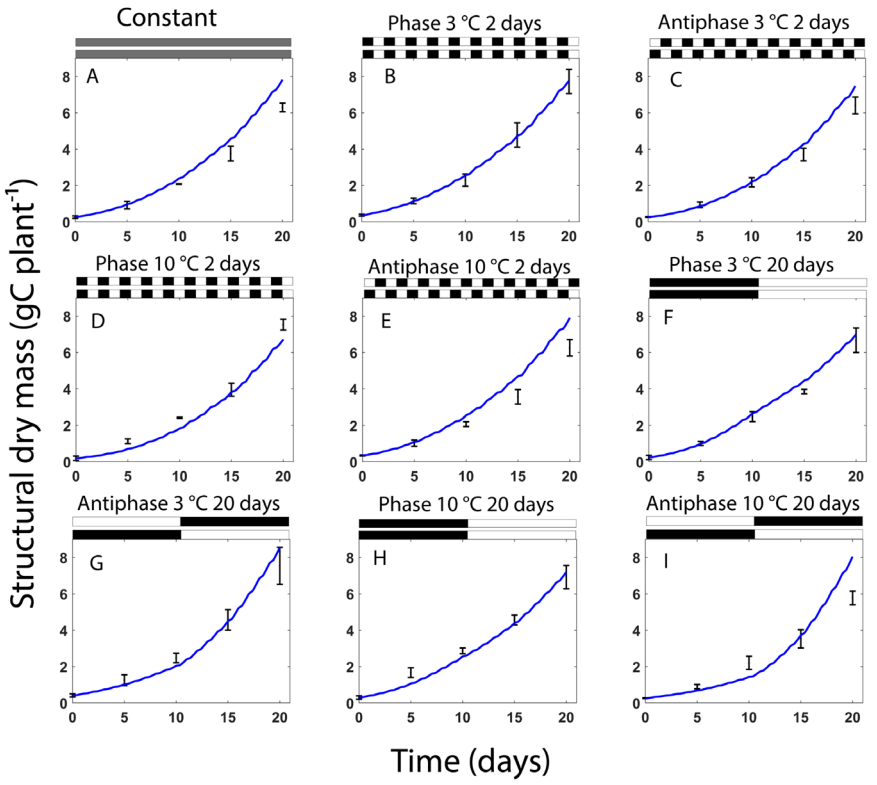

***Figure 5.4**. Measured (error bars) and simulated (bold lines) soluble sugar (glucose, fructose, sucrose) concentration as a function of time as described in equation 1. Treatments are as described in Figure 2. White bars above the graphs indicate a low light and temperature level and black bars indicate a high level of light intensity and temperature. Data are means of three blocks (n=3) with 6 replicate plants per block.*

5.4 Discussion

Starch and sugar pools in plants are regulated by a complex enzymatic network (Dong & Beckles, 2019; Rasse & Tocquin, 2006) causing concentrations to fluctuate on short (<1 day) and long (> 1 day) timescales. These variations have a profound effect on plant structural growth (Gent, 1986; Smith & Stitt, 2007) but often they are not explicitly included in crop models. The aim of this paper was to develop a plant growth model that can explain the day-to-day variations in observed carbohydrate levels and growth of vegetative plants grown at daily and weekly fluctuations in light and temperature. We describe the interconversion between the soluble sugar and

starch pool using a kinetic reversible reaction. Our three-state model has only an additional state (X_{Sol}) and two additional parameters (k_1 and k_2) compared with the two-state model from van Henten (1994). The model described most of the trends observed for soluble sugars and starch accumulation and depletion in plants grown at fluctuating light and temperature.

5.4.1 Structural growth and carbohydrate accumulation

Our model assumes a linear relationship between relative growth rate and soluble sugar concentration in leaves. This assumption is supported by observations from Thornley and Hurd (1976), that show a direct correlation between the two variables (Fig. 3 in Thornley & Hurd, 1976). This relationship is highly sensitive to increasing concentrations of soluble sugars. This assumption can lead to a large overestimation of structural mass. This does not mean that the formulation is wrong, instead, it suggests that this function is only suited for plants grown at source-limited conditions (i.e., when the potential supply of photosynthesis is low compared to the potential demand for assimilates). This reasoning could explain the higher structural growth rates observed at high light intensity and low temperatures in our simulations. While at low temperatures the relative growth rate is decreased following an equation with a Q_{10} factor =1.6, the increased NSC concentration from the high PPFD levels will lead to an overall increase in the relative growth rate. A more suitable formulation for our model would be that the correlation between soluble sugars and relative growth rate follows a saturation type of curve (i.e., a Michaelis-Menten saturation function). Beyond a saturation point, temperature becomes the primary factor influencing growth rate, rather than the carbohydrate availability (Fatichi et al., 2019).

5.4.2 Sink limitation of growth at low temperatures and high light intensity

In high-tech greenhouses, optimal temperatures are maintained, and water and nutrient availability are not limiting factors, thus growth is primarily limited by light availability (source-limited growth). However, elevated CO_2 and high light intensities generally lead to an accumulation of carbohydrates. The factors limiting growth in this case are metabolism or sink activity (tissue expansion and cell division) rather than source activity (C assimilation, Fatichi et al., 2014). At high light intensity and low temperature, there is a higher allocation of C to starch at the cost of structural growth, however this cannot be well simulated by our model. Leuzinger et al. (2013) incorporated sink-limited growth in their tree model based on the assumption that maximum plant growth is reached asymptotically as growing degree days increase. Bucksch et al. (2017) improved the simulation accuracy of tree growth in Dynamic

Global Vegetation models by considering intrinsic limitations of meristems and cellular growth rates, though the model remains complex with many parameters.

It is important to note that from our perspective, source-limited and sink-limited growth are not mutually exclusive but rather dependent on the environmental conditions. Whichever mechanism dominates can change over time and with changes in the environment. For example, Escobar Gutierrez et al. (1998) modelled structural growth over time as the minimum of supply and demand (see Eq. 20 Escobar Gutierrez et al., 1998b), similar to the approach used by Seginer & Gent (2014).

In our model, there is an implicit assumption that carbohydrates act solely as a substrate for structural growth. However, it is likely that carbohydrates have a signalling role (Pollock & Farrar, 1996). Low temperature can reduce the sink (meristem) activity, and thus result in an increase in carbohydrate levels. Changes in sugar concentration over a period of hours to few days can indicate imbalance between assimilate production in source tissues and consumption in sink tissues. This emphasizes the need to consider carbohydrates as both a substrate and signal in crop models for more accurate predictions of growth and productivity. Future improvements must include the implementation of these signalling mechanisms.

5.4.3 Feedback inhibition of photosynthesis due to high concentration of carbohydrates

Our model currently overestimates structural dry weight and total dry weight when there is a low temperature relative to available light. This may be due to feedback inhibition of photosynthesis caused by carbohydrate accumulation, which is not included in our model. However, when plants are exposed to more balanced conditions (e.g., light level is adjusted to temperature, Figure 5.2F) our model predictions are accurate for starch, soluble sugars, and structural dry weight. Sink activity can regulate source leaf photosynthesis via assimilate accumulation (Stitt, 1996). An increase in carbohydrate concentration can directly downregulate photosynthesis by inducing phosphate deficiency or a high concentration of triose-phosphate which inhibits RuBP-carboxylase activity (Azcon-bieto, 1983; Paul & Foyer, 2001a). Although net photosynthesis substantially increases when plants are grown at high atmospheric CO_2, this increase is not sustained in some species (Stitt, 1991) after doubling CO_2 concentrations. Because fluctuating temperature and light can lead to an accumulation of carbohydrates, it is necessary to improve crop model predictions by including the feedback mechanisms between carbohydrates and photosynthesis. It is important to note that photosynthesis inhibition might not occur in high-producing crops. Experiments in semi-closed greenhouse with elevated CO_2

levels did not cause feedback inhibition in fruiting tomato or cucumber crops. This is because these plants had sufficient sink organs (fruits) to use the extra assimilates (Marcelis, 1991; Qian et al., 2012). However, vegetative tomato plants can much more easily reach sink limitation compared to fruiting crops (Li et al., 2015). Gent & Seginer (2012) incorporated photosynthesis inhibition in their vegetative plant model; it occurs whenever the assimilate pool is completely full (Seginer & Gent, 2014). Similarly, Vanthoor et al. (2011) included an inhibition term that is activated once the carbohydrate amount in the buffer exceeds its maximum storage capacity (see eq. 9.11 in Vanthoor et al., 2011). However, neither of these implementations have been validated or based on experimental quantification of photosynthesis inhibition. Therefore, a more accurate mathematical approximation based on experimental data is needed to describe this process. Our results highlight the importance of further investigating the impact of high soluble sugar on photosynthesis inhibition and its effect on plant growth.

5.4.4 Starch accumulation mechanisms

One of the main limitations in our model is its inability to accurately predict starch accumulation at high light intensities and low temperatures. Rasse & Tocquin (2006) simulated starch accumulation through two mechanisms: (1) a programmed baseline rate of starch synthesis when photosynthesis is low (Sun et al., 1999) and (2) an overflow mechanism when photosynthesis exceeds organ growth demand and respiratory costs (Stitt, 1996). An overflow mechanism could be implemented in our model by linking k_1 (soluble sugar conversion to starch) to the soluble sugar levels wherein, above a certain threshold, k_1 would be higher to promote more sugar accumulation. However, we could not retrieve sufficient information in literature to quantitatively relate sugar concentration with starch accumulation. The interconversion between soluble sugars and starch in plants is likely influenced by temperature (Sperling et al., 2019; Zwieniecki et al., 2015). This can be modelled by considering the temperature kinetics of both compounds. At high light, starch production is high, but if temperature is low, degradation of starch into soluble sugars will also reduce due to a lower reaction rate of starch degrading enzymes

5.4.5 Possible model extensions

Our model represents an appealing scheme to introduce C allocation and sink control in a mechanistic way. Here, we identify major knowledge gaps that can further refine the model and generalize it towards a larger range of crops and climate fluctuations.

1. First, the model should be extended with functions that describe growth under sink-limited conditions. Elevated CO_2, low temperatures and high light intensities generally lead to carbohydrate accumulation. The factors limiting growth in this case are metabolism or sink activity (tissue expansion and cell division) rather than source activity (C assimilation Fatichi et al., 2014). However, there is not enough quantitative information that describes the relationship between high levels of NSC accumulation and growth. A first attempt to describe sink-limited growth could be to determine the relationship between relative growth rate and carbohydrate level experimentally. Our model assumes a linear relationship, however relative growth rate and carbohydrate levels may share a non-linear relationship. It needs to be determined whether additional feedback mechanisms must be included. As pointed out in previous reviews of crop growth models (e.g., Poorter et al., 2013) inclusion of source-sink interaction in mechanistic models should be prioritized to improve understanding on how physiology responds when the environment changes.
2. Second, improvements are needed in the estimation of rate constants for starch and soluble sugars (k_1 and k_2) across a wider range of temperatures, as it is likely that these rate constants are temperature-dependent (Sperling et al., 2019; Zwieniecki et al., 2015). As such, the kinetics of these parameters should be included, specifically with respect to their temperature dependence.
3. Third, future extensions of the model should include the regulation of C partitioning via the circadian clock (endogenous rhythm), for example with phase oscillators (e.g. Seki et al., 2017). In this way the model could account for changes in the daylength.

5.4.6 Practical implications

Improving energy use efficiency while maintaining crop yield can be realized by a flexible control of the climate set points, which can reduce energy consumption of the greenhouse up to 20% (Körner & Challa, 2004; Van Beveren et al., 2015). One major bottleneck for improvement in optimal climate control is the need for a suitable crop model. Fine climate control requires integration over different time scales (hourly, daily, monthly); therefore, the crop models should include refined physiological processes that account for short-term responses. Our model could be used to predict the effect of climate control strategies on the diurnal or hourly C balance of the plant, in order to steer the climate towards desired state trajectories and to avoid unwanted trajectories (e.g., too high or too low starch levels). Seginer (2022) showed that the

choice of crop model used for indoor environmental control of a greenhouse (e.g., a model without a NSC pool vs a model with an NSC pool) has a large influence on the control strategies. It is essential to note that the reproductive processes of crops become the primary bottleneck for implementing flexible climate control once the crop has flowered, as discussed in **Chapter 4.** To accurately simulate realistic greenhouse scenarios, it is crucial to include the simulation of processes such as fruit and seed set. By doing so, the implementation of flexible climate control can be optimized, and more realistic results can be obtained.

5.5 Conclusions

In conclusion, the trends of soluble sugar and starch accumulation and depletion in plants grown under day-to-day fluctuating light and temperature can be explained by a model that incorporates an interconversion between the soluble sugar and starch pool using a kinetic reversible reaction. This increases the model complexity only slightly, with the addition of one state and two parameters compared to a previous two-state model (Van Henten, 1994). The simulation model shows reasonable agreement with measurements; however, one limitation of our model is its inability to predict structural growth under sink-limiting conditions, such as high light intensity and low temperature.

5.6 Acknowledgements

The authors would like to thank Ido Seginer for providing valuable feedback on earlier versions of the manuscript, and to Jordan van Brenk for proofreading the manuscript.

5.7 Appendices

5.7.1 Appendix A: Additional tables

Table A 5.1. *Nominal and optimal parameters of the two-state variable growth model.*

Parameter	Nominal Value	Lower bound	Upper bound	Optimal value	Units	Source
c_β	0.8 (can only go from 0 to 1)	0.6	0.8	0.7	-	Sweeney et al. (1981)
$c_{car,1}$	-1.32×10^{-5}	-6.6×10^{-6}	-2.64×10^{-5}	-1.32×10^{-5}	m s^{-1} $°C^{-2}$	estim. from Goudriaan (1987)
$c_{car,2}$	5.94×10^{-4}	2.97×10^{-4}	1.2×10^{-3}	5.94×10^{-4}	m s^{-1} $°C^{-1}$	estim. from Goudriaan (1987)
$c_{car,3}$	-2.64×10^{-3}	-1.3×10^{-3}	-5.3×10^{-3}	-2.64×10^{-3}	m s^{-1}	estim. from Goudriaan (1987)
c_ϵ	17×10^{-9}	7×10^{-9}	1.9×10^{-8}	17×10^{-9}	kg J^{-1}	Goudriaan et. al (1985)
$c_{r,gr,max}$	5.6×10^{-6}	1×10^{-6}	8.6×10^{-6}	5.6×10^{-6}	s^{-1}	van Holsteijn (1981)

Table A 5.2. *Average and standard deviation of the cross-validation predictions.*

	RMSE soluble sugars ($gCHOgDM^{-1}$)	RMSE starch ($gCHOgDM^{-1}$)	RMSE structural dry weight	Weighted RMSE total (-)
Average	0.013	0.036	0.623	3.22
Standard deviation	0.0106	0.0136	0.3252	1.79

General discussion

Chapter 6

Ana Cristina Zepeda

Precise control of the indoor climate in greenhouses allows for consistent crop production and high yields, regardless of external weather conditions (Bot, 2001). However, this requires high energy inputs, particularly during the cold and dark winter months in temperate climates (Van Beveren et al., 2015). The Dutch horticultural sector has set a goal to become climate neutral by 2050 (Landbouw & Zaken, 2020) and achieving this requires substantial reductions in energy use in the greenhouse. Flexible greenhouse climate control based on plant physiological processes has the potential to save a significant amount of energy (Körner & Challa, 2003). The aim of this thesis was to contribute to the understanding of the crop's ability to buffer climate fluctuations, and to capture this knowledge into a model.

6.1 Plants as a 'Battery' – The Role of a Dynamic C Pool

Plants adapt to fluctuations in light intensity and temperature through the storage and remobilization of non-structural carbohydrates (NSC). Plants distribute the recently assimilated carbon (C) from the leaves, which serves as a source, to sinks for growth, metabolic maintenance, storage, and defence (Chapin et al., 1990). NSC are accumulated as soluble sugars and starch (Martínez-Vilalta et al., 2016) when the net production of carbohydrates exceeds the demand and growth is limited by assimilate usage. **Chapter 3** showed that when plants are exposed to different temperature and light fluctuations, the differences in total dry mass are relatively small while NSC are highly dynamic. This highlights that changes in NSC levels do not necessarily result in substantial alterations in the overall total plant biomass. Instead, temperature and light fluctuations impact growth of structural mass. This insight is crucial, as it implies that plants could serve as an effective 'battery' for C storage, buffering asynchronies between supply and demand for assimilates.

Defining the buffering capacity is a crucial aspect of the 'plants-as-a-battery' analogy. In vegetative plants, the buffering capacity depends on the characteristics of the C pool, such as how much C the plant can accumulate before growth is significantly reduced, how quickly C can be remobilized, and whether a fraction of C remains non-mobilizable. However, in mature plants with flowers, the hierarchy of limitations changes as here, crop flexibility will be determined by the thermosensitivity of reproductive processes rather than by the C pool itself. However, this will be further discussed in section 6.4.

6.2 The 'balanced crop': source-sink ratio vs. photothermal ratio

There is significant interest among researchers and growers in maintaining a 'balanced crop' in order to optimize vegetative growth and prevent the risk of physiological disorders (Elings et al., 2006; Geelen et al., 2015; Li et al., 2015). Physiologically, this balance refers to the source-sink ratio, which is the ratio between the supply of assimilates and the demand for assimilates. The supply of assimilates in an adult crop is primarily determined by the net rate of CO_2 assimilation, which is largely influenced by incoming radiation and CO_2 concentration. The demand for assimilates, or potential growth rate, is determined by the competition between organs for assimilates and the individual demand of each organ, the latter of which is highly temperature sensitive. While the source-sink ratio can give an indication on the 'C status' of the plant (i.e. whether growth is source- or sink-limited), it is a complex parameter that cannot be easily measured as it requires calculating the source and sink strength with a crop growth model. The photothermal ratio (PTR) is an easily measured alternative and practical tool that can provide insight into the balance between the supply of sugars through photosynthesis and the demand of sugars through the rate of cell division (Poorter et al., 2016). PTR is calculated as the ratio of daily light to the average daily temperature above 0°C (Liu & Heins, 1998; Poorter et al., 2016). Balanced growth through the PTR (Geelen et al., 2015) is achieved by adjusting the daily mean temperature to the daily light integral (see Figure 6.1).

While the PTR offers more flexibility as a guideline for controlling greenhouse climate compared to predetermined climate set points, it does not necessarily result in energy savings in the greenhouse. With the PTR, the decision to heat up the greenhouse, thereby consuming gas, is primarily based on the radiation levels, rather than factors such as gas prices or wind speed. An alternative would be to widen the temperature bandwidth, allowing the temperature to fluctuate within certain limits. This has been shown to result in energy savings from 4% at a bandwidth of 2 °C in tomato (Elings et al., 2005), and up to 13% at a bandwidth of 10 °C for a rose crop (Buwalda et al., 1999). Despite the flexibility of this approach, the constrains are still directly on climatic factors (although based on the crop). The ultimate goal for a flexible climate control based on the concept of 'plants as a battery', is to replace direct constraints on climate set points by constraints determined by the crop's response and physiology (Van Straten et al., 2000). However, this requires a reliable crop prediction model that can accurately account for varying climate conditions, which is also one of the main goals of this thesis as discussed in **Chapter 4** and **Chapter 5.**

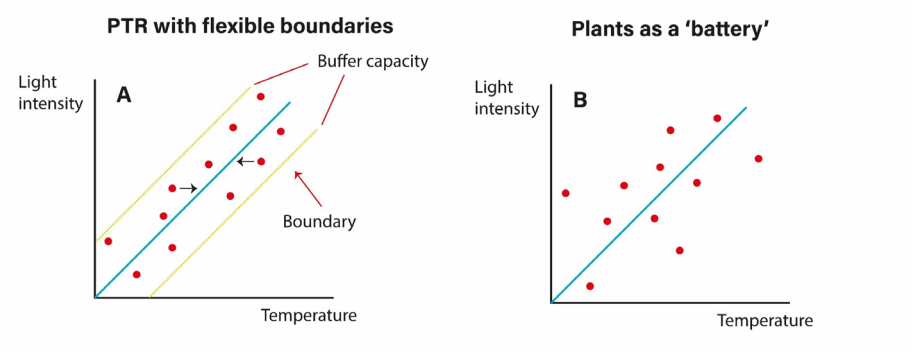

Figure 6.1. *Graphical illustration of two different forms of flexible climate control in the greenhouse. (A) Photothermal ratio (PTR, daily light integral to daily temperature integral). Here, temperature constrains can be widened to allow more flexibility on the climate control, however the constrains are on the temperature set points. (B) Flexible climate control using the 'plants as a battery', where direct constraints on climate set points are replaced by the crops physiological response, which requires a crop growth model that can account by reversible and irreversible processes.*

6.2.1 Temperature integration

Temperature integration has long been recognized as a strategy to minimize the energy required to heat a greenhouse (Körner, 2003). The objective here is to shift heating to times when heat loss is low, such as low-wind days or during the night when the thermal screens are in use (Huang & Chalabi, 1995). Heating the greenhouse above the desire temperature during the day for free (by the sun), then compensating by less heating at night to maintain a desired average temperature is a diurnal approach for energy savings (Hemming et al., 2019b). Over long-term seasons, reducing heating by a few degrees on cold days when the forecast predicts warmer weather in the future could also save energy without significant yield losses. However, determining the optimal temperature setpoint trajectory over a certain period requires forecasting the windspeed or temperature, which represents an additional challenge due to the inherent uncertainty of these inputs (Payne et al., 2022).

6.2.1.1 Starch accumulation over structural growth

Chapter 3 shows that vegetative tomato plants have a large temperature integration capacity (up to 20 days) when looking at the total dry mass of the plants. Specifically, plants grown under daily alternating temperature (18 °C and 28 °C) and light conditions (200 and 400 µmol m^{-2} s^{-1}) for 20 days showed no significant difference in total dry mass accumulation compared to plants grown for 10 days at 28 °C and 200 µmol m^{-2} s^{-1}, followed by 10 days at 18 °C and 400 µmol m^{-2} s^{-1}. The main difference

was that plants under high light levels and low temperature allocated more C into starch, at the expense of structural growth (Figure 6.2). This supports the argument made in **Chapter 2**, plants can buffer the temperature and light fluctuations through the starch pool specifically. One question that remains unclear is whether the increased C storage is the result of active allocation by the plants, or whether it is it simply a consequence of reduced structural growth?

In any case, this change in allocation has a significant impact according to the phenology of the plant: if C storage is prioritized over structural growth during the exponential growth phase, it could result in a reduction in leaf area (an irreversible process), which ultimately decreases the amount of light captured. However, our research did not observe this effect as the plants were grown with a high leaf area index, resulting in linear growth. In general, prioritizing C storage (as starch) over structural growth has implications on the overall morphology of plants, as the lack of resources for growth may limit the development of various organs. Focusing on structural growth might be appropriate when the plants are young, while prioritizing the accumulation of starch might be desirable in adult crops (as an increased concentration of starch or soluble sugar content in the leaves is sometimes described as a quality trait).

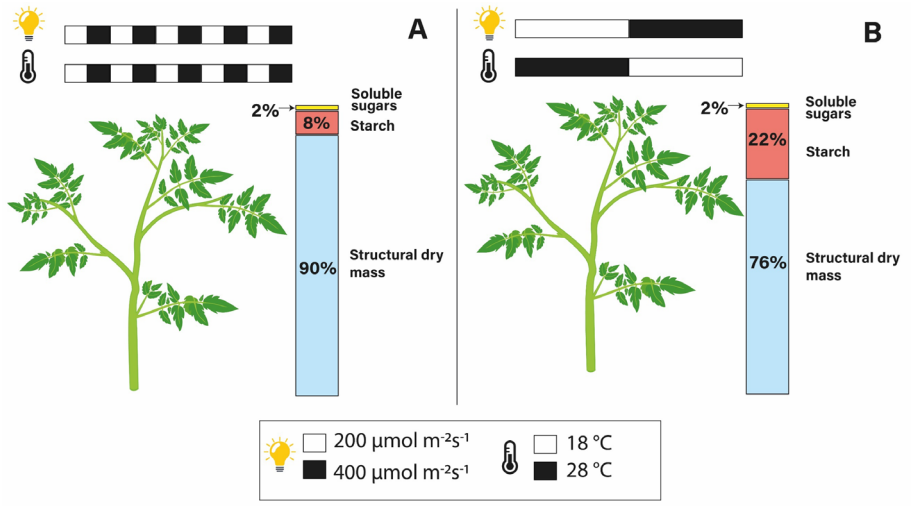

Figure 6.2. *Graphical illustration of findings from* ***Chapter 2.*** *Tomato plants were grown for 20 days at (A) an alternating light intensity of 200 µmol m^{-2} s^{-1} and 18 °C for 1 day followed by 400 µmol m^{-2} s^{-1} and 28 °C the next day or (B) light intensity of 200 µmol m^{-2} s^{-1} and 28 °C for 10 days followed by 400 µmol m^{-2} s^{-1} and 18 °C for the next 10 days. At the end of the treatment both (A) and (B) had the same light and temperature integral.*

When exploring boundaries for temperature integration, a distinction must be made between reversible processes and irreversible ones. Reversible processes are those that can be restored by adjusting the temperature, for example, the C balance, as seen in **Chapter 3**. Negative irreversible processes must be avoided – for example, delayed LAI development during the beginning of the season, could lead to a reduced light interception and thus a lower growth. Abortion of flowers is another irreversible process that should be considered in the temperature integration strategy; however, reproductive processes will be further discussed in **subsection 6.3.**

6.3 Modelling the C pool: how far are we?

Models are simplifications of complex systems, defined by specific boundaries. Mechanistic models offer an understanding of the underlying processes, making them valuable tools for testing and exploring hypotheses (Hammer et al., 2004). In **Chapter 2** I argue that current crop growth models inadequately represent the dynamic C pool. Crop growth models often include storage as a passive process whenever there is excess of C. However, modelling the accumulation and remobilization of C (a dynamic C pool) is challenging due to the complexity of the process. Two key mechanisms for the active regulation of storage are identified in **Chapter 2:** (i) partitioning of assimilates between soluble sugars and starch and (ii) degradation and remobilization of storage compounds. Other research (e.g. Gibon et al., 2009; Pokhilko et al., 2014.; Stitt & Zeeman, 2012) has primarily focused on studying starch turnover and its relationship with biomass in *Arabidopsis* on a diurnal basis. Several models have been proposed to explain the 'near to complete' starch degradation at night, with the simplest being the 'Arithmetic Division' model (Scialdone et al., 2013). This model assumes that the plant adjusts the rate of starch degradation at the end of the day, such that it is nearly entirely consumed by the end of the night. However, a critical aspect in this model is that physiologically, this 'near to complete' remobilization occurs only when plants are source-limited. As a result, this model does not account for progressive accumulation of starch under conditions of high light intensity and low temperatures, as observed in **Chapter 3.**

The initial model proposed in **Chapter 2** had a complex structure with many parameters and rule-based processes, which requires the estimation of numerous thresholds and limits. This complexity made the model less robust. By contrast, in **Chapter 5,** we adopted a different approach by modelling the starch-soluble sugar dynamics using a reversible kinetic reaction that only required two additional parameters. This approach has been used in other studies, such as simulating the rates of conversion from starch to soluble sugars at fruit maturation in tomato (Luo et al.,

2020). This new model predicted the minimum and maximum starch and soluble sugar concentrations as inherent properties of the model, which improved its robustness.

The model developed in **Chapter 5** proved to be a simple and accurate model for predicting starch, soluble sugars and structural growth in plants under different light and temperature fluctuations. However, there are some limitations in the experimental dataset used for model calibration and evaluation. Data was collected every 5 days, which does not provide a comprehensive understanding of the diurnal dynamics of these C pools. A more complete study in the future should include measurements of starch and soluble sugar concentrations at the beginning and end of both the light and the dark periods. Additionally, the experimental design should incorporate a wider range of C status in the plant, from very source-limited (e.g., low light intensity) to very sink-limited (e.g., high light intensity) at various temperatures. The model could be further improved by considering the effects of varying photoperiods, such as alternating long and short days (Feugier & Satake, 2014; Webb et al., 2019). This would provide a more comprehensive representation of the plant's growth under different photoperiodic conditions.

6.4 Flexible climate control and fruit, seed set – the weak link

As highlighted in **subsection 6.1**. is important to differentiate between reversible and irreversible processes when exploring the boundaries for temperature integration strategies. In this general discussion I have focused so far on the C balance of vegetative plants, where C can accumulate and later be depleted without adverse effects on total plant mass. However, reproductive processes are highly thermosensitive, and temperature stress during the reproductive phase is usually irreversible, although it depends on the duration (or 'dosage') of the stress (Körner, 2019). Many studies (e.g., Chaturvedi et al., 2021; Pham et al., 2020; Santiago & Sharkey, 2019; Sato et al., 2006; Zinn et al., 2010) have extensively quantified the effects of temperature stress on reproductive processes in field crops, including cereals and grains. However, little of this has focused on stress duration, although there are exceptions (e.g., Prasad et al. 1999). Results in **Chapter 4** show the consequences of the 'temperature-dose' response (temperature × duration) on the germination of tomato pollen. Specifically, the study found that exposure to 30°C for one day resulted in a relatively high rate of pollen germination leading to a seeded fruit with high mass. However, exposure to 30°C for three days or longer resulted in a close to zero germination rate, leading to reduced seed set and reduced fruit mass.

Simple regression models that account for temperature effects on flower abortion, fruit set, or harvest index are often introduced to field crop models to predict yield. In a horticultural context, fruit set is often modelled as a function of the source-sink balance, or simply set to be a fixed fraction under the assumption that temperature is maintained within certain bounds to maximize fruit set. Excluding the simulation of reproductive processes in crop models can lead to inaccurate yield predictions. For example, **Chapter 3** showed that plants grown for 10 days at 18 °C and the following 10 days at 28 °C did not have reduced total plant mass, but rather showed increased allocation of C to storage (NSC) and less to structural mass. However, the fruit mass prediction model developed in **Chapter 4** estimates a potential 50% reduction in individual fruit mass for flowering plants.

6.4.1 Coupling fruit set models with crop growth models is essential to explore boundaries for temperature integration

In the context of greenhouse climate control, including the prediction of reproductive processes as a function of temperature (intensity and duration) has important implications for the optimal control algorithm. When computing optimal trajectories or climate set points, the controller must consider the presence of flowers, as well as the amplitude and duration of the temperature fluctuations. This will then involve a balancing of costs to maintain optimal temperature conditions against the economic losses that may result from harvesting a lower number or fruits or smaller fruits. For the controller to effectively make these decisions, a reliable fruit set and fruit mass model is necessary to account for these factors. The predictive model for fruit mass developed in **Chapter 4** could be coupled to a fruiting crop to predict the effect of different temperature integration regimes on individual fruit mass. Furthermore, to accurately predict the yield per truss, the independent quadratic relationship between temperature and fruit set that was observed can be incorporated into the model. A key consideration is that the crop model must accurately distinguish the developmental stage of the flowers or trusses. This is because the model developed in **Chapter 4** only accounts for effects prior to anthesis. One way forward could be to adopt the method used by Challinor et al. (2005), which involves identifying periods of temperature stress and relating them to trusses that are vulnerable to failure.

6.5 Do we need more complex models?

Measuring feedback (from sensors) and estimating the crop state is required to make rational control decisions in the greenhouse or for the decision support system to give advice to the grower (Körner, 2019) as highlighted in **Chapter 1** (Figure 1.1).

However, in optimal control, very complex crop models are often undesirable because they make optimization difficult (Van Straten et al., 2010). In many cases, this results in an oversimplification of the problem where the crop is not explicitly included in the optimization algorithms, but rather represented as user-defined set points (e.g., Van Beveren et al., 2015). However, when we do not have enough information, then there is a higher likelihood of obtaining a bad advice from the optimal control algorithm. In **Chapter 5,** we developed a model that provided new information that previous crop models did not have. This was done by considering two different assimilate pools (soluble sugars and starch) that operate at different time scales and have distinct functions. Overall, the model complexity increased only to an additional state and three additional parameters compared to Van Henten's (1994) two-state model. Seginer (2022) demonstrated that the optimal control advice for the greenhouse climate depends on the crop model structure. By incorporating an assimilate pool into a crop model, he found that the correlation between mean daily temperature and mean daily global radiation (PTR) was improved (i.e. 'balanced growth') compared to models without an assimilate pool. The improved PTR in this study was an inherent consequence of using a model with more information (i.e. an assimilate buffer). This highlights the importance of choosing the right crop model and incorporating a sufficient level of complexity to ensure accurate control advice. The three-state model developed in **Chapter 5,** represents a promising option for improving the precision and accuracy of greenhouse crop control; or at the very least, it simulates more realistic scenarios under fluctuating climate conditions, though this potential remains to be tested.

6.6 Dynamic climate control – the gap with practice

Dynamic climate control has the potential to save significant amounts of energy (e.g. Körner & Van Straten, 2008; Sigrimis et al., 2000; van Beveren et al., 2015)but it requires the acceptance from growers (Van Straten et al., 2000). Growers may be reluctant to adopt energy-saving measures when energy costs are not high and the revenues are still acceptable (Van Straten et al., 2000). However, with recent energy price increases, there is increased interest in reducing energy costs. Growers may also be concerned that long-term temperature integration can lead to an 'unbalanced crop' and negatively impact crop yield. Adoption of new methods by growers will ultimately depend on the accurate quantification of benefits and a thorough assessment of associated risks (Van Straten et al., 2000).

Summary

Summary

Precise control of the indoor climate in greenhouses allows for consistent crop production and high yields, regardless of external weather conditions (Bot, 2001). However, this requires high energy inputs, particularly during the cold and dark winter months in temperate climates (Van Beveren et al., 2015). The Dutch horticultural sector has set a goal to become climate neutral by 2050 (LTO Glaskracht, 2015), and achieving this requires substantial reductions in energy use in the greenhouse. Flexible greenhouse climate control based on plant physiological processes has the potential to save a significant amount of energy (Körner & Challa, 2003). The aim of this thesis is to contribute to the understanding of the crop's ability to buffer climate fluctuations, and to capture this knowledge into a model.

In **Chapter 1** (general introduction) the relevance of using flexible climate control to reduce the energy consumption in the greenhouses is highlighted. By using a systems approach, the research problem is clearly defined. In this chapter I propose the analogy of plants as a battery: plants store energy in the form of sugars (soluble sugars and starch) produced through photosynthesis, and the stored sugars can be used for the growth and survival of the plant, similar to how batteries store and release energy. Additionally, the chapter highlights how reproductive processes in plants limit flexible temperature control in greenhouses and provides a brief overview of the role of models in explaining crop flexibility. The chapter concludes by presenting the research approach for this thesis.

In **Chapter 2,** the aim was to provide arguments supporting the view that an active C pool needs to be included in simulation models to improve our understanding of plant growth in fluctuating environments. Carbon (C) storage allows a plant to support growth whenever there is a temporal asynchrony between supply (source strength) and demand of C (sink strength). This asynchrony is strongly influenced by changes in light and temperature. In most crop models, C storage is included as a passive process that occurs whenever there is an excess of C from photosynthesis compared with the demand of C for metabolism. However, there are numerous studies that challenged this concept, and provided experimental evidence that C storage is an active process that allows buffering of environmental fluctuations to support long-term plant growth. In this opinion paper, we argue that an active C pool needs to be included in simulation models for a better understanding of plant growth patterns under fluctuating environment. Specifically, we propose that the two main mechanisms actively regulating C storage in plants are the partitioning of assimilates between soluble sugars and starch and the degradation and remobilization of storage

compounds. The insights gained here are important to optimize crop performance under fluctuating conditions and thus for developing more resource-efficient crop production systems.

Despite the central role of C in plant growth, our understating of the dynamics of C storage and remobilization under short-term (days) and long-term (weeks) climate fluctuations is limited. In **Chapter 3,** the aim was to test the hypothesis that C storage and remobilization can buffer the effects of temperature and light fluctuations on growth of tomato plants. Differences in final structural dry weight were relatively small, while NSC concentrations were highly dynamic and followed changes of light and temperature (a positive correlation with decreasing temperature and increasing light intensity). High temperature and low light intensity lead to depletion of the NSC pool, but NSC level never dropped below 8% of the plant weight and this fraction was not mobilizable. Our results suggest that growing plants under fluctuating conditions do not necessarily have detrimental effects on plant growth and may improve biomass production in plants. These findings highlight the importance in the NSC pool dynamics to buffer fluctuations of light and temperature on plant structural growth

While **Chapter 2** and **Chapter 3** focus on the flexibility of vegetative plants, it should be noted that the reproductive processes in flowering plants are highly sensitive to temperature. As a result, these processes are often inflexible or irreversible. These processes are often neglected in crop growth models, which can limit their accuracy and reliability in predicting yield under fluctuating conditions. In **Chapter 4,** we developed a quantitative model to predict seed set and fruit mass based on the effect of temperature and duration of the temperature on pollen quality (pollen number, viability, and germination). To develop the model, we conducted an experiment where we exposed dwarf tomato plants to 14°C for 4, 6, or 8 days, 30°C and 34°C for 1, 3, or 4 days, and a control treatment at 18°C. Temperatures of 30°C and 34°C reduced pollen viability and germination, resulting in lower seed set and fruit mass. While fruit set remained unaffected at 30°C, both 14°C and 34°C led to reduced fruit set. No correlation was observed between fruit set and pollen number, germination, or viability. At low temperatures (14 °C) yield was predicted to decrease due to a lower number of fruits in the truss (as a consequence of low fruit set) and due to a reduced fruit mass compared to optimal temperatures (18 °C). At high temperatures (30 °C) yield was predicted to decrease mainly due to a reduced individual fruit mass (as a consequence of low seed set). Our model overestimates fruit mass at very high temperatures (34 °C) and long durations (3 or 4 days). By coupling this model with a crop growth model, a control algorithm could weight the presence of flowers and the impact of temperature fluctuations against the economic losses from harvesting

smaller fruits or a reduced number of fruits, making it a valuable tool for optimizing greenhouse temperature strategies.

Because soluble sugars and starch have distinct functions and respond differently to environmental conditions, it is crucial to explicitly differentiate between these two pools in models to accurately predict the effect of NSC on growth. In **Chapter 5** the aim is to develop a plant growth model that can explain the day-to-day variations in soluble sugars, starch and structural growth of vegetative plants grown at day-to-day fluctuations in light and temperature. To achieve this, we extended the existing crop growth model by separating the non-structural carbohydrate pool into a soluble sugar and starch pool. The interconversion between the soluble sugar and starch pool was described by a kinetic reversible reaction. The model results agreed with the measured starch, soluble sugars, and structural dry mass of plants grown for 20 days under 8 conditions of varying light and temperature conditions. The model only failed to accurately predict growth at high light intensities and low temperatures. Under these sink-limited conditions the model overestimated structural dry mass and underestimated starch concentration. The model can be improved by incorporating the direct influence of temperature on meristem activity or on the rate of starch degradation into soluble sugars.

Chapter 6 concludes with an insightful discussion on the practical implications of the concepts of temperature integration, photothermal ratio, and source-sink ratio. The chapter also reflects on the current state of crop flexibility modelling and identifies potential areas of improvement. Additionally, the gap between dynamic control in theory and its implementation in practice is discussed and an outlook is provided to bridge this gap.

References

Ahmed, F. E., Hall, A. E., & DeMason, D. A. (1992). Heat Injury During Floral Development in Cowpea (Vigna Unguiculata, Fabaceae). *American Journal of Botany*, *79*(7), 784–791. https://doi.org/10.1002/j.1537-2197.1992.tb13655.x

Alexander, M. P. (1969). *Differential Staining of Aborted and Non Aborted Pollen* (Vol. 44, Issue 3).

Athanasiou, K., Dyson, B. C., Webster, R. E., & Johnson, G. N. (2010). Dynamic acclimation of photosynthesis increases plant fitness in changing environments. *Plant Physiology*, *152*(1), 366–373. https://doi.org/10.1104/pp.109.149351

Atkin, O. K., & Tjoelker, M. G. (2003a). Thermal acclimation and the dynamic response of plant respiration to temperature. *Trends in Plant Science*, *8*(7), 343–351. https://doi.org/10.1016/S1360-1385(03)00136-5

Atkin, O. K., & Tjoelker, M. G. (2003b). Thermal acclimation and the dynamic response of plant respiration to temperature. *Trends in Plant Science*, *8*(7), 343–351. https://doi.org/10.1016/S1360-1385(03)00136-5

Azcon-bieto, J. (1983). *Inhibition of Photosynthesis by Carbohydrates in Wheat Leaves*. 681–686.

Baena-González, E., & Hanson, J. (2017). Shaping plant development through the SnRK1–TOR metabolic regulators. *Current Opinion in Plant Biology*, *35*, 152–157. https://doi.org/10.1016/j.pbi.2016.12.004

Baena-González, E., Rolland, F., Thevelein, J. M., & Sheen, J. (2007). A central integrator of transcription networks in plant stress and energy signalling. *Nature*, *448*(7156), 938–942. https://doi.org/10.1038/nature06069

Bakker, J. C. (1989). The effects of air humidity on flowering, fruit set, seed set and fruit growth of glasshouse sweet pepper (Capsicum annuum L.). *Scientia Horticulturae*, *40*(1), 1–8. https://doi.org/10.1016/0304-4238(89)90002-2

Bangerth, F., & Ho, L. C. (1984). Fruit position and fruit set sequence in a truss as factors determining final size of tomato fruits. *Annals of Botany*, *53*(3), 315–320. https://doi.org/10.1093/oxfordjournals.aob.a086695

Barbaroux, C., & Bréda, N. (2002). Contrasting distribution and seasonal dynamics of carbohydrate reserves in stem wood of adult ring-porous sessile oak and

diffuse-porous beech trees. *Tree Physiology*, *22*(17), 1201–1210. https://doi.org/10.1093/treephys/22.17.1201

Bertin, N. (1995). Competition for assimilates and fruit position affect fruit set in indeterminate greenhouse tomato. *Annals of Botany*, *75*(1), 55–65. https://doi.org/10.1016/S0305-7364(05)80009-5

Bertin, N., & Gary, C. (1993). *Tomato fruit set: a case study for validation of the model TOMGRO*.

Bheemanahalli, R., Sunoj, V. S. J., Saripalli, G., Prasad, P. V. V., Balyan, H. S., Gupta, P. K., Grant, N., Gill, K. S., & Jagadish, S. V. K. (2019). Quantifying the impact of heat stress on pollen germination, seed set, and grain filling in spring wheat. *Crop Science*, *59*(2), 684–696. https://doi.org/10.2135/cropsci2018.05.0292

Bhuiyan, R., & Iersel, M. W. van. (2021). *Only Extreme Fluctuations in Light Levels Reduce Lettuce Growth Under Sole Source Lighting*. *12*(January), 1–12. https://doi.org/10.3389/fpls.2021.619973

Boscutti, F., Vianello, A., & Casolo, V. (2018). *‘ Last In – First Out ’: seasonal variations of non-structural carbohydrates , glucose-6-phosphate and ATP in tubers of two Arum species*. *20*, 346–356. https://doi.org/10.1111/plb.12673

Bot, G. P. A. (2001). Developments in indoor sustainable plant production with emphasis on energy saving. *Computers and Electronics in Agriculture*, *30*(1–3), 151–165. https://doi.org/10.1016/S0168-1699(00)00162-9

Bours, R. (2014). *Antiphase light and temperature cycles disrupt rhytmic plant growth*. Wageningen University.

Bucksch, A., Buck-Sorlin, G., Ouest, A., Simone Fatichi, F., Zurich, E., Hayat, A., Hacket-Pain, A. J., Pretzsch, H., Rademacher, T. T., & Friend, A. D. (2017). Modeling Tree Growth Taking into Account Carbon Source and Sink Limitations. *Frontiers in Plant Science | Www.Frontiersin.Org*, *8*, 182. https://doi.org/10.3389/fpls.2017.00182

Buwalda, F., Eveleens, B., & Wertwijn, R. (2000). *Ornamental crops tolerate large temeperature fluctuations: a potential for more efficient greenhouse strategies*.

Buwalda, F., Rijsdijk A.A., Vogelezang J.V.M., Hattendorf A., & Batta L.G.G. (1999). An energy efficient strategy for cut rose. *Acta Horticulturae*, *507*, 117–125.

Camara, M., Martins, M., Hejazi, M., Fettke, J., Steup, M., Feil, R., Krause, U., Arrivault, S., Vosloh, D., Figueroa, C. M., Ivakov, A., Yadav, U. P., Piques, M., Metzner, D., Stitt, M., & Lunn, J. E. (2013). Feedback Inhibition of Starch Degradation in Arabidopsis Leaves Mediated by Trehalose 6-Phosphate. *Plant Physiology*, *163*(November 2013), 1142–1163. https://doi.org/10.1104/pp.113.226787

Cannell, M. G. R., & Dewar, R. C. (1994). *Carbon Allocation in Trees : a Review of Concepts for Modelling*.

Cerasuolo, M., Richter, G. M., Richard, B., Cunniff, J., Girbau, S., Shield, I., Purdy, S., & Karp, A. (2016). Development of a sink-source interaction model for the growth of short-rotation coppice willow and in silico exploration of genotype×environment effects. *Journal of Experimental Botany*, *67*(3), 961–977. https://doi.org/10.1093/jxb/erv507

Challinor, A. J., Wheeler, T. R., Craufurd, P. Q., & Slingo, J. M. (2005). Simulation of the impact of high temperature stress on annual crop yields. *Agricultural and Forest Meteorology*, *135*(1–4), 180–189. https://doi.org/10.1016/j.agrformet.2005.11.015

Chapin, F. S., Schulze, E., & Mooney, H. A. (1990). The Ecology and Economics of Storage in Plants. *Annual Review of Ecology and Systematics*, *21*(1), 423–447. https://doi.org/10.1146/annurev.es.21.110190.002231

Chatterton, N. J., & Silvius, J. E. (1980). Photosynthate partitioning into leaf starch as affected by daily photosynthetic period duration in six species. *Physiologia Plantarum*, *49*(2), 141–144. https://doi.org/10.1111/j.1399-3054.1980.tb02642.x

Chaturvedi, P., Wiese, A. J., Ghatak, A., Záveská Drábková, L., Weckwerth, W., & Honys, D. (2021). Heat stress response mechanisms in pollen development. *New Phytologist*, *231*(2), 571–585. https://doi.org/10.1111/nph.17380

Chuste, P.-A., Maillard, P., Bréda, N., Levillain, J., Thirion, E., Wortemann, R., & Massonnet, C. (2020). Sacrificing growth and maintaining a dynamic carbohydrate storage are key processes for promoting beech survival under prolonged drought conditions. *Trees*, *34*, 381–394. https://doi.org/10.1007/s00468-019-01923-5

C.J. Pollock, & J.F. Farrar. (1996). Source-Sink Relations: The Role of Sucrose. In *Photosynthesis and the Environment* (Vol. 5, pp. 261–279).

Clarke, P. J., Burrows, G. E., Enright, N. J., & Knox, K. J. E. (2013). *Tansley review Resprouting as a key functional trait : how buds , protection and resources drive persistence after fire*. 19–35.

Coast, O., Murdoch, A. J., Ellis, R. H., Hay, F. R., & Jagadish, K. S. V. (2016). Resilience of rice (Oryza spp.) pollen germination and tube growth to temperature stress. *Plant Cell and Environment*, *39*(1), 26–37. https://doi.org/10.1111/pce.12475

Couée, I., Sulmon, C., Gouesbet, G., & El Amrani, A. (2006). Involvement of soluble sugars in reactive oxygen species balance and responses to oxidative stress in plants. *Journal of Experimental Botany*, *57*(3), 449–459. https://doi.org/10.1093/jxb/erj027

Da Silva, D., Qin, L., DeBuse, C., & DeJong, T. M. (2014). Measuring and modelling seasonal patterns of carbohydrate storage and mobilization in the trunks and root crowns of peach trees. *Annals of Botany*, *114*(4), 643–652. https://doi.org/10.1093/aob/mcu033

De Jong, M., Mariani, C., & Vriezen, W. H. (2009). The role of auxin and gibberellin in tomato fruit set. *Journal of Experimental Botany*, *60*(5), 1523–1532. https://doi.org/10.1093/jxb/erp094

de Koning, A. N. M. (1990). Long-term temperature integration of tomato. Growth and development under alternating temperature regimes. *Scientia Horticulturae*, *45*(1–2), 117–127. https://doi.org/10.1016/0304-4238(90)90074-O

De Souza, A. P., Massenburg, L. N., Jaiswal, D., Cheng, S., Shekar, R., & Long, S. P. (2017). Rooting for cassava: insights into photosynthesis and associated physiology as a route to improve yield potential. *New Phytologist*, *213*(1), 50–65. https://doi.org/10.1111/nph.14250

De Swaef, T., Driever, S. M., Van Meulebroek, L., Vanhaecke, L., Marcelis, L. F. M., & Steppe, K. (2013). Understanding the effect of carbon status on stem diameter variations. *Annals of Botany*, *111*(1), 31–46. https://doi.org/10.1093/aob/mcs233

Dieleman, J. A., & Meinen, E. (2007). Interacting effects of temperature integration and light intensity on growth and development of single-stemmed cut rose plants. *Scientia Horticulturae*, *113*(2), 182–187. https://doi.org/10.1016/j.scienta.2007.03.004

Dietze, M. C., Sala, A., Carbone, M. S., Czimczik, C. I., Mantooth, J. A., Richardson, A. D., & Vargas, R. (2014). Nonstructural Carbon in Woody Plants. *Annual Review of Plant Biology*, *65*(1), 667–687. https://doi.org/10.1146/annurev-arplant-050213-040054

Dong, S., & Beckles, D. M. (2019). *Dynamic changes in the starch-sugar interconversion within plant source and sink tissues promote a better abiotic stress response*. https://doi.org/10.1016/j.jplph.2019.01.007

Edwards, K. D., Akman, O. E., Knox, K., Lumsden, P. J., Thomson, A. W., Brown, P. E., Pokhilko, A., Kozma-bognar, L., Nagy, F., Rand, D. A., & Millar, A. J. (2010). Quantitative analysis of regulatory flexibility under changing environmental conditions. *Molecular Systems Biology*, *6*(424), 1–11. https://doi.org/10.1038/msb.2010.81

Elings, A., Kempkes, F. L. K., Kaarsemaker, R. C., Ruijs, M. N. A., van de Braak, N. J., & Dueck, T. A. (2005). The energy balance and energy-saving measures in greenhouse tomato cultivation. *Acta Horticulturae*, *691*, 67–74. https://doi.org/10.17660/ActaHortic.2005.691.5

Escobar Gutierrez, A. J., Daudet, F. A., Gaudillere, J. P., Maillard, P., & Frossard, J. S. (1998a). Modelling of Allocation and Balance of Carbon in Walnut (Juglans regia L .) Seedlings during Heterotrophy – autotrophy Transition. *Journal of Theoretical Biology*, *194*, 29–47.

Escobar Gutierrez, A. J., Daudet, F. A., Gaudillere, J. P., Maillard, P., & Frossard, J. S. (1998b). Modelling of Allocation and Balance of Carbon in Walnut (Juglans regia L .) Seedlings during Heterotrophy – autotrophy Transition. *Journal of Theoretical Biology*, *194*, 29–47.

Farquhar, A. G. D., Caemmerer, S. Von, & Berry, J. A. (1980). A Biochemical Model of Photosynthetic COz Assimilation in Leaves of C3 Species. *Planta*, *149*(1), 78–90.

Fatichi, S., Leuzinger, S., & Körner, C. (2014). Moving beyond photosynthesis: From carbon source to sink-driven vegetation modeling. *New Phytologist*, *201*(4), 1086–1095. https://doi.org/10.1111/nph.12614

Fatichi, S., Pappas, C., Zscheischler, J., & Leuzinger, S. (2019). Modelling carbon sources and sinks in terrestrial vegetation. *New Phytologist*, *221*(2), 652–668. https://doi.org/10.1111/NPH.15451

Feugier, F. G., & Satake, A. (2014). Hyperbolic features of the circadian clock oscillations can explain linearity in leaf starch dynamics and adaptation of plants to diverse light and dark cycles. *Ecological Modelling*, *290*(C), 110–120. https://doi.org/10.1016/j.ecolmodel.2013.11.011

Feugier, F. G., Satake, A., Shabala, S., & Newman, I. A. (2013). *Dynamical feedback between circadian clock and sucrose availability explains adaptive response of starch metabolism to various photoperiods*. https://doi.org/10.3389/fpls.2012.00305

Fink, M. (1993). Effects of short-term temperature fluctuations on plant growth and conclusions for short-term temperature optimization in greenhouses. In *Environmental Stress and Horticulture Crops* (Vol. 328, pp. 147–154).

Firon, N., Shaked, R., Peet, M. M., Pharr, D. M., Zamski, E., Rosenfeld, K., Althan, L., & Pressman, E. (2006). Pollen grains of heat tolerant tomato cultivars retain higher carbohydrate concentration under heat stress conditions. *Scientia Horticulturae*, *109*(3), 212–217. https://doi.org/10.1016/j.scienta.2006.03.007

Fisher, D. B., & Gifford, R. M. (1986). *Accumulation and Conversion of Sugars by Developing Wheat Grains '*. 1024–1030.

Flis, A., Mengin, V., Taylor, J., Christopher, L., Tindal, C., Thomas, H., Ougham, H. J., Reffye, P. De, Stitt, M., Williams, M., Halliday, K. J., Millar, A. J., Tindal, C., Thomas, H., & Ougham, H. J. (2015). *Multiscale digital Arabidopsis predicts individual organ and whole-organism growth*. *112*(19). https://doi.org/10.1073/pnas.1506983112

Furze, M. E., Trumbore, S., & Hartmann, H. (2018). Detours on the phloem sugar highway: stem carbon storage and remobilization. *Current Opinion in Plant Biology*, *43*, 89–95. https://doi.org/10.1016/j.pbi.2018.02.005

Geelen P.A.M., Voogt J.O., & van Weel P.A. (2015). *HET NIEUWE TELEN*. www.ltoglaskrachtnederland.nl

Geiger, D. R., Servaties, J. C., & Fuchs, M. A. (2000). Role of starch in carbon translocation and partitioning at the plant level. *Australian Journal of Plant Physiology*, *27*.

Gent, M. P. N. (1986). *Carbohydrate Level and Growth of Tomato Plants*. 1075–1079.

Gent, M. P. N., & Seginer, I. (2012a). A carbohydrate supply and demand model of vegetative growth: Response to temperature and light. *Plant, Cell and*

Environment, *35*(7), 1274–1286. https://doi.org/10.1111/j.1365-3040.2012.02488.x

Gent, M. P. N., & Seginer, I. (2012b). A carbohydrate supply and demand model of vegetative growth: Response to temperature and light. *Plant, Cell and Environment*, *35*(7), 1274–1286. https://doi.org/10.1111/j.1365-3040.2012.02488.x

Gessler, A., & Grossiord, C. (2019). Coordinating supply and demand: plant carbon allocation strategy ensuring survival in the long run. *New Phytologist*, *222*(1), 5–7. https://doi.org/10.1111/nph.15583

Gibon, Y., Bläsing, O. E., Palacios-Rojas, N., Pankovic, D., Hendriks, J. H. M., Fisahn, J., Höhne, M., Günther, M., & Stitt, M. (2004). Adjustment of diurnal starch turnover to short days: Depletion of sugar during the night leads to a temporary inhibition of carbohydrate utilization, accumulation of sugars and post-translational activation of ADP-glucose pyrophosphorylase in the followin. *Plant Journal*, *39*(6), 847–862. https://doi.org/10.1111/j.1365-313X.2004.02173.x

Gibon, Y., Pyl, E.-T., Sulpice, R., Lunn, J. E., Hohne, M., Gunther, M., & Stitt, M. (2009). Adjustment of growth, starch turnover, protein content and central metabolism to a decrease of the carbon supply when Arabidopsis is grown in very short photoperiods. *Plant, Cell & Environment*, *32*(7), 859–874. https://doi.org/10.1111/j.1365-3040.2009.01965.x

Goudriaan, J., & van Laar, H. H. (1978). Calculation of daily totals of the gross CO2 assimilation of leaf canopies. In *Neth. J. agric. Sei* (Vol. 26).

Goudriaan, J., & van Laar, H. H. (1992a). *Modelling Potential Crop Growth Processes*.

Goudriaan, J., & van Laar, H. H. (1992b). *Modelling Potential Crop Growth Processes*.

Goudriaan J., van Laar H.H., van Keulen H., & Louwerse W. (1985). Photosynthesis, CO2 and Plant Production. In *Wheat and Growth Modeling* (Vol. 86, pp. 107–123).

Graf, A., Schlereth, A., Stitt, M., & Smith, A. M. (2010a). Circadian control of carbohydrate availability for growth in Arabidopsis plants at night. *Proceedings*

of the National Academy of Sciences of the United States of America, *107*(20), 9458–9463. https://doi.org/10.1073/pnas.0914299107

Graf, A., Schlereth, A., Stitt, M., & Smith, A. M. (2010b). *Circadian control of carbohydrate availability for growth in Arabidopsis plants at night*. *107*(20). https://doi.org/10.1073/pnas.0914299107

Graf, A., & Smith, A. M. (2011). Starch and the clock : the dark side of plant productivity. *Trends in Plant Science*, *16*(3), 169–175. https://doi.org/10.1016/j.tplants.2010.12.003

Gu, S., Zhang, L., Yan, Z., Van Der Werf, W., & Evers, J. B. (2018). Quantifying within-plant spatial heterogeneity in carbohydrate availability in cotton using a local-pool model. *Annals of Botany*, *121*(5), 1005–1017. https://doi.org/10.1093/aob/mcx210

Hammer, G. L., Kropff, M. J., Sinclair, T. R., & Porter, J. R. (2002). *Future contributions of crop modelling-from heuristics and supporting decision making to understanding genetic regulation and aiding crop improvement*. *18*.

Hammer, G. L., Sinclair, T. R., Chapman, S. C., & van Oosterom, E. (2004). On systems thinking, systems biology, and the in silico plant. *Plant Physiology*, *134*(3), 909–911. https://doi.org/10.1104/pp.103.034827

Hammer, G., Messina, C., Wu, A., & Cooper, M. (2019). Biological reality and parsimony in crop models - Why we need both in crop improvement! *In Silico Plants*, *1*(1), 1–21. https://doi.org/10.1093/insilicoplants/diz010

Hartmann, H., McDowell, N. G., & Trumbore, S. (2015). Allocation to carbon storage pools in Norway spruce saplings under drought and low CO2. *Tree Physiology*, *35*(3), 243–252. https://doi.org/10.1093/treephys/tpv019

Hartmann, H., & Trumbore, S. (2016). Understanding the roles of nonstructural carbohydrates in forest trees - from what we can measure to what we want to know. *The New Phytologist*, *211*(2), 386–403. https://doi.org/10.1111/nph.13955

Hedhly, A. (2011). Sensitivity of flowering plant gametophytes to temperature fluctuations. *Environmental and Experimental Botany*, *74*, 9–16. https://doi.org/10.1016/j.envexpbot.2011.03.016

Hedhly, A., Hormaza, J. I., & Herrero, M. (2005). The effect of temperature on pollen germination, pollen tube growth, and stigmatic receptivity in peach. *Plant Biology*, *7*(5), 476–483. https://doi.org/10.1055/s-2005-865850

Hemming, S., Bakker, J. C., Campen, J. B., & Kempkes, F. L. K. (2019a). Sustainable use of energy in greenhouses. In *Achieving sutainable greenhouse cultivation* (pp. 445–493).

Hemming, S., Bakker, J. C., Campen, J. B., & Kempkes, F. L. K. (2019b). *Sustainable use of energy in greenhouses* (pp. 445–492). https://doi.org/10.19103/as.2019.0052.07

Henten, E. J. Van. (1994). *Validation of a Dynamic Lettuce Growth Model for Greenhouse Climate Control*. *45*, 55–72.

Heuvelink, E. (1996). Dry matter partitioning in tomato: Validation of a dynamic simulation model. *Annals of Botany*, *77*(1), 71–80. https://doi.org/10.1006/anbo.1996.0009

Hikosaka, K., Ishikawa, K., Borjigidai, A., Muller, O., & Onoda, Y. (2006). Temperature acclimation of photosynthesis : mechanisms involved in the changes in temperature dependence of photosynthetic rate. *Journal of Experimental Botany*, *57*(2), 291–302. https://doi.org/10.1093/jxb/erj049

Hilty, J., Muller, B., Pantin, F., & Leuzinger, S. (2021). Plant growth: the What, the How, and the Why. In *New Phytologist* (Vol. 232, Issue 1, pp. 25–41). John Wiley and Sons Inc. https://doi.org/10.1111/nph.17610

Horton, P. (1985). Interactions between electron transfer and carbon assimilation. In *Photosynthetic Mechanisms and the Environment (Barber, J. Baker, N.R.)*.

Huang, J., Forkelová, L., Unsicker, S. B., Forkel, M., Griffith, D. W. T., Trumbore, S., & Hartmann, H. (2019). Isotope labeling reveals contribution of newly fixed carbon to carbon storage and monoterpenes production under water deficit and carbon limitation. *Environmental and Experimental Botany*, *162*(February), 333–344. https://doi.org/10.1016/j.envexpbot.2019.03.010

Huang, J., Hammerbacher, A., Weinhold, A., Reichelt, M., Gleixner, G., Behrendt, T., Dam, N. M. van, Sala, A., Gershenzon, J., Trumbore, S., & Hartmann, H. (2018). *Eyes on the future – evidence for trade-offs between growth , storage and defense in Norway spruce*. https://doi.org/10.1111/nph.15522

Huang, Z., & Chalabi, Z. S. (1995). Use of time-series analysis to model and forecast wind speed. *Journal of Wind Engineering and Industrial Aerodynamics*, *56*(2–3), 311–322. https://doi.org/10.1016/0167-6105(94)00093-S

Huner, N. P. A., Oquist, G., Hurry, V. M., Krol, M., Falk, S., & Griffith, M. (1993). *Photosynthesis , photoinhibition and low temperature acclimation in cold tolerant plants*. 19–39.

Hurd, R. G., & Graves, C. J. (1984). the Influence of Different Temperature Patterns Having the Same Integral on the Earliness and Yield of Tomatoes. In *Acta Horticulturae* (Issue 148, pp. 547–554). https://doi.org/10.17660/ActaHortic.1984.148.69

Jing, Q., Qian, B., Bélanger, G., VanderZaag, A., Jégo, G., Smith, W., Grant, B., Shang, J., Liu, J., He, W., Boote, K., & Hoogenboom, G. (2020). Simulating alfalfa regrowth and biomass in eastern Canada using the CSM-CROPGRO-perennial forage model. *European Journal of Agronomy*, *113*(October 2019), 125971. https://doi.org/10.1016/j.eja.2019.125971

Kaiser, E., Morales, A., & Harbinson, J. (2018). Fluctuating light takes crop photosynthesis on a rollercoaster ride. *Plant Physiology*, *176*(2), 977–989. https://doi.org/10.1104/pp.17.01250

Kang, M., Yang, L., Zhang, B., & de Reffye, P. (2010). Correlation between dynamic tomato fruit-set and source-sink ratio: a common relationship for different plant densities and seasons? *Annals of Botany*. https://doi.org/10.1093/aob/mcq244

Kearns, C. A., & Inouye, D. W. (1993). *Techniques for pollination biologists*. University Press of Colorado.

Keunen, E., Peshev, D., Vangronsveld, J., Ende, W. Van Den, & Cuypers, A. (2013). Plant sugars are crucial players in the oxidative challenge during abiotic stress : extending the traditional concept. *Plant Cell and Environment*, *36*, 1242–1255. https://doi.org/10.1111/pce.12061

Kiran, A., Sharma, P. N., Awasthi, R., Nayyar, H., Seth, R., Chandel, S. S., Siddique, K. H. M., Zinta, G., & Sharma, K. D. (2021). Disruption of carbohydrate and proline metabolism in anthers under low temperature causes pollen sterility in chickpea. *Environmental and Experimental Botany*, *188*(December 2020), 104500. https://doi.org/10.1016/j.envexpbot.2021.104500

Klopotek, Y., & Kläring, H. P. (2014). Accumulation and remobilisation of sugar and starch in the leaves of young tomato plants in response to temperature. *Scientia Horticulturae*, *180*, 262–267. https://doi.org/10.1016/j.scienta.2014.10.036

Kolbe, A., Tiessen, A., Schluepmann, H., Paul, M., Ulrich, S., & Geigenberger, P. (2005). *Trehalose 6-phosphate regulates starch synthesis via posttranslational redox activation of ADP-glucose pyrophosphorylase*. *102*(31), 2–7. https://doi.org/10.1073/pnas.0503410102

Körner, C. (2015). Paradigm shift in plant growth control. *Current Opinion in Plant Biology*, *25*, 107–114. https://doi.org/10.1016/j.pbi.2015.05.003

Körner, O. (2003). *Crop Based Climate Regimes for Energy Saving in Greenhouse Cultivation*. 240. https://doi.org/10.13140/RG.2.1.1433.4165

Körner, O. (2019). Models, sensors and decision support systems in greenhouse cultivation. In *Achieving Sustainable Greenhouse Cultivation* (pp. 379–412). https://doi.org/10.19103/as.2019.0052.15

Körner, O., Andreassen, A. U., & Aaslyng, J. M. (2006). Simulating dynamic control of supplementary lighting. *Acta Horticulturae*, *711*(35), 151–156. https://doi.org/10.17660/ActaHortic.2006.711.17

Körner, O., & Challa, H. (2003). Design for an improved temperature integration concept in greenhouse cultivation. *Computers and Electronics in Agriculture*, *39*(1), 39–59. https://doi.org/10.1016/S0168-1699(03)00006-1

Körner, O., & Challa, H. (2004). *Temperature integration and process-based humidity control in chrysanthemum*. *43*, 1–21. https://doi.org/10.1016/j.compag.2003.08.003

Körner, O., Heuvelink, E., & Niu, Q. (2009). Quantification of temperature, CO2, and light effects on crop photosynthesis as a basis for model-based greenhouse climate control. *Journal of Horticultural Science and Biotechnology*, *84*(2), 233–239. https://doi.org/10.1080/14620316.2009.11512510

Körner, O., & van Straten, G. (2008). Decision support for dynamic greenhouse climate control strategies. *Computers and Electronics in Agriculture*, *60*(1), 18–30. https://doi.org/10.1016/j.compag.2007.05.005

Kozlowski, T. T. (1992). Carbohydrate sources and sinks in woody plants. *The Botanical Review*, *58*(2), 107–222. https://doi.org/10.1007/BF02858600

Kromdijk, J., Głowacka, K., Leonelli, L., Gabilly T., S., Iwai, M., Niyogi K., K., & Long, S. P. (2016). Improving photosynthesis and crop productivity by accelerating recovery from photoprotection. *Science*, *354*(6314), 857–862.

Lacointe, A., Kajji, A., Daudet, F. A., Archer, P., Frossard, J. S., Saint-Joanis, B., & Vandame, M. (1993). Mobilization of carbon reserves in young walnut trees. *Acta Botanica Gallica*, *140*(4), 435–441. https://doi.org/10.1080/12538078.1993.10515618

Landbouw, V., & Zaken, S. V. E. (2020). *Meerjarenafspraak Energietransitie Glastuinbouw 2014-2020*. 1–6.

Landhäusser, S. M., & Lieffers, V. J. (2003). Seasonal changes in carbohydrate reserves in mature northern Populus tremuloides clones. *Trees - Structure and Function*, *17*(6), 471–476. https://doi.org/10.1007/s00468-003-0263-1

Lastdrager, J., Hanson, J., & Smeekens, S. (2014). Sugar signals and the control of plant growth and development. *Journal of Experimental Botany*, *65*(3), 799–807. https://doi.org/10.1093/jxb/ert474

Lawlor, D. W., & Paul, M. J. (2014). Source/sink interactions underpin crop yield: The case for trehalose 6-phosphate/SnRK1 in improvement of wheat. *Frontiers in Plant Science*, *5*(AUG), 1–14. https://doi.org/10.3389/fpls.2014.00418

Legros, S., Mialet-Serra, I., Clement-Vidal, A., Caliman, J. P., Siregar, F. A., Fabre, D., & Dingkuhn, M. (2009). Role of transitory carbon reserves during adjustment to climate variability and sourcesink imbalances in oil palm (Elaeis guineensis). *Tree Physiology*, *29*(10), 1199–1211. https://doi.org/10.1093/treephys/tpp057

Leuzinger, S., Manusch, C., Bugmann, H., & Wolf, A. (2013). A sink-limited growth model improves biomass estimation along boreal and alpine tree lines. *Global Ecology and Biogeography*, *22*(8), 924–932. https://doi.org/10.1111/GEB.12047

Li, L., & Sheen, J. (2016). Dynamic and diverse sugar signaling. *Current Opinion in Plant Biology*, *33*, 116–125. https://doi.org/10.1016/j.pbi.2016.06.018

Li, T., Heuvelink, E., & Marcelis, L. F. M. (2015). Quantifying the source-sink balance and carbohydrate content in three tomato cultivars. *Frontiers in Plant Science*, *6*(June), 1–10. https://doi.org/10.3389/fpls.2015.00416

LIANG, X. gui, SHEN, S., GAO, Z., ZHANG, L., ZHAO, X., & ZHOU, S. li. (2021). Variation of carbon partitioning in newly expanded maize leaves and plant adaptive growth under extended darkness. *Journal of Integrative Agriculture*, *20*(9), 2360–2371. https://doi.org/10.1016/S2095-3119(20)63351-2

Liebig, H. P. (1988). *Temperature integration by kohlrabi growth*.

Liu, B., & Heins D., R. (1998). Modeling poinsettia vegetative growth and development: the response to the ratio of radiant to thermal energy. *Acta Horticulturae*, *456*.

Liu, B., Liu, L., Asseng, S., Zhang, D., Ma, W., Tang, L., Cao, W., & Zhu, Y. (2020). Modelling the effects of post-heading heat stress on biomass partitioning, and grain number and weight of wheat. *Journal of Experimental Botany*, *71*(19), 6015–6031. https://doi.org/10.1093/JXB/ERAA310

LTO Glaskracht. (2015). *Visie 2030 Glastuinbouw Energie en Klimaat*.

Luo, A., Kang, S., Chen, J., & Bailey, B. N. (2020a). *SUGAR Model-Assisted Analysis of Carbon Allocation and Transformation in Tomato Fruit Under Different Water Along With Potassium Conditions*. *11*(June). https://doi.org/10.3389/fpls.2020.00712

Luo, A., Kang, S., Chen, J., & Bailey, B. N. (2020b). *SUGAR Model-Assisted Analysis of Carbon Allocation and Transformation in Tomato Fruit Under Different Water Along With Potassium Conditions*. *11*(June). https://doi.org/10.3389/fpls.2020.00712

MacNeill, G. J., Mehrpouyan, S., Minow, M. A. A., Patterson, J. A., Tetlow, I. J., & Emes, M. J. (2017a). Starch as a source, starch as a sink: The bifunctional role of starch in carbon allocation. In *Journal of Experimental Botany* (Vol. 68, Issue 16, pp. 4433–4453). Oxford University Press. https://doi.org/10.1093/jxb/erx291

MacNeill, G. J., Mehrpouyan, S., Minow, M. A. A., Patterson, J. A., Tetlow, I. J., & Emes, M. J. (2017b). Starch as a source, starch as a sink: The bifunctional role of starch in carbon allocation. In *Journal of Experimental Botany* (Vol. 68, Issue 16, pp. 4433–4453). Oxford University Press. https://doi.org/10.1093/jxb/erx291

MacRae, E., & Lunn, J. (2006). Control of sucrose biosynthesis. In W. Plaxton & M. T. McManus (Eds.), *Annual Plant Reviews, Control of Primary Metabolism in Plants* (pp. 234–250). Blackwell Publishing Ltd.

Marcelis, L. F. M. (1991). Effects of Sink Demand on Photosynthesis in Cucumber. *Journal of Experimental Botany*, *42*(11), 1387–1392. https://doi.org/10.1093/JXB/42.11.1387

Marcelis, L. F. M. (1994). A simulation model for dry matter partitioning in cucumber. *Annals of Botany*, *74*(1), 43–52. https://doi.org/10.1093/aob/74.1.43

Marcelis, L. F. M., & Baan Hofman-Eijer, L. R. (1997). Effects of Seed Number on Competition and Dominance among Fruits in Capsicum annuum L. In *Annals of Botany Company* (Vol. 79).

Marcelis, L. F. M., Heuvelink, E., & Goudriaan, J. (1998a). Modelling biomass production and yield of horticultural crops: A review. *Scientia Horticulturae*, *74*(1–2), 83–111. https://doi.org/10.1016/S0304-4238(98)00083-1

Marcelis, L. F. M., Heuvelink, E., & Goudriaan, J. (1998b). Modelling biomass production and yield of horticultural crops: A review. *Scientia Horticulturae*, *74*(1–2), 83–111. https://doi.org/10.1016/S0304-4238(98)00083-1

Margalha, L., Confraria, A., & Baena-González, E. (2019). SnRK1 and TOR: Modulating growth–defense trade-offs in plant stress responses. *Journal of Experimental Botany*, *70*(8), 2261–2274. https://doi.org/10.1093/jxb/erz066

Martínez-Vilalta, J., Sala, A., Asensio, D., Galiano, L., Hoch, G., Palacio, S., Piper, F. I., & Lloret, F. (2016). Dynamics of non-structural carbohydrates in terrestrial plants: A global synthesis. *Ecological Monographs*, *86*(4), 495–516. https://doi.org/10.1002/ecm.1231

Mengin, V., Stitt, M., Pyl, E. T., & Moraes, T. A. (2017). *Photosynthate partitioning to starch in Arabidopsis thaliana is insensitive to light intensity but sensitive to photoperiod due to a restriction on growth in the light in short photoperiods*. 2608–2627. https://doi.org/10.1111/pce.13000

Millar, A. J., Pokhilko, A., Seaton, D. D., & Ebenho, O. (2014). *Regulatory principles and experimental approaches to the circadian control of starch turnover*.

Muller, B., & Martre, P. (2019). Plant and crop simulation models: powerful tools to link physiology, genetics, and phenomics. *Journal of Experimental Botany*, *70*(9), 2339–2344. https://doi.org/10.1093/JXB/ERZ175

Müller, F., Xu, J., Kristensen, L., Wolters-Arts, M., De Groot, P. F. M., Jansma, S. Y., Mariani, C., Park, S., & Rieu, I. (2016). High-temperature-induced defects in tomato (Solanum lycopersicum) anther and pollen development are associated with reduced expression of B-class floral patterning genes. *PLoS ONE*, *11*(12), 1–14. https://doi.org/10.1371/journal.pone.0167614

Nagele, T., Henkel, S., Ho, I., Sauter, T., Sawodny, O., & Systemdynamik, S. H. (2010). *Mathematical Modeling of the Central Carbohydrate Metabolism in Arabidopsis Reveals a Substantial Regulatory Influence of Vacuolar Invertase on Whole*. *153*(May 2010), 260–272. https://doi.org/10.1104/pp.110.154443

Nunes, C., O'Hara, L. E., Primavesi, L. F., Delatte, T. L., Schluepmann, H., Somsen, G. W., Silva, A. B., Fevereiro, P. S., Wingler, A., & Paul, M. J. (2013). The trehalose 6-phosphate/snRK1. signaling pathway primes growth recovery following relief of sink limitation. *Plant Physiology*, *162*(3), 1720–1732. https://doi.org/10.1104/pp.113.220657

Ohnishi, S., Miyoshi, T., & Shirai, S. (2010). Low temperature stress at different flower developmental stages affects pollen development, pollination, and pod set in soybean. *Environmental and Experimental Botany*, *69*(1), 56–62. https://doi.org/10.1016/j.envexpbot.2010.02.007

Osman, R., Zhu, Y., Cao, W., Ding, Z., Wang, M., Liu, L., Tang, L., & Liu, B. (2021). Modeling the effects of extreme high-temperature stress at anthesis and grain filling on grain protein in winter wheat. *The Crop Journal*, *9*(4), 889–900. https://doi.org/10.1016/J.CJ.2020.10.001

Palacio, S., Hoch, G., Sala, A., Körner, C., & Millard, P. (2014). Does carbon storage limit tree growth? *New Phytologist*, *201*(4), 1096–1100. https://doi.org/10.1111/nph.12602

Pan, J., Zhu, Y., & Cao, W. (2007). Modeling plant carbon flow and grain starch accumulation in wheat. *Field Crops Research*, *101*(3), 276–284. https://doi.org/10.1016/j.fcr.2006.12.005

Pandolfini, T., Molesini, B., & Spena, A. (2009). *Parthenocarpy in Crop Plants*. https://doi.org/10.1002/9781119312994.apr0416

Parent, B., Turc, O., Gibon, Y., Stitt, M., & Tardieu, F. (2010). Modelling temperature-compensated physiological rates, based on the co-ordination of responses to temperature of developmental processes. *Journal of Experimental Botany*, *61*(8), 2057–2069. https://doi.org/10.1093/jxb/erq003

Paul, M. J., & Foyer, C. H. (2001a). Sink regulation of photosynthesis. *Journal of Experimental Botany*, *52*(360), 1383–1400. https://doi.org/10.1093/jexbot/52.360.1383

Paul, M. J., & Foyer, C. H. (2001b). Sink regulation of photosynthesis. *Journal of Experimental Botany*, *52*(360), 1383–1400. https://doi.org/10.1093/jexbot/52.360.1383

Payne, H. J., Hemming, S., van Rens, B. A. P., van Henten, E. J., & van Mourik, S. (2022). Quantifying the role of weather forecast error on the uncertainty of greenhouse energy prediction and power market trading. *Biosystems Engineering*, *224*, 1–15. https://doi.org/10.1016/J.BIOSYSTEMSENG.2022.09.009

PBL. (2022). *Klimaat- en Energieverkenning 2022*. www.pbl.nl/kev

Peet, M. M., Sato, S., & Gardner, R. G. (1998). Comparing heat stress effects on male-fertile and male-sterile tomatoes. *Plant, Cell and Environment*, *21*(2), 225–231. https://doi.org/10.1046/j.1365-3040.1998.00281.x

Peet, M. M., Willits, D. H., & Gardner, R. (1997). Response of ovule development and post-pollen production processes in male-sterile tomatoes to chronic, sub-acute high temperature stress. *Journal of Experimental Botany*, *48*(306), 101–111. https://doi.org/10.1093/jxb/48.1.101

Peng, B., Guan, K., Tang, J., Ainsworth, E. A., Asseng, S., Bernacchi, C. J., Cooper, M., Delucia, E. H., Elliott, J. W., Ewert, F., Grant, R. F., Gustafson, D. I., Hammer, G. L., Jin, Z., Jones, J. W., Kimm, H., Lawrence, D. M., Li, Y., Lombardozzi, D. L., … Zhou, W. (2020). Towards a multiscale crop modelling framework for climate change adaptation assessment. *Nature Plants*, *6*(4), 338–348. https://doi.org/10.1038/s41477-020-0625-3

Penning De Vries, F. W. T., Brunsting~, P. A. H. M., & van Laar$, H. H. (1974). Products, Requirements and Efficiency of Biosynthesis : A Quantitative Approach. *J. Theor. Biol*, *45*, 339–377.

Pereira, J., Revi, A., Rose, S., Sanchez-Rodriguez, R., Lisa Schipper Sweden, E. F., Schmidt, D. U., Schoeman, D., Shaw, R., Singh, C., Solecki, W., & Stringer, L. (2022). *IPCC Summary for Policy Makers*. Morgan Wairiu. https://doi.org/10.1017/9781009325844.001

Pham, D., Hoshikawa, K., Fujita, S., Fukumoto, S., Hirai, T., Shinozaki, Y., & Ezura, H. (2020). A tomato heat-tolerant mutant shows improved pollen fertility and fruit-setting under long-term ambient high temperature. *Environmental and Experimental Botany*, *178*(March), 104150. https://doi.org/10.1016/j.envexpbot.2020.104150

Pilkington, S. M., Encke, B., Krohn, N., Höhne, M., Stitt, M., & Pyl, E. T. (2015). Relationship between starch degradation and carbon demand for maintenance and growth in Arabidopsis thaliana in different irradiance and temperature regimes. *Plant, Cell and Environment*, *38*(1), 157–171. https://doi.org/10.1111/pce.12381

Pokhilko, A., Seaton, D. D., Ebenhöh, O., & Millar, A. J. (n.d.). *Regulatory principles and experimental approaches to the circadian control of starch turnover*. https://doi.org/10.1098/rsif.2013.0979

Pollock, C. J., & Cairns, A. J. (1991). *GRASSES AND CEREALS*.

Pommerrenig, B., Ludewig, F., Cvetkovic, J., Trentmann, O., Klemens, P. A. W., & Neuhaus, H. E. (2018a). In concert: Orchestrated changes in carbohydrate homeostasis are critical for plant abiotic stress tolerance. *Plant and Cell Physiology*, *59*(7), 1290–1299. https://doi.org/10.1093/pcp/pcy037

Pommerrenig, B., Ludewig, F., Cvetkovic, J., Trentmann, O., Klemens, P. A. W., & Neuhaus, H. E. (2018b). In concert: Orchestrated changes in carbohydrate homeostasis are critical for plant abiotic stress tolerance. *Plant and Cell Physiology*, *59*(7), 1290–1299. https://doi.org/10.1093/pcp/pcy037

Poorter, H., Anten, N. P. R., & Marcelis, L. F. M. (2013a). Physiological mechanisms in plant growth models: Do we need a supra-cellular systems biology approach? *Plant, Cell and Environment*, *36*(9), 1673–1690. https://doi.org/10.1111/pce.12123

Poorter, H., Anten, N. P. R., & Marcelis, L. F. M. (2013b). Physiological mechanisms in plant growth models: Do we need a supra-cellular systems biology approach? *Plant, Cell and Environment*, *36*(9), 1673–1690. https://doi.org/10.1111/pce.12123

Poorter, H., Fiorani, F., Pieruschka, R., Putten, W. H. van der, Kleyer, M., & Schurr, U. (2016). *Tansley review Pampered inside , pestered outside ? Differences and similarities between plants growing in controlled conditions and in the field*. 838–855.

Prasad, P. V. V., Craufurd, P. Q., Summerfield, R. J., & Ad, R. R. G. (1999). *Fruit Number in Relation to Pollen Production and Viability in Groundnut Exposed to Short Episodes of Heat Stress Author*. *84*(3), 381–386.

Prasad, V., Craufurd, P., & Summerfield, R. (1999). Fruit number in relation to pollen production and viability in groundnut exposed to short episodes of heat stress. *Annals of Botany*, *84*(3), 381–386. https://doi.org/10.1006/anbo.1999.0926

Pressman, E. (2002). The Effect of Heat Stress on Tomato Pollen Characteristics is Associated with Changes in Carbohydrate Concentration in the Developing Anthers. *Annals of Botany*, *90*(5), 631–636. https://doi.org/10.1093/aob/mcf240

Pyl, E. T., Piques, M., Ivakov, A., Schulze, W., Ishihara, H., Stitt, M., & Sulpice, R. (2012). Metabolism and growth in Arabidopsis depend on the daytime temperature but are temperature-compensated against cool nights. *Plant Cell*, *24*(6), 2443–2469. https://doi.org/10.1105/tpc.112.097188

Qian, T., Dieleman, J. A., Elings, A., & Marcelis, L. F. M. (2012). Leaf photosynthetic and morphological responses to elevated CO2 concentration and altered fruit number in the semi-closed greenhouse. *Scientia Horticulturae*, *145*, 1–9. https://doi.org/10.1016/J.SCIENTA.2012.07.015

Rasse, D. P., & Tocquin, P. (2006). Leaf carbohydrate controls over Arabidopsis growth and response to elevated CO2: An experimentally based model. *New Phytologist*, *172*(3), 500–513. https://doi.org/10.1111/j.1469-8137.2006.01848.x

Richardson, A. D., Carbone, M. S., Keenan, T. F., Czimczik, C. I., Hollinger, D. Y., Murakami, P., Schaberg, P. G., & Xu, X. (2013). Seasonal dynamics and age of stemwood nonstructural carbohydrates in temperate forest trees. *New Phytologist*, *197*(3), 850–861. https://doi.org/10.1111/nph.12042

RIVM. (2021). *Greenhouse Gas Emissions in the Netherlands 1990-2019*. www.rivm.nl/en

Rodriguez, M., Parola, R., Andreola, S., Pereyra, C., & Martínez-Noël, G. (2019). TOR and SnRK1 signaling pathways in plant response to abiotic stresses: Do they always act according to the “yin-yang” model? *Plant Science*, *288*(April). https://doi.org/10.1016/j.plantsci.2019.110220

Ruan, Y. L., Patrick, J. W., Bouzayen, M., Osorio, S., & Fernie, A. R. (2012). Molecular regulation of seed and fruit set. *Trends in Plant Science*, *17*(11), 656–665. https://doi.org/10.1016/j.tplants.2012.06.005

Ruan, Y.-L. (2014). Sucrose Metabolism: Gateway to Diverse Carbon Use and Sugar Signaling. *The Annual Review of Plant Biology*, *65*, 33–67. https://doi.org/10.1146/annurev-arplant-050213-040251

Ruelland, E., Vaultier, M. N., Curie, M., Galile, R., & Seine, I. (2009a). Cold Signalling and Cold Acclimation in Plants ˚ Plant Science Centre , Department of Plant Physiology , I . INTRODUCTION. In *Advances in Botanical Research* (1st ed., Vol. 49, Issue 08). Elesvier Ltd. https://doi.org/10.1016/S0065-2296(08)00602-2

Ruelland, E., Vaultier, M. N., Curie, M., Galile, R., & Seine, I. (2009b). Cold Signalling and Cold Acclimation in Plants ˚ Plant Science Centre , Department of Plant Physiology , I . INTRODUCTION. In *Advances in Botanical Research* (1st ed., Vol. 49, Issue 08). Elesvier Ltd. https://doi.org/10.1016/S0065-2296(08)00602-2

Sala, A., Woodruff, D. R., & Meinzer, F. C. (2012). Carbon dynamics in trees: feast or famine? *Tree Physiology*, *32*(6), 764–775. https://doi.org/10.1093/treephys/tpr143

Santiago, J. P., & Sharkey, T. D. (2019). Pollen development at high temperature and role of carbon and nitrogen metabolites. *Plant Cell and Environment*, *42*(10), 2759–2775. https://doi.org/10.1111/pce.13576

Sato, S., Kamiyama, M., Iwata, T., Makita, N., Furukawa, H., & Ikeda, H. (2006). Moderate increase of mean daily temperature adversely affects fruit set of Lycopersicon esculentum by disrupting specific physiological processes in male reproductive development. *Annals of Botany*, *97*(5), 731–738. https://doi.org/10.1093/aob/mcl037

Sato, S., Peet, M. M., & Gardner, R. G. (2001). Formation of parthenocarpic fruit, undeveloped flowers and aborted flowers in tomato under moderately elevated temperatures. *Scientia Horticulturae*, *90*(3–4), 243–254. https://doi.org/10.1016/S0304-4238(00)00262-4

Sato, S., Peet, M. M., & Thomas, J. F. (2000a). Physiological factors limit fruit set of tomato (Lycopersicon esculentum Mill.) under chronic, mild heat stress. *Plant,*

Cell and Environment, *23*(7), 719–726. https://doi.org/10.1046/j.1365-3040.2000.00589.x

Sato, S., Peet, M. M., & Thomas, J. F. (2000b). Physiological factors limit fruit set of tomato under chronic, mild heat stress. *Plant, Cell & Environment*, *23*, 719–726. https://doi.org/10.1046/j.1365-3040.2000.00589.x

Sato, S., Peet, M. M., & Thomas, J. F. (2002). Determining critical pre- and post-anthesis periods and physiological processes in Lycopersicon esculentum Mill. exposed to moderately elevated temperatures. *Journal of Experimental Botany*, *53*(371), 1187–1195. https://doi.org/10.1093/jexbot/53.371.1187

Schapendonk, A. H. C. M., Stol, W., Kraalingen, D. W. G. Van, & Bouman, B. A. M. (1998). *LINGRA , a sink / source model to simulate grassland productivity in Europe*. *9*, 87–100.

Schmitz, J., Heinrichs, L., Scossa, F., Fernie, A. R., Oelze, M., Dietz, K., Rothbart, M., Grimm, B., Flügge, U., & Häusler, R. E. (2014). *The essential role of sugar metabolism in the acclimation response of Arabidopsis thaliana to high light intensities*. *65*(6), 1619–1636. https://doi.org/10.1093/jxb/eru027

Schnyder H. (1993). The role of carbohydrate storage and redistribution in the source-sink relations of wheat and barley during grain filling — a review. *New Phytologist*, *123*(2), 233–245. https://doi.org/10.1111/j.1469-8137.1993.tb03731.x

Scialdone, A., Mugford, S. T., Feike, D., Skeffington, A., Borrill, P., Graf, A., Smith, A. M., & Howard, M. (2013). Arabidopsis plants perform arithmetic division to prevent starvation at night. *ELife*, *2013*(2), 1–24. https://doi.org/10.7554/eLife.00669

Seginer, I. (2022). Sub-optimal control of the greenhouse environment : Crop models with and without an assimilates buffer. *Biosystems Engineering*, *221*, 236–257. https://doi.org/10.1016/j.biosystemseng.2022.06.011

Seginer, I., & Gent, M. P. N. (2014). Short and long term vegetative growth response to temperature, interpreted by the dynamics of a carbohydrate storage. *Scientia Horticulturae*, *171*, 14–26. https://doi.org/10.1016/j.scienta.2014.03.020

Seki, M., Ohara, T., Hearn, T. J., Frank, A., da Silva, V. C. H., Caldana, C., Webb, A. A. R., & Satake, A. (2017). Adjustment of the Arabidopsis circadian oscillator

by sugar signalling dictates the regulation of starch metabolism. *Scientific Reports*, *7*(1). https://doi.org/10.1038/s41598-017-08325-y

Serrago, R. A., Alzueta, I., Savin, R., & Slafer, G. A. (2013). Field Crops Research Understanding grain yield responses to source – sink ratios during grain filling in wheat and barley under contrasting environments. *Field Crops Research*, *150*, 42–51. https://doi.org/10.1016/j.fcr.2013.05.016

Sigrimis, N., Anastasiou, A., & Rerras, N. (2000). Energy saving in greenhouses using temperature integration: A simulation survey. *Computers and Electronics in Agriculture*, *26*(3), 321–341. https://doi.org/10.1016/S0168-1699(00)00083-1

Silpi, U., Lacointe, A., Kasempsap, P., Thanysawanyangkura, S., Chantuma, P., Gohet, E., Musigamart, N., Clément, A., Améglio, T., & Thaler, P. (2007). Carbohydrate reserves as a competing sink: Evidence from tapping rubber trees. *Tree Physiology*, *27*(6), 881–889. https://doi.org/10.1093/treephys/27.6.881

Smith, A. M., & Stitt, M. (2007). Coordination of carbon supply and plant growth. *Plant, Cell and Environment*, *30*(9), 1126–1149. https://doi.org/10.1111/j.1365-3040.2007.01708.x

Smith, A. M., & Zeeman, S. C. (2020). *Starch : A Flexible , Adaptable Carbon Store Coupled to Plant Growth*. 217–245.

Smith, N. G., & Dukes, J. S. (2013). Plant respiration and photosynthesis in global-scale models: Incorporating acclimation to temperature and CO2. *Global Change Biology*, *19*(1), 45–63. https://doi.org/10.1111/j.1365-2486.2012.02797.x

Sonnewald, U., & Fernie, A. R. (2018). Next-generation strategies for understanding and influencing source-sink relations in crop plants This review comes from a themed issue on Physiology and metabolism The concepts of source and sinks. *Current Opinion in Plant Biology*, *43*, 63–70. https://doi.org/10.1016/j.pbi.2018.01.004

Sperling, O., Kamai, T., Tixier, A., Davidson, A., Jarvis-Shean, K., Raveh, E., DeJong, T. M., & Zwieniecki, M. A. (2019). Predicting bloom dates by temperature mediated kinetics of carbohydrate metabolism in deciduous trees. *Agricultural and Forest Meteorology*, *276–277*(July), 107643. https://doi.org/10.1016/j.agrformet.2019.107643

Spitters, C. J. T., Keulen, H. van, & Kraalingen, D. W. G. Van. (1987a). A simple universal crop growth simulator: SUCROS87. In *Simulation and systems management in crop protection* (pp. 147–181).

Spitters, C. J. T., Keulen, H. van, & Kraalingen, D. W. G. Van. (1987b). A simple universal crop growth simulator: SUCROS87. In *Simulation and systems management in crop protection* (pp. 147–181).

Steduto, P., Hsiao, T. C., Raes, D., & Fereres, E. (2009). Aquacrop-the FAO crop model to simulate yield response to water: I. concepts and underlying principles. *Agronomy Journal*, *101*(3), 426–437. https://doi.org/10.2134/agronj2008.0139s

Stitt, M. (1991). *Rising CO2 levels and their potential significance for carbon flow in photosynthetic cells*. 741–762.

Stitt, M., & Zeeman, S. C. (n.d.). *Starch turnover: pathways, regulation and role in growth | Elsevier Enhanced Reader*. Retrieved November 27, 2020, from https://reader.elsevier.com/reader/sd/pii/S1369526612000519?token=9D6AD377AF80250E0B4FD98959D61ACD05CE9BAD3BB99A31EE480D36D741F99ADD7D59DE5140C543E9011678596D7D4B

Stitt, M., & Zeeman, S. C. (2012). Starch turnover: Pathways, regulation and role in growth. *Current Opinion in Plant Biology*, *15*(3), 282–292. https://doi.org/10.1016/j.pbi.2012.03.016

Stitt Mark. (1996). Metabolic Regulation of Photosynthesis. In *Photosynthesis and the Environment* (Vol. 5, pp. 151–190).

Sulpice, R., Flis, A., Ivakov, A. A., Apelt, F., Krohn, N., Encke, B., Abel, C., Feil, R., Lunn, J. E., & Stitt, M. (2014). Arabidopsis Coordinates the Diurnal Regulation of Carbon Allocation and Growth across a Wide Range of Photoperiods. *Molecular Plant* •, *7*, 137–155. https://doi.org/10.1093/mp/sst127

Sun, J., Okita, T. W., & Edwards, G. E. (1999). Modification of carbon partitioning, photosynthetic capacity, and O2 sensitivity in Arabidopsis plants with low ADP-glucose pyrophosphorylase activity. *Plant Physiology*, *119*(1), 267–276. https://doi.org/10.1104/pp.119.1.267

Sweetlove, L. J., Nielsen, J., & Fernie, A. R. (2017). Engineering central metabolism – a grand challenge for plant biologists. *Plant Journal*, *90*(4), 749–763. https://doi.org/10.1111/tpj.13464

Talbott, L. D., & Zeiger, E. (1998). The role of sucrose in guard cell osmoregulation. *Journal of Experimental Botany*, *49*(Special issue: Stomatal biology), 329–337. https://doi.org/10.1093/jxb/49.special_issue.329

Thakur, P., Kumar, S., Malik, J. A., Berger, J. D., & Nayyar, H. (2010). *Cold stress effects on reproductive development in grain crops : An overview*. *67*, 429–443. https://doi.org/10.1016/j.envexpbot.2009.09.004

Thalmann, M., & Santelia, D. (2017a). Starch as a determinant of plant fitness under abiotic stress. *New Phytologist*, *214*(3), 943–951. https://doi.org/10.1111/nph.14491

Thalmann, M., & Santelia, D. (2017b). Starch as a determinant of plant fitness under abiotic stress. *New Phytologist*, *214*(3), 943–951. https://doi.org/10.1111/nph.14491

Thornley, J. (2016). Temperature and CO2Responses of Leaf and Canopy Photosynthesis : a Clarification using the Non-rectangular Hyperbola Model of Photosynthesis Temperature and CO 2 Responses of Leaf and Canopy Photosynthesis : a Clarification using the Non-rectangular Hyper. *Annals of Botany*, *82*(January), 883–892.

Thornley, J. H. (1976). *Mathematical models in plant physiology*. Academic Press.

Thornley, J. H. M., & Hurd, R. G. (1974). An analysis of the growth of young tomato plants in water culture at different light integrals and CO2 concentrations: II. A mathematical model. *Annals of Botany*, *38*(2), 389–400. https://doi.org/10.1093/oxfordjournals.aob.a084822

Thornley, J. H. M., & Hurd, R. G. (1976a). An analysis of the growth of young tomato plants in water culture at different light integrals and CO2 concentrations: II. A mathematical model. *Annals of Botany*, *38*(2), 389–400. https://doi.org/10.1093/oxfordjournals.aob.a084822

Thornley, J. H. M., & Hurd, R. G. (1976b). An analysis of the growth of young tomato plants in water culture at different light integrals and CO2 concentrations: II. A mathematical model. *Annals of Botany*, *38*(2), 389–400. https://doi.org/10.1093/oxfordjournals.aob.a084822

Tixier, A., Cochard, H., Badel, E., Dusotoit-Coucaud, A., Jansen, S., & Herbette, S. (2013). Arabidopsis thaliana as a model species for xylem hydraulics: Does size

matter? *Journal of Experimental Botany*, *64*(8), 2295–2305. https://doi.org/10.1093/jxb/ert087

van Beveren, P. J. M., Bontsema, J., van Straten, G., & van Henten, E. J. (2015). Optimal control of greenhouse climate using minimal energy and grower defined bounds. *Applied Energy*, *159*, 509–519. https://doi.org/10.1016/j.apenergy.2015.09.012

Van Der Ploeg, A., & Heuvelink, E. (2005). Influence of sub-optimal temperature on tomato growth and yield: A review. *Journal of Horticultural Science and Biotechnology*, *80*(6), 652–659. https://doi.org/10.1080/14620316.2005.11511994

van der Velden, N., & Smit, P. (2019). *Energiemonitor van de Nederlandse glastuinbouw 2018*. https://doi.org/10.18174/505786

van Henten, E. J. (1994). *Validation of a Dynamic Lettuce Growth Model for Greenhouse Climate Control*. *45*, 55–72.

van Mourik, S., van der Tol, R., Linker, R., Reyes-Lastiri, D., Kootstra, G., Koerkamp, P. G., & van Henten, E. J. (2021). Introductory overview: Systems and control methods for operational management support in agricultural production systems. *Environmental Modelling and Software*, *139*. https://doi.org/10.1016/J.ENVSOFT.2021.105031

van Straten, G., Challa, H., & Buwalda, F. (2000). Towards user accepted optimal control of greenhouse climate. *Computers and Electronics in Agriculture*, *26*(3), 221–238. https://doi.org/10.1016/S0168-1699(00)00077-6

van Straten, G., van Willigenburg, G., van Henten, E., & van Ooteghem, R. (2010). Optimal control of greenhouse cultivation. *Optimal Control of Greenhouse Cultivation*, 1–297. https://www.taylorfrancis.com/books/mono/10.1201/b10321/optimal-control-greenhouse-cultivation-gerrit-van-straten-gerard-van-willigenburg-eldert-van-henten-rachel-van-ooteghem

Vanthoor, B. H. E., Visser, P. H. B. de, Stanghellini, C., & Henten, E. J. van. (2011a). A methodology for model-based greenhouse design : Part 2 , description and validation of a tomato yield model. *Biosystems Engineering*, *110*(4), 378–395. https://doi.org/10.1016/j.biosystemseng.2011.08.005

Vanthoor, B. H. E., Visser, P. H. B. De, Stanghellini, C., & Henten, E. J. Van. (2011b). A methodology for model-based greenhouse design : Part 2 , description and validation of a tomato yield model. *Biosystems Engineering*, *110*(4), 378–395. https://doi.org/10.1016/j.biosystemseng.2011.08.005

Varga, A., & Bruinsma, J. (1976). Roles of Seeds and Auxins in Tomato Fruit Growth. *Zeitschrift Für Pflanzenphysiologie*, *80*(2), 95–104. https://doi.org/10.1016/s0044-328x(76)80146-8

Vialet-chabrand, S., Matthews, J. S. A., Simkin, A. J., Raines, C. A., & Lawson, T. (2017). Importance of Fluctuations in Light on Plant. *Plant Physiology*, *173*(April), 2163–2179. https://doi.org/10.1104/pp.16.01767

Walters, R. G. (2005). Towards an understanding of photosynthetic acclimation. *Journal of Experimental Botany*, *56*(411), 435–447. https://doi.org/10.1093/jxb/eri060

Webb, A. A. R., Satake, A., & Caldana, C. (2019). Continuous dynamic adjustment of the plant circadian oscillator. *Nature Communications*, 4–9. https://doi.org/10.1038/s41467-019-08398-5

Weber, R., Gessler, A., & Hoch, G. (2019). High carbon storage in carbon-limited trees. *New Phytologist*, *222*(1), 171–182. https://doi.org/10.1111/nph.15599

Weber, R., Schwendener, A., Schmid, S., Lambert, S., Wiley, E., Landh, S. M., & Weber, R. (2018). *Living on next to nothing : tree seedlings can survive weeks with very low carbohydrate concentrations*. *2014*, 107–118. https://doi.org/10.1111/nph.14987

Welham, T., Brachmann, A., Pike, M., Pike, J., Perry, J., Parniske, M., Sato, S., Tabata, S., Smith, A. M., Wang, T. L., Biology, M., Centre, J. I., Nr, N., V, U. K. C., & Pike, M. (2010). A Suite of Lotus japonicus Starch Mutants Reveals Both Conserved and Novel Features of Starch Metabolism. *Plant Physiology*, *154*(October 2010), 643–655. https://doi.org/10.1104/pp.110.161844

Wiese-klinkenberg, A., Parent, B., Mielewczik, M., & Schurr, U. (2010). *Diel time-courses of leaf growth in monocot and dicot species : endogenous rhythms and temperature effects*. 1–9. https://doi.org/10.1093/jxb/erq049

Wiley, E., King, C. M., & Landhäusser, S. M. (2019). Identifying the relevant carbohydrate storage pools available for remobilization in aspen roots. *Tree Physiology*, *39*(7), 1109–1120. https://doi.org/10.1093/treephys/tpz051

Wubs, A. M. (2010). *Towards stochastic simulation of crop yield: a case study of fruit set in sweet pepper*.

Yamori, W., Hikosaka, K., & Way, D. A. (2014). Temperature response of photosynthesis in C3, C4, and CAM plants: Temperature acclimation and temperature adaptation. *Photosynthesis Research*, *119*(1–2), 101–117. https://doi.org/10.1007/s11120-013-9874-6

Yin, X., & Struik, P. C. (2009). C3 and C4 photosynthesis models: An overview from the perspective of crop modelling. *NJAS - Wageningen Journal of Life Sciences*, *57*(1), 27–38. https://doi.org/10.1016/j.njas.2009.07.001

Zepeda, A. C., Heuvelink, E., & Marcelis, L. F. M. (2022a). Carbon storage in plants: a buffer for temporal light and temperature fluctuations. *In Silico Plants*. https://doi.org/10.1093/insilicoplants/diac020

Zepeda, A. C., Heuvelink, E., & Marcelis, L. F. M. (2022b). *Non-structural carbohydrate dynamics and growth in tomato plants grown at fluctuating light and temperature*. *October*, 1–13. https://doi.org/10.3389/fpls.2022.968881

Zhang, Y., & Kaiser, E. (2020). *Salt stress and fluctuating light have separate effects on photosynthetic acclimation , but interactively affect biomass*. *May*, 2192–2206. https://doi.org/10.1111/pce.13810

Zhang, Y., Primavesi, L. F., Jhurreea, D., Andralojc, P. J., Mitchell, R. A. C., Powers, S. J., Schluepmann, H., Delatte, T., Wingler, A., & Paul, M. J. (2009). Inhibition of SNF1-related protein kinasel activity and regulation of metabolic pathways by trehalose-6-phosphate1[w][OA]. *Plant Physiology*, *149*(4), 1860–1871. https://doi.org/10.1104/pp.108.133934

Zinn, K. E., Tunc-ozdemir, M., & Harper, J. F. (2010). *Temperature stress and plant sexual reproduction : uncovering the weakest links*. *61*(7), 1959–1968. https://doi.org/10.1093/jxb/erq053

Zwieniecki, M. A., Tixier, A., & Sperling, O. (2015). Temperature-assisted redistribution of carbohydrates in trees. *American Journal of Botany*, *102*(8), 1216–1218. https://doi.org/10.3732/ajb.1500218

Acknowledgements

Seven years ago, I left my sunny life in Mexico to start a new adventure in the not-so-sunny Netherlands. Never in my wildest dreams I image that this bold move would lead me to obtaining a PhD degree. These past four years have been very challenging, especially when you're far away from the comfort of home and family. This challenge became even heavier in the midst of a global pandemic. Nevertheless, the result has been also very rewarding. I was lucky enough to have landed in a place where people were warm and kind to me. In the end, growth is a continuous process, and I feel that these past four years I have grown enormously, both as a scientist and as a person. Now I have the opportunity to thank all the people that were part of this journey, but I must warn you, this section might end up being even longer than my general introduction!

Ep, you were a constant source of reliability throughout my PhD, thanks for always being so available. You taught me how to be concise and pragmatic, as exemplified by your general rule: *'if it fits in the email subject line, no need to write a full email'*. You were also very good at suggesting 'no-panic' solutions whenever I had unexpected results. From you I learned that no matter how puzzled you are, after a few meetings things always become clearer. I always felt that 'we were on the same page' on many topics or issues. I also want to thank you for the enjoyable moments, like sharing funny stories about the past (we both like history of things in general) and the fun gala dinner we had in Angers. Thanks to you and Mariko also for open you home for a delicious dinner. You definitely set a very good example on how a good supervisor should be.

Leo, you were the creative, out-of-the-box mind in our team. Thank you for always being present, engaged, and effective. I learned a lot from your ability to approach problems with creativity. I have very present how, when I was struggling with a draft or ideas, you would tell *'many times I don't know where this idea is going but after a few meetings with Ep, it becomes something'*. I am especially grateful that you made it clear from our first meeting that you were open to discuss problems and feelings, which for me is essential to grow as an academic and as a human; I never felt alone in this process. You always encouraged to be confident and reassured me in moments of uncertainty. Your 'dad' jokes always lightened up tedious meetings (and remined me of my own dad 'dad' jokes). I still wonder what your secret is to be so energetic.

Gerrit (Stunnenberg), you were my saving angel. I am not particularly skilful at technical tasks; therefore, this PhD could have never been done without your technical

support. Beyond that, you were also there for me in cloudy moments, whenever an experiment would fail and I was in the brink of tears, you would always say *'don't worry, we will find a solution'*. Ook bedankt omdat je bent de enige Nederlander die mij actief heeft aangemoedigd om Nederlands te spreken. **David (Brink),** thank you also for all the technical support! For trying to find solutions to my experimental problems, and for always say hello with a big smile. You three (Gerrit, David and Jannick) were a key piece in this thesis.

To my paranymphs, **David (Katzin),** you were an essential piece during my PhD that prevented me from going insane. Thank you for listening and always offering a different perspective (usually, a less dramatic one). We for sure shared many tears, but we shared many more happy moments: birthdays, zarpes, zarpesitos, zarpesones, celebrations of publications, food, concerts. Somewhere along the PhD, we developed the healthy habit of going for a run every Wednesday, which for me is still like a therapy. You were also the first one that thought me how to model (remember the MinCHO?!), 5 hours straight debugging code. Thanks for being so critical and for giving me feedback on my manuscripts. Two years ago, I was your paranymph and now is your turn. **Cecile,** I am so grateful you came into my life, that you were not shy to say hello in the coffee corner, and that we quickly and easily became very close. You are what in Mexico would say *'a sister from a different mother!'*. Thanks for listening to all my dramas, taking care of me whenever I was sad or sick (which often involved cooking for me) and thanks for coming to Mexico with me. It was because of you that I was introduced to the ferret world, and now I have my beautiful ladies Sukla and Olivia, so I owe you that. You are one of the most committed friends I've ever had, and I am very lucky to have you.

Nicole, for me you are the equivalent of my third paranymph. Destiny made us neighbors and since then, we have been like family. Thanks for your *gezelligheid,* for listening to me, for irradiating so much positiveness, for our nice adventures, for the tea nights and long after dinner conversations. **Wouter,** thanks for having such an amazing girlfriend, but also for all those moments when I was feeling stressed, and you knew exactly how to cheer me up: food! **Priscila,** I learned how to be a good supervisor from you. You know how the saying goes: *'Dios las hace y ellas se juntan'.* I ended my MSc thesis with a job, but also with a best friend. You are my stable place in Wageningen. I hope we can celebrate many more birthdays, Christmas, and New Year's Eve together. **Simon** thanks for all the constant support throughout the PhD. I could have never done this without all your encouragement. Thanks for teaching me how to model and new methods (you really opened a whole new world for me), although sometimes I think you arrived late when God was spreading the habit of *patience.* For all those long walks (up to 30 km walks…) where we talked about

everything and nothing, like in Seinfeld. But most importantly, thank you for having so much faith on me and encourage me to *'not to sell myself short'*.

To my lovely office mates: **Martina**, is so special that we started our PhD on the same day and now we are defending our thesis 1 day apart. I am lucky that I went through the last months of my PhD with you by my side (literally) because we could share all our frustrations and just be crazy together. **Yifei,** with you is also very special because life always found a way to put us together. During the MSc studies, we ended together in the same ACT group, did the thesis at the same time, we started the PhD more or less at the same time, and now we are office mates. Thanks for the girls gossip, and for the mutual sharing of our frustration with Dutch culture. **Jordan**, even though you joined the HPP later on, I am so grateful that you did. Being around you makes me feel relaxed and comfortable. Thank you for your care and thoughtfulness, like bringing me tea during my moments of crisis and asking, 'what do you need?' instead of 'what happened?'. You are a *fantastic* concert partner, and your positive energy is contagious

Wim, you were the first person who ever planted the seed of curiosity in me about 'doing a PhD' when I was working on my master's thesis. Thank you for encouraging me back then. **Elias,** you have been a constant presence in my academic journey since my master's studies. I appreciate your critical thinking, your support and encouragement, and your willingness to listen to my concerns and crises. Your academic and life advice has been very valuable to me. **Silvere,** you are a funny and very smart addition to the team. Thanks for all the jokes that make lunch time less awkward, for your scientific discussions, for your help with coding when I desperately send you an e-mail titled 'you are my last hope' at the middle of the night. If I would have to describe you with a meme, you would be the old wise Yoda. **Katharina,** I see you as a fundamental piece in the group that was long time missing. You came to the HPP and gave the warmth human feeling that sometimes we forget and overlook in academia. Thanks for all the little encouragement notes, for believing in me, and for always having an open door. We are very lucky to have you. **Paul,** the biggest lesson I've learned from you is the importance of allowing space without a tight agenda (which I am an expert on, tight straight agendas…) so that creativity can flow. I feel very fortunate that we can now work together. Thank you for our stimulating conversations - there's never a dull moment with you.

To all my students **Francesco, Youri, Pinglin, Willem, Philippe, Marloes** and **Stefan** (although you were not my student). This thesis would have never been possible without your contribution. **Stefan (Vorage),** I am so happy that you jumped in for the last part of the dwarf tomato experiment. I am proud that you are a co-author.

I enjoyed so much working with you, and all our interesting talks while measuring. Thanks for your very helpful comments on my manuscripts and proofreading one of my chapters. **Francesco,** you were my first student and you set the bar quite high since the very beginning. **Marloes, Philippe and Willem,** I appreciate a lot your commitment as students. **Pinglin,** you really make a huge step with all the testing for pollen measurements, and you were always very proactive.

Julia, I am so happy that you are back in the Netherlands! Thanks for the nice coffee breaks and our warmth conversations. Thanks to you and **Koty** for the nice *'uitjes'* and dinners. **Willy,** thanks for being so *you,* expressive, organised, enthusiastic, and for irradiating that '*latin spice'* that we all need in our dull academic lives. **Balta,** you are the only Zepeda that I know that is not a relative of mine. You bring a lot of enthusiasm to the group, thanks for being my punching bag (literally). **Hadriensito,** thanks for sharing your amazing girlfriend with me, for the nice dinners, and the good memories in Mexico. To the enthusiastic PV members that I haven't thanked yet: **Yongran, Britt** and **Roel,** I'm proud of the nice things that we have managed to organize together! **Sarah (Berman)** your constant smile always brightens my day. **Wannida** and **Sijia**, my conference partners, thanks for being so kind and cute to me. **Kevin** thanks for the philosophical in-depth talks. Thanks also to all my HPP colleagues **Maggie, Stefan, Killian, Elena, Diego, Lucas, Kartika, Marijke, Tijmen, Michele, Katharina (Huntenberg), Maria, Ying, Xixi, Mexx, Rachel, Bartian, Samikshya, Evi, Jiayu, Linda, Sil, Arjen, Joke, Maarten** (and whoever I forgot: I owe you a beer!).

Henry, thanks for the enriching conversations, and for the meetings that turned into a walk in the park, ice cream and laying on the grass. **Ambra** thanks for all the nice moments and for sharing little pieces of culture like the Three Kings (you still need to cook tamales!), for teaching me how to cook pasta, and for cooking for me when I was stressed or sick. **Claudius,** thank you for all the valuable advice, especially in moments of crisis. **Hua,** thanks for your kindness and encouragement. I wish I could be half as perseverant as you are. **Alejandro,** se te extraña, gracias por toda tu ayuda con experimentos, y por todos los buenos momentos con la Priscilla. **Daniel (Reyes)** gracias por todas esas buenas conversaciones con una birrita, y por animarte a supervisar un estudiante conmigo (deberíamos repetir!).

Ido, I greatly admire your work, but what impresses me the most is your great enthusiasm for science even after officially retiring 20 years ago. Thank you for your recent visit to Wageningen and the insightful discussion we had. I still hope that we can collaborate in the future. **Silke, Leon, Fokke, Eldert** and **Klaas** (the Flexcrop team), thanks for your insightful discussions during the project meetings. **Jeroen,**

Max and Bram, thanks for your engagement with the project, you are always very curious and asking the challenging questions.

Ana (Vals). Two years ago, in the middle of the pandemic I boldly decided to start sewing lessons. This decision has given me such a nice friend. Thanks for introducing me to the sewing world, for being a refreshing person to talk to (no science) and for waking up that creative side from me. **Gloria (Paniagua)**, thank you for your support since I was a child. Over the years, you have taught me to break the stigma surrounding mental health and therapy, and you have helped me grow emotionally. I appreciate you always offering me a fresh and pragmatic alternative perspective. **Emma and Margret,** thank you for being so kind and warmth with me. **Michel, Gjerrit and Nicole,** I am happy that I met you! Thanks for the nice company during holidays, all the delicious dinners and very insightful conversations.

Dani, todo empezó contigo. Desde tu ayuda para hacer el mini invernadero en el Tec o explicarme los mapas de Karnaugh. Tu eras el inteligente, el de la mención honorifica, yo era la matada. Por incentivarme a buscar algo mas allá, que me llenara como persona y como profesionista. Por ensenarme como usar LaTex y Matlab. Por siempre tener un buen consejo (por ejemplo, multiplicar todo por 10 para que los cálculos cuadren). Por toda tu positividad (no conozco a nadie más positivo que tu). Por creer en mí, por ser mi cómplice gastronómico. Gracias infinitas soon to be Dr. Cárdenas. A mis *'amiwis'* **Mariana y Laura,** la vida nos separó cuando teníamos 18 años. Aun así, hoy a nuestros 31 años, seguimos juntas a la distancia, ya sea mediante voice notes (que parecen podcasts), o por videollamadas. Ojalá la vida nos mantenga juntas otros 60 años más. **Ale Balderrama, mi nabita.** Although my decision about coming to the Netherlands meant that we would be apart, and that broke my heart, I still feel you very close to me. You are my sister from a different mother. During my bachelor you were my constant source of support, we shared so many tears togethers but lately, we share many happy moments. I am very proud of what you have become.

Damian, Picho y Cata. We came from the same university and ended up together doing the same master in the same group. And now the three of us ended up staying in the Netherlands. It was always nice being around with you three because it felt like being back to Mexico. You guys are the only ones that fully understand my Spanish sayings. **Toneli,** although we lived in the same city only briefly, I always enjoyed our long gossipy talks, and I am happy that we still keep the contact.

Priscila (Mariscal), comadre. Gracias por ser lo mas cercano a familia que tengo por acá. Porque me haces sentir que tengo un hogar en Santiago de Compostela, y porque cuando siento que mi batería se agota, ir a verte me llena de energía. **Maria y Juan**

Pablo, ustedes son unos niños que irradian felicidad, los extraño todos los días. Querida ahijada, mi **Lu**, estoy muy orgullosa y feliz de ser tu Madrina. **Juan,** gracias por siempre abrirme las puertas de tu hogar, y por su calidez.

Tía Tali, gracias por recibirme como tu hija en Monterrey, por venir a mi graduación de maestría y ahora a la de doctorado, y por ensenarme a cocinar (todos mis amigos te lo agradecen). **Madrina Rocío**, gracias por estar conmigo en momentos importantes, sobre todo cuando era niña, todavía recuerdo cuando me vestiste de veracruzana en el baile típico del Salesiano. **Primo Jorge**, realmente de lo más difícil de irme de Monterrey, después de años y años de vivir en la misma ciudad y ser tan cercanos, fue decirte adiós. **Padrino Carlos, tíos Marco, Celina y Rodolfo, primos Sofi, Marquito y Rodolfito,** gracias por darse la vuelta y acompañarme en este día tan importante para mí.

Papá y mamá, a ustedes podría escribirles un libro entero para agradecerles todo lo que me han dado. **Papá,** gracias por darme las alas para volar tan lejos como quisiera. Primero durante mi carrera, y después para estudiar la maestría. Gracias por apoyarme cuando tome la decisión de vivir en Holanda, porque tus sabias que eso implicaba no tenerme cerca de ti. Pero en lugar de cortarme las alas, me diste seguridad en las decisiones que tome, y a pesar de los 10,000 km que nos separan, jamás me he sentido sola. **Mamá,** tu camino a través de la EM me ha enseñado a siempre ver el lado positivo de la vida. Hablar contigo siempre me hace poner mis problemas en perspectiva. Siempre eres mi más grande motivación. Admiro mucho tu fortaleza, tu positivismo y tu fe. Desde chiquita tuviste mucha dedicación para ensenarnos a estudiar, llevarnos al piano y a la natación. Eras nuestra cómplice. Toda tu dedicación nos ha hecho ser las mujeres que somos hoy.

And finally, my baby, my dear **Juli**. First, thank you for being a part of this journey through developing the design concept of my thesis (I am fully aware that I am a difficult client). Thank you also for counting all that pollen for me! You are the greatest gift that life has given me and my best friend. Despite being apart from you, we still find ways to stay close: almost every day, we cook together through a video call. But we also paint together, we knit together, we exercise together. Whenever things get tough, whenever I am scared, when days seem to only say *'no'* to me, I am always with you.

About the author

Ana Cristina Zepeda Cabrera was born in April 1992 in Uruapan Michoacán, the world capital of avocados, in México. Described by her parents, she was a 'restless' child, that would get anyone taking care of her exhausted. She liked doing all sort of extra activities, like swimming, playing piano, playing football (or better said, warming up the bench), and baking cookies. She completed her high school education in the same city, where she chose to focus on chemistry and biological sciences.

After graduating from high school, Cristy moved all the way to the north of Mexico to study a 5-year BSc in Biotechnology Engineering, at the Instituto Tecnológico y de Estudios Superiores de Monterrey. After one year, she realized that the biotechnology aspect was *'not her cup of tea'* and made the decision to switch her specialization to agrobiotechnology. This came as a surprise to her family, considering she had never been able to keep a plant alive. During her BSc, she became an active member of the Asociación de Estudiantes de Michoacán, a student association that promoted the culture of her home state. Cristy held different roles within the association, including treasurer and president. Together with a group of enthusiastic students, she participated in gastronomic contests and cultural expositions. During her BSc, she did an exchange semester in the Universidad Politécnica de Madrid, where she took different courses including viticulture and oenology.

Upon graduating in August 2015, Cristy started working in the quality assurance department of a food company in Monterrey. Life in the big city and a monotonous job from 8 am to 6 pm made her feel like she was living in an infinite loop of boredom. In the midst of an existential crisis, sitting in her car in the parking lot of Walmart during the lunch break, Cristy realized that it was time for a change. In September 2016 she left her office life to start a MSc in Plant Sciences in Wageningen, the Netherlands.

Cristy did her MSc thesis in the Horticulture and Product Physiology group, under the supervision of Dr. Wim van Ieperen and Priscilla Malcolm MSc., exploring the effects of far-red light on plant water relations. During this time, she realized doing research really *'sparked the joy'* and she subsequently pursued a PhD in modelling and plant physiology under the guidance of Dr. Leo Marcelis and Dr. Ep Heuvelink.

During her stay in the Netherlands, she grew to appreciate the Dutch way of life, which she found to be both safe and liberating, despite the limited food culture, which seemed to revolve around the potato, as van Gogh famously depicted in '*De aardappeleters'.* Luckily enough, cooking was something she enjoyed. Aside from science, Cristy picked up hobbies during her PhD such as knitting and sewing, a hobby that all her colleagues are very aware of.

She submitted her thesis in March 2023 and began a new adventure as a postdoc in the Horticulture and Product Physiology group, where she models and investigates the effect of the environment on tip burn in lettuce. Cristy currently lives in Wageningen with her two ferrets, Olivia and Sukla.

List of publications in peer-reviewed journal articles

A.C. Zepeda, E. Heuvelink, L.F.M. Marcelis. **Carbon storage in plants: a buffer for temporal light and temperature fluctuations**. Published in In Silico Plants (2023), 5. DOI: https://doi.org/10.1093/insilicoplants/diac020

A.C. Zepeda, E. Heuvelink, L.F.M. Marcelis (2022). **Non-structural carbohydrate dynamics and growth in tomato plants grown at fluctuating light and temperature.** Published in Frontiers in Plant Science (2022), 13. DOI: https://doi.org/10.3389/fpls.2022.968881

Talks and presentations

Too cold or too hot? modelling seed set and fruit size in different temperature and durations (oral presentation). Symposium of adaptation of Horticultural Plants to Abiotic Stress (Angers, France 2022)

Modelling, control and crop physiology for flexible crop production (oral presentation). Frontiers in Agricultural Genomics seminar, UNAM (Online, 2022).

Modelling crop flexibility to fluctuations in light and temperature (oral presentation). Crops in Silico (Online, 2021)

Carbohydrate Pool and Growth of Tomato Plants Under Fluctuating Light and Temperature Regimes (Oral presentation). American Society for Horticultural Science (Online, 2021)

Flexcrop: Energy management in greenhouses using crop flexibility (poster presentation). ISHS International Workshop on Vertical Farming. (Wageningen, The Netherlands; 2019)

Energy management in greenhouses using crop flexibility (poster presentation). Commit2data NWO meeting. (Amsterdam, The Netherlands; 2018)

Awards

Young Minds Award best oral presentation. Symposium of adaptation of Horticultural Plants to Abiotic Stress (Angers, France 2022)

Graduate Oral Presentation Award, 3rd place. ISHS International Workshop on Vertical Farming. (Wageningen, The Netherlands; 2019)

Poster award 3rd place. Commit2data NWO meeting. (Amsterdam, The Netherlands; 2018)

PE&RC Training and Education Statement

With the training and education activities listed below the PhD candidate has complied with the requirements set by the C.T. de Wit Graduate School for Production Ecology and Resource Conservation (PE&RC) which comprises of a minimum total of 32 ECTS (= 22 weeks of activities)

Review/project proposal (4.5 ECTS)

- Carbon storage in plants: a buffer for temporal light and temperature fluctuations

Post-graduate courses (12.7 ECTS)

- Introduction to R for statistical analysis; PE&RC (2018)
- The art of modelling; PE&RC (2019)
- Statistical uncertainty analysis of dynamic models (2019)
- Tidy data and data visualization with ggplot; PE&RC (2019)
- Introduction to LaTex; PE&RC (2019)
- Linear models; PE&RC (2020)
- R Markdown; PE&RC (2021)
- Integrated modelling and optimization; BioSB (2022)

Competence strengthening/skills courses (4.6 ECTS)

- Bridging across cultural differences; WGS (2018)
- Mindful scientific writing; ….. (2020)
- Scientific artwork; ….. (2021)
- Scientific journalism; PE&RC (2022)

Scientific integrity/ethics in science activities (0.6 ECTS)

- Scientific integrity; WGS (2019)

PE&RC Annual meetings, seminars and the PE&RC weekend (2.1 ECTS)

- PE&RC First years weekend (2019)
- PE&RC Midterm years weekend (2020)
- PE&RC Last year weekend (2021)

Discussion groups/local seminars or scientific meetings (6.9 ECTS)

- Frontiers literature in plant science (2018-2022)
- 1rst ISHS International workshop on vertical farming (2019)
- Modelling and simulation discussion group (2019)
- Frontiers in agricultural genomics seminar (2022)

International symposia, workshops and conferences (5.4 ECTS)

- Symposium of adaptation of Horticultural Plants to Abiotic Stress (Angers, France 2022)
- Frontiers in Agricultural Genomics seminar, UNAM (Online, 2022).
- Crops in Silico (Online, 2021)
- American Society for Horticultural Science (Online, 2021)
- ISHS International Workshop on Vertical Farming. (Wageningen, The Netherlands; 2019)
- Commit2data NWO meeting. (Amsterdam, The Netherlands; 2018)

Committee work (4 ECTS)

- Horticulture and Product Physiology Personeelsvereniging (2018-2022)

Lecturing/supervision of practicals/tutorials (3.6 ECTS)

- Crop ecology (2019, 2020)
- Greenhouse technology (2020)
- Concepts in environmental physiology (2020)

BSc/MSc thesis supervision (17 ECTS)

- Effect of temperature integration on young tomato plants; growth, development and assimilate pool dynamic changes in response to temperature and light fluctuations

- Effect of temperature on growth and photosynthesis of tomato plants
- Carbohydrate pool dynamics in response of temperature and light fluctuations
- Modelling carbohydrate pool dynamic of tomato plants: calibration of the two-state dynamic model
- Low Pollen quality and high abortion of tomato flower under short-term heat stress
- Pollen quality and quantity, and flower abortion affected by moderate heat and cold stress
- The effect of light and temperature integration period on *Solanum lycopersicum*

This project (647003006) was funded by Netherlands Organization for Scientific Research (NWO) with contributions from LTO Glastuinbouw, AgroEnergy, Blue Radix, B-Mex, LetsGrow.com, Delphy, and WUR Greenhouse Horticulture.

Cover design

Julieta Zepeda Cabrera

Plants as a Battery Exploring Crop Flexibility to Buffer Enviromental Fluctuations Cristina Zepeda